Republic of Iraq
Ministry of Higher Education
and Scientific Research
Babylon University
College of Engineering
Dept. of Mech. Eng.

OPTIMUM DIMENSIONS OF UNSYMMETRICAL ANNULAR FIN ARRAY

A THESIS SUBMITTED TO THE COLLEGE OF ENGINEERING OF THE UNIVERSITY OF BABYLON IN PARTIAL FULFILLMENT OF THE REQUIREMENTS FOR THE DEGREE OF MASTER OF SCIENCE IN MECHANICAL ENGINEERING

By

ALI SAFA NOURI AL-SA'EGH

B.Sc., 2001

November, 2005 **Shawal, 1426**

﴿اللـهُ نُـورُ ألسَّـمَاوَاتِ وَألأَرْضِ مَثَـلُ نُـورِهِ كَمِشْـكَاةٍ فِيهَـا مِصْبَاحٌ أَلْمِصْبَاحُ فِي زُجَاجَـةٍ أَلزُّجَاجَـةُ كَأَنَّـهَا كَوْكَبٌ دُرِّيٌّ يُوقَدُ مِن شَجَرَةٍ مُّبَارَكَةٍ زَيْتُونَـةٍ لا شَرْقِيَّةٍ وَلا غَرْبِيَّـةٍ يَكَـادُ زَيْتُهَا يُضِيءُ وَلَوْ لَمْ تَمْسَسْهُ نَـارٌ نُّـورٌ عَلَى نُـورٍ يَهْدِي الله لِنُورِهِ مَن يَشَآءُ وَيَضْرِبُ الله أَلأَمْثَالَ لِلنَّاسِ وَالله بِكُلِّ شَيْءٍ عَلِيمٌ ﴾

سورة النـور/ الآيه 35

الإهداء

إلى ..... الشمعةِ أَلَتي طالَما أَضاءَتْ لِي أَلطَّريقْ.

إلى ..... معلمي أَلأَوَلْ و أُسْتاذيْ أَلفاضِلْ.

إلى ..... من شَجَعَني و أَلْهَمَني أَلصَبْر و أَلعَطاء.

إلى ..... أَلحَبيبْ أَلخالِدْ أَلذِكْر.

إلى ..... ذكرى والِدي أَلحبَيبْ.

أُهْدي هذا أَلْجُهد أَلمُتَواضِعْ .

علي صفاء
تشرين الأول،
2005

EXAMINING COMMITTEES CERTIFICATE

We certify that we have read this thesis entitled **"Optimum Dimensions of Unsymmetrical Annular Fin Array"** and as an examining committee, examined the student, **"Ali Safa Nouri"**, in its contents and that in our opinion it meets standard of a thesis for the degree of Master of Science in Mechanical Engineering.

Signature:
Name: Asst. Prof.
Dr. Adil A. Al- Moosway
(Chairman)
Date: / 11 / 2005

Signature:
Name: Asst. Prof.
Dr. Majid I. Abdul Wahab
(Member)
Date: / 11 / 2005

Signature:
Name: Asst. Prof.
Dr. Falah K. Matloob
(Member)
Date: / 11 / 2005

Signature:
Name: Asst. Prof.
Dr. Tahseen A.Al-Hattab
(Supervisor)
Date: / 11 / 2005

Signature:
Name: Asst. Prof.
Dr. Emad S. Ali
(Supervisor)
Date: / 11 / 2005

Approval of the Mechanical Engineering Department.
Head of the Mechanical Engineering Department.

Signature:
Name: Asst .Prof.
Dr. Alaa M. Hussian
Date: / 11 / 2005

Approval of the College of Engineering.
Dean of the College of Engineering.

Signature:
Name: Asst. Prof.
Dr. Haroun A. K. Shahad
Date: / 11 / 2005

SUPERVISOR CERTIFICATION

We certify that this thesis entitled **"Optimum Dimensions of Unsymmetrical Annular Fin Array"** was prepared by **"Ali Safa Nouri"** under our supervision at the **Babylon University**, College of Engineering in partial fulfillment of the requirements for the degree of Master of Science in Mechanical Engineering (Power Engineering).

Signature

Name: Asst. Prof.

Dr. Tahseen A. Al-Hattab

(Supervisor)

Date: / 11 / 2005

Signature

Name: Asst. Prof.

Dr. Emad S. Ali

(Supervisor)

Date: / 11 / 2005

ACKNOWLEDGMENTS

Praise be to **ALLAH**, Most gracious, Most Merciful, who gave me the ability and desire to complete this research work.

I wish to express my cordial thanks and deepest gratitude to my supervisors ***Ass. Prof. Dr. Emad S. Ali*** and ***Ass. Prof. Dr. Tahseen A. Al-Hattab*** for their generous guidance, and valuable and active interest in this work.

My great appreciation is expressed to the Dean of the College of Engineering ***Dr. Haroun A. K. Shahad*** and also to the head of Mechanical Engineering ***Dr. Alaa M. Hussein*** and to the advanced computer laboratory staff for their kind help and invaluable advice.

My special thanks and deepest and warmest gratitude are due to my family with special gratitude to my wife for their kindness, love, support and encouragement during the period of preparing this work.

Furthermore, deepest thanks to my friends for their help to accomplish this study. Finally, I would like to express my deepest thanks and gratitude to all those who have helped me in one way or another in carrying out this research.

Ali Safa
2005

ABSTRACT

A two-dimensional fin analysis is considered in this work to study an optimization approach for a rectangular annular fin array with constant thermal properties. In this work, a design procedure based on the determination of the maximum heat dissipation from a rectangular annular fin array with non-uniform fin length taken into account the variation of the base temperature.

Fin effectiveness is the most characteristic parameter that can be used to distinguish the operation of the fin. In order to determine the fin effectiveness more precisely, the effect of the existence of the fin on the fin base temperature was taken into account, which was neglected by many other researchers.

A finite element technique of Galerkin's method is presented to solve the governing equations of rectangular profile annular fin array. Straight elements with triangular shape were used.

The force convection mode of heat transfer is taken into consideration, neglecting the heat transfer by natural convection and radiation. The total heat flow and fin array effectiveness were developed. The heat conduction within the base surface to which the fins are attached, the heat transfer from the spacing between fins, and the heat transfer from the outmost edge of the fins are also included.

Hooke and Jeeves numerical optimization method is used to find the optimum fin length corresponding to maximum heat dissipation for two cases: The first is based on non-equal fin length and equal spacing between fins (FAM) and the second is based on equal fin length and equal spacing between fins (SFM). The optimization criterion is based on a maximum effectiveness per the volume of the array. A comparison is made between the results obtained from the optimization procedure based on uniform fin length (SFM) of the array with that of non-uniform fin length (FAM). The results indicated that the optimization

procedure based on (FAM) produce higher performance with fewer amounts of materials.

In order to investigate the effect of the base temperature profile on the heat transfer, the fin length profile and so the effectiveness and its optimum values, two base temperature profiles were used. First sinusoidal base temperature profile, second linear base temperature profile. The results indicated that the length profile was always different from base temperature profile. It was shown that the total heat removed based on sinusoidal base temperature was always higher than that for the linear base temperature. Also, The effectiveness corresponding to linear profile were always higher than that for sinusoidal one, and the mass of the array for the case of linear profile was less than that in sinusoidal case.

The values of the total heat removed, the total fins length, and the fin array effectiveness per the volume of the array were drawn versus Biot number. It was found that increasing the Biot number would decrease the values of the total heat removed from the fin array and so the total fins length.

In order to examine the effect of Γ parameter, the total heat removed, The total fins length and the fin effectiveness per the volume of the fins were also drawn for different values of Biot number and Γ. The results indicated that decreasing Γ would increase the fin array effectiveness.

Analytical one-dimensional and two-dimensional analyses for single annular fin and fin array are used to verify the validity of the present analysis. It was found that the numerical solution is valid.

CONTENTS

NOMENCLATURE

The following symbols are used generally throughout the text. Other are defined as when used.

Symbol	Description	Unit
A	Area of Triangular Element	m^2
A_b	Area of Fin Base	m^2
A_e	Surface Area of Triangular Element Subjected to Boundary Condition	m^2
A_f	Total Surface Area of One Fin	m^2
A_o	Total External Surface Area of Pipe	m^2
a_t	Maximum Root Depression (Evaluation) Temperature in Equation (2.3)	K
$[B]$	Gradient Matrix	–
B_i	Biot Number $(Bi) = \frac{hL_c}{k}$	–
B_w	Dimensionless Thickness of Pipe Wall	–
b_t	a_t/θ_b	–
b_w	Thickness of Pipe Wall	m
dr	Increment in r-direction	m
dz	Increment in z-direction	m
$\{gv\}$	Gradient Vector	–
H	Height of Pipe Wall (Base Surface)	m
h	Convection Heat Transfer Coefficient	$W/m^2.K$
$\{I\}$	Inter Element Vector	–
k	Thermal Conductivity of Fin Material	W/m.K
$[K]$	Element Stiffness Matrix	–

$[K_D]$	Element Stiffness Matrix to the Conduction Equation	_
$[K_m]$	Element Stiffness Due to Boundary Condition	_
L	Dimensionless Fin Length in Equation (3.3)	_
L_c	Characteristic Length	m
L_e	Dimensionless Height of the Pipe Wall	_
L_t	Total Length of Fins	m
l	Fin Length in Equation (2.2)	m
ℓ	Fin Length	m
$[N]$	Shape Function Matrix	_
N_e	Number of Element	_
N_i, N_j, N_k	Shape Functions	_
n_f	Number of Fins	_
$(ne)_r$	Number of Element in r-Direction	_
$(ne)_z$	Number of Element in z-Direction	_
n_p	Number of Points	_
$(n_p)_r$	Number of Points in r-Direction	_
$(n_p)_z$	Number of Points in z-Direction	_
q_e	Heat Transfer from Each Element	W
q_{max}	Maximum Heat Transfer from the Fin Array	W
q_{nf}	Heat Transfer without Fin	W
q_t	Total Heat Flow from the Fin Array	W
R	Radial Distance of any Point in Fin Array	m
$R_{Cond.}$	Conduction Resistance	K/W
$R_{Conv.}$	Convection Resistance	K/W
r_{in}	Dimensionless Inner Radius of Pipe	_
r_{out}	Dimensionless Outer Radius of Pipe	_
$\{R\}$	The Residual Vector	_

r	Dimensionless Radial Distance of any Point in Fin Array	_
r'	Radial Distance to the Centroid of a Triangular Element	m
r_1	Outer Radius of Pipe	m
r_o	Inner Radius of Pipe	m
S	Spacing between Fins	m
T	Fin Temperature at any Location	K
T_b	Fin Base (Root) Temperature	K
T_e	Average Temperature over Element Surface	K
T_f	Fluid Temperature	K
t	Half Fin Thickness of Fin in Equation (2.2)	m
y	Transverse Coordinate (y-Axis)	_
Z	Axial Position of any Point in Fin Array	m
z	Dimensionless Axial Distance	_

Greek Symbols

ψ	The Angle of the Outward Normal on the Boundary	deg.
ε	Effectiveness of Single Fin in Equation (2.1)	_
ε_{fa}	Fin Array Effectiveness	_
ε_{fopt}	Optimum fin effectiveness	_
$\alpha_1, \alpha_2, \alpha_3$	Coefficients of the Interpolation Polynomial in Equation (3.29)	_
β	r_2/r_1	_
δ	Half Fin thickness	m
δ'	Dimensionless Half Fin thickness	_
$\eta_{h\ const}$	Fin efficiency with uniform heat transfer coefficient in Equation (2.2)	_

$\eta_{h\ Nonunif.}$	Fin efficiency with non-uniform heat transfer coefficient in Equation (2.2)	–
Φ	Dimensionless temperature	–
$\Gamma_1, \Gamma_2, \Gamma_3, \Gamma_4$	The Element Boundary	–
ρ	Density of fin material	kg/m^3
θ_c	Circumferential Direction	
θ_b	T_b-T_f	K

Superscripts

(e)	element
m	Exponent of the periodic base temperature
T	Transpose

Abbreviation

Ann.	Annular
Cir.	Circular
DGFSSE	Decomposes the Global Force Vector and Solves the System of Equations
DGSM	Decomposes the Global Stiffness Matrix
ESMFV	Evaluation of Stiffness Matrix and Force Vector
FAM	Fin Array Method
Hyp.	Hyperbolic
MSE	Modifying System of Equations
NBW	Number of Bandwidth
NDBC	Number of Derivative Boundary Condition
OFL	Optimum Fin Length

Pra.	Parabolic
Rec.	Rectangular
SFM	Single Fin Method
SSAHTUAF	Steady State Heat Transfer from Unsymmetrical Annular Fin Array
Trap.	Trapezoidal
Tri.	Triangular

CHAPTER ONE

1

INTRODUCTION

1.1 General

The term “extended surface” is commonly used in reference to a solid that experiences energy transfer by conduction within its boundaries, as well as energy transfer by convection (and/or radiation) between its boundaries and its surroundings. Although there are many different situations that involve combined conduction-convection effects, the most frequent application is one in which an extended surface is used specifically to enhance the heat transfer rate between a solid and an adjoining fluid. Such an extended surface is termed a fin.

The surface area of a wall, in principle, is increased in two ways. In the first way, the extended surfaces are integral parts of the base material, obtained by a casting or extruding process. The extended surfaces in the second way which may or may not be made from the base material, are attached to the base by pressing, soldering, or welding. The same geometry is obtained, though less frequently, by machining the base material. In practice, manufacturing technology and cost dictate the selection of the most desirable form, (***Arpaci, 1966***) [1].

Consider the plane wall of figure (1-1). If the base temperature (T_b) is fixed, there are two ways in which the heat transfer rate may be increased. The convection coefficient (***h***) could be increased by increasing the fluid velocity, and/or the fluid temperature (T_f) could be reduced. However, many situations would be encountered in which increasing ***h*** to the maximum possible values is

either insufficient to obtain the decider heat transfer rate or the associated costs are prohibitive. Such costs are related to the blower or pump power requirements needed to increase ***h*** through increased fluid motion. Moreover, the second option of reducing T_f is often impractical, (***Incropera*** and ***DeWitt, 1996***) [2].

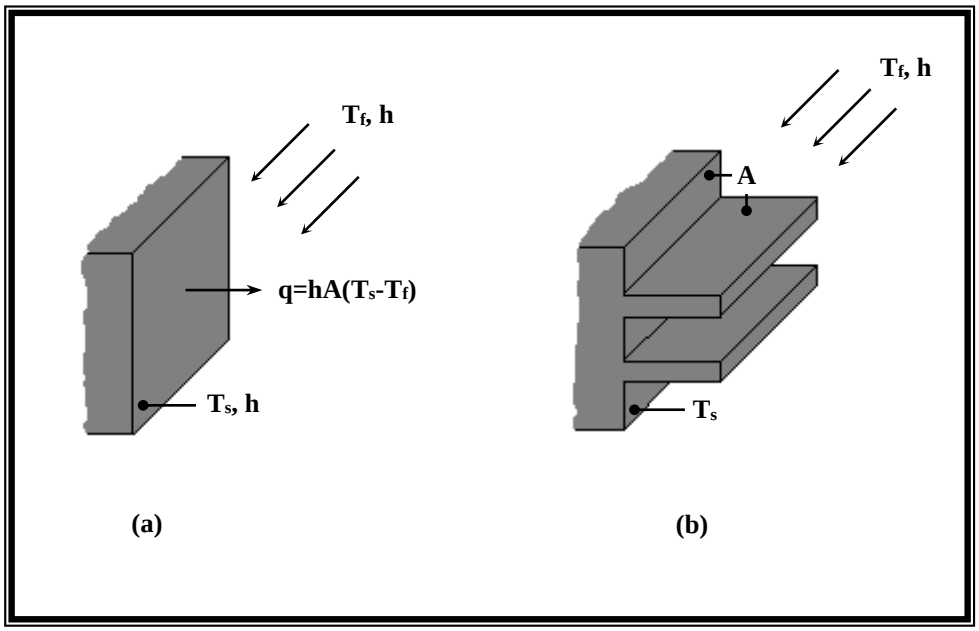

Figure (1-1) Use of Fins to Enhance Heat Transfer from a Plane Wall. (a) Bare Surface. (b) Finned Surface.

If the value of heat transfer coefficient is very large, as it is with high velocity fluids or liquids vapor (boiling and condensation), the fin may cause a reduction in heat transfer rate due to the existence of the conduction resistance which represents a large impediment to the heat flow than the convective resistance, (***Holman, 1989***) [3].

Accordingly a fin can be defined as an extra surface added to a prime surface to increase the heat transfer through a unit of its surface area, (***Abdul-Rahman, 1978***) [4].

The use of fins on one side of a wall separating two heat-exchanging fluids is exploited most if the fins are attached to or made an integral part of that face on which the thermal surface resistively is the greatest. In such a case the fins serve the purpose of artificially increasing the surface trasmittance. It is on this

principle that fins find numerous applications in electrical apparatuses in which generated heat must be efficiently dissipated, and in such specialized installations as single and double-tube heat exchanger for boilers and radiators, in cylinders of air-cooled internal combustion engines, and so on, (***Schneider, 1974***) [5]. Annular fins are of great practical importance in compact heat exchangers, finned tubes, and fuel cans in nuclear reactors, etc., (***Elias, 1998***) [6].

The primary surface usually takes the form either a plane wall or a cylindrical tube. However, the extended surfaces are not so limited in variety. They range from pin fins of cylindrical, conical, and parabolic profile, through longitudinal fins of rectangular, trapezoidal, and parabolic profile, to annular and helical fins of rectangular, trapezoidal, and parabolic profile. Figure (1-2) illustrates some of the more frequently encountered configurations. The pin fins and the longitudinal fins are used with both plane walls and cylindrical tubes, but the annular and helical fins are only suitable for use with cylindrical tubes, (***Manzoor, 1984***) [7].

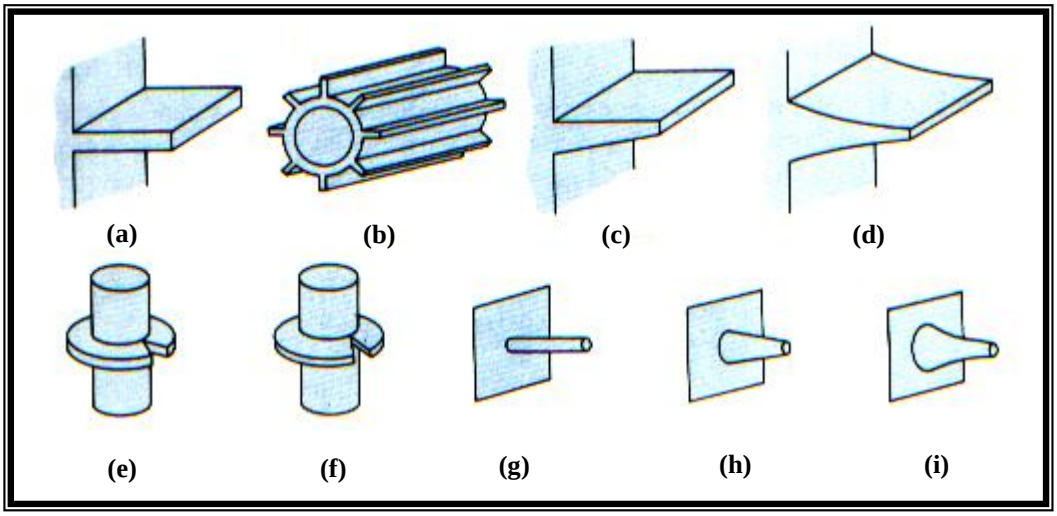

Figure (1-2) Schematic Diagrams of Different Types of Fins:
(a) Longitudinal Fin of Rectangular Profile; (b) Cylindrical Tube with Fins of Rectangular Profile; (c) Longitudinal Fin of Trapezoidal Profile; (d) Longitudinal Fin of Parabolic Profile; (e) Cylindrical Tube with Radial Fin of Rectangular Profile; (f) Cylindrical Tube with Fins of Truncated Conical Profile; (g) Cylindrical Pin Fin; (h) Truncated Conical Spine; (i) Parabolic Spine, Ref. [2].

The selection of fins is made on the basis of thermal performance and cost. The selection of suitable fin geometry requires a compromise among the cost, the weight, the available space, and the pressure drop of the heat transfer fluid, as well as the heat transfer characteristics of extended surface, (***Krith*** and ***Bohn, 1997***) [8].

It is interesting to note that the fin efficiency reaches its maximum value for the trivial case of (ℓ=**0**), or no fin at all. It is therefore not possible to maximize fin performance with respect to fin length. It is normally more important to maximize the efficiency with respect to the quantity of fin material (mass, volume, or cost), because such an optimization has obvious economic significance, (***Kern*** and ***Kraus, 1972***) [9].

When fins are used they should be placed on the side of the heat exchange surface where the heat transfer coefficient between the fluid and the surface is lower. A thin, slender, closely spaced fin is superior to fewer and thicker fins from the heat transfer standpoint. Obviously, fins made of materials having a high thermal conductivity are desirable, (***Myers, 1971***) [10].

In practice, fins are usually found in assemblies or arrays, and not as a single fin. Heat transfer from these assemblies to the surrounding occurs by convection and/or radiation. The total heat transfer depends on the following as described by, (***Mousa, 2000***) [11]:

1. Temperature distribution along the fin length as well as the assembly's base.
2. Fin geometry.
3. Air flow rate.
4. Orientation of the fin assembly.

Recent investigations of the combined fin and supporting surface have shown that the presence of fins induces two-dimensional effects within the supporting surface and these may have two-dimensional variations within the fin, (***Suryanarayana, 1977***) [12].

The design of a fin thus becomes an open-ended matter of optimizing, subject to many factors. Some of the factors that have to be considered include the following as reported by, (***Lienhard IV*** and ***Lienhard V, 2004***) [13]:

- The weight of material added by the fin. This might be a cost factor or it might be an important consideration in its own right.
- The possible dependence of h on $(T-T_f)$, flow velocity past the fin, or other influences.
- The influence of the fin (or fins) on the heat transfer coefficient (h), as the fluid moves around it (or them).
- The geometric configuration of the channel that the fin lies in.
- The cost and complexity of manufacturing fins.
- The pressure drop introduced by the fins.

The designer should be interested in choosing the best shape of fin in regard to economical and manufacturing consideration but after the shape has been chosen, the designer should aspire to the optimized dimensions. The optimum design for a given profile is defined as the fin base width and height which maximize the heat dissipation for a specified profile area, heat transfer coefficient and thermal conductivity, (***Chung et al., 1989***) [14].

The optimized dimension of the fin can be defined in either one of two ways:

1- The minimum weight (material) for dissipating a given heat amount.
2- The maximum amount of heat dissipation for a given quantity of weight.

The least material method is selected because the fins are frequently made of high conducting or corrosion resistance metals, which may be expensive.

The other methods, the maximum heat dissipation for a given volume, which is used later, is suitable for numerous applications of fin in a different practices.

1.2 Objective and Scope

The objective of the present thesis is to study the optimum dimension (lengths) of unsymmetrical annular fin array which comprises of n_f of equally spaced rectangular fins attached to cylindrical wall (pipe). This study consists of the following sequential steps:

1- The governing equation is solved using Finite-element method "*Galerkin-method*" to find the temperature distribution in the annular fin array (see Chapter Three).

2- Evaluating the effectiveness of the fin array (see Chapter three).

3- Hooke and Jeeves numerical optimization method, (***Bunday, 1985***) [15], is used to determine the optimum length of each fin in the array (see Chapter Four).

The effects of fin tip and periodic and non-periodic base temperature on an optimum dimension are also examined. Force convection heat transfer mode is studied in the present analysis.

This thesis is organized in six chapters:

Chapter One: introduces and explains briefly the problem of the study, the aim of the study and the subjects included in other chapters.

Chapter Two: contains a brief review of previous studies on the subject under consideration.

Chapter Three: presents the formulation of the mathematical model on the general finite element method formulation of the problem.

Chapter Four: deals with the optimization procedure and the computer program, which is constructed to perform all calculations based on the analysis.

Chapter Five: presents and discusses the results and the behavior for the selected range of parameters.

Chapter Six: gives a summary of the conclusions drawn from this study and suggestions for further related works.

CHAPTER TWO

2

LITERATURE REVIEW

2.1 Introduction

The work in extended surfaces started as early as the end of the eighteenth century. All the early works were directed towards finding an analytical solution of the governing equations of various types of fins making use of the same assumptions. Later works on extended surfaces were involved in analyzing the effect of some of the assumptions as well as finding numerical solution which in turn paved the way to analyzing more complex types of fins as well as reaching for the optimum dimensions of fins, **(*Elias*, 1998)**[6].

Reviews of relevant previous works including a general work in annular fins, longitudinal fins, fin arrays, and the optimum design problems are presented in this chapter.

2.2 Single Annular Fins

The problem of temperature distribution, heat transfer, fin efficiency, and the performance of annular fin which has been solved by many workers is considered in this article.

Some early measurements of temperature distribution in long metallic rods were available in the experimental determination of the thermal conductivities of iron and copper by ***Stewart*** [16] **(1893)**. ***Parson*** and ***Harper*** [17] **(1922**) derived an equation for the efficiency of straight fins of constant thickness in the course of a paper on airplane-engine radiator. The earliest mathematically rigorous

investigation pertaining to the heat flow within extended surfaces which was performed by ***Harper*** and ***Brown*** [18] **(1922)** was referred to as the first comprehensive treatment of the temperature gradient and efficiency of straight fins of rectangular, triangular, and trapezoidal profile, and annular fins of rectangular profile. They introduced a method to correct the length of fin using the tip effect.

Murray [19] **(1938)** presented equations for the temperature gradient and the effectiveness of annular fins of constant thickness with a symmetrical temperature distribution around the base of the fin. The solution was given in terms of Bessel function and simplifying graphs were given.

Herman and ***Arnold*** [20] **(1939)** proposed an investigation to determine and correlate the experimental surface heat transfer coefficients of finned cylinders with different air-stream cooling. The investigation covered the termination of the effect of fin width, fin space, fin thickness, and cylinder diameter on the heat transfer.

Carrier and ***Anderson*** [21] **(1944)** discussed straight fins of constant thickness, annular fins of constant thickness, and annular fins of constant cross-sectional area, presenting equations for the fin efficiency of each one. In the latter two cases, the solutions were given in the form of infinite series.

Gardner [22] **(1945)** generalized the extended surface problem by deriving general equations for the efficiency from the generalized Bessel equation. Gardner also defined the fin effectiveness, then he showed that the effectiveness is related to fin efficiency by

$$\varepsilon = \left(\frac{A_f}{A_b} \right) \eta \qquad \textbf{….(2.1)}$$

The results were perfectly general for eleven common profiles of longitudinal fins, radial fins, and spines; substituting the order n of the

appropriate differential equation identifies the equations of previous investigators.

Zabronsky [23] **(1952)** presented an exact solution for the efficiency of square fins on round tubes. All four rectangular fin edges were considered adiabatic, as would occur in a heat exchanger, where a large single fin sheet was penetrated by symmetrically bank of normal tubes. The efficiency of such fins was found to be nearly identical to that of circular fin of the same surface area.

Keller and ***Somers*** [24] **(1959)** obtained the two-dimensional analytical solution for annular fins, given in graphical form with the efficiency plotted versus the design parameter group. They supplied needed design information for fins of small height-to-thickness ratio and large height-to-inner radius ratio, and had compared it with one-dimensional heat flow of ***Gardner*** [22]. Their conclusion of the approximation is valid only for length to thickness ratio of more than ten where curvature is important; i.e., where the fin height is comparable to the inner diameter.

Yudin and ***Tokhtarova*** [25] **(1973)** investigated the effects of heat transfer nonuniformity from an annular rectangular fin, and on the basis of a combined analytic and experimental study derived the equation,

$$\eta_{h\ Nonuniform} = \left(1.0 - 0.058\frac{l}{t}Bi^{1/2}\right)\eta_{h\ Constant} \qquad \textbf{....(2.2)}$$

Lau and ***Tan*** [26] **(1973)** treated the annular and straight fin using Biot number as an independent parameter and discussed the error in one-dimensional approximation. They obtained analysis solutions for two types and concluded that: (1) the validity of one-dimensional approximation or not was depending on the value of Biot number (2) the error of one-dimensional from two-dimensional analysis decreases with decreasing values of fin length.

Abdul-Rahman [4] **(1978)** studied the heat transfer performance of annular fins of constant thickness with respect to the validity of assuming

one-dimensional heat flow and arrived at some limit by which the one and two- dimensional cases can be distinguished. He constructed an analogous system simulating heat flow through the fin using an electrical network. To verify the results obtained practically, a numerical technique was used to solve the governing conduction equation under the two conditions of the one- and two-dimensional heat flow.

Hegs et al. [27] **(1981)** attained an analytical solution for the temperature distribution within an annular triangular fin with linearly varying heat transfer coefficient derived, and the corresponding fin efficiency is compared with experimental results. It was apparent from the results that for given value of the average heat transfer coefficient, the maximum fin efficiency is given by (h = constant) and the minimum by (h at the base $\cong 0$).

Ünal [28] **(1988)** derived an analytical solution to find the one-dimensional temperature distribution on a straight (or a cylindrical) fin with and without internal heat generation. There were two different boundary conditions at the fin tip, i.e. the condition where heat transfer takes place at the fin tip (*real b.c.*) and the condition where no heat transfer takes place there (*hypothetical b.c.*). The heat transfer coefficient was a power function of the temperature difference between the fin and its surroundings.

Charters and ***Theerakulpisut*** [29] **(1989)** presented one-dimensional analytical solution to generate simplified relationships for determining fin efficiencies of constant thickness annular fins. These relationships may also be extended in order to be used with constant thickness rectangular and hexagonal fins with minimum effort. They concluded that these relationships are simple and capable of predicting the fin efficiency with high degree of accuracy. The analysis was based on insulated tip assumption.

Look [30] **(1995)** presented an analytical solution of a radial fin of uniform thickness on a pipe with insulated tip in one and two dimensions. Comparisons

were made of the one-dimensional and two-dimensional centerline temperature profiles and heat lost ratios for a radial fin of uniform thickness on a pipe. Effects of Biot number, fin thickness, and size ratio (ratio of radial distances of the tip and root) were investigated. In particular, the more restrictive two-dimensional results as to the usefulness of the fin are demonstrated. Further, the distortion of the two-dimension temperature profile for intermediate values of the Biot number exhibit regions where waste of material in this shape of fin occurs. Finally, information is presented which relates the fin size (radially) and the Biot number magnitude for which the fin is beneficial.

Look [31] **(1999)** studied the two-dimensional effects by comparing the results of one and two-dimensional analysis of a rectangular fin on a pipe with convection from the tip as a function of Biot number and the relative fin size. That is, the difference in the two results was pointed out through a compression of heat transfer situations using the fin effectiveness versus the Biot number. Constant heat transfer coefficient and constant base temperature were assumed. It has been found that the fin effectiveness decreases with an increase of Biot number.

2.3 Longitudinal Fins

The problems of longitudinal fins only in contact with the present work are considered in this article.

Sparrow and ***Hennecke*** [32] **(1970)** solved the coupled two-dimensional heat-conduction problem encompassing the longitudinal fin and the wall by using finite difference technique. The results of this investigation demonstrated that fins could not be properly designed without consideration of the thermal interaction between the fin and the wall to which it was affixed. The following conclusions were derived:

- Consideration must be given to the depression of the temperature of the fin base and the adjacent wall surface.

- The base temperature depression associated with an ensemble of fins would be greater than that calculated for the case of isolated fin.

Levitsky [33] **(1972)** showed that the two-dimensional solution can be reduced to one-dimensional solution only if Biot number based upon thickness is less than unity. A circular fin has been used in this analysis.

Look [34] **(1989)** presented the results of an investigation of the effect of an idealized non-constant fin root temperature on the heat loss from the rectangular fin. The convection coefficients of all surfaces were not equal and thermal radiation effects were neglected.

Look and ***Kang*** [35] **(1991)** described the effects of non-constant root temperature and the effect of unequal top, bottom, and tip surface convection coefficients on the heat lost from a single fin of rectangular profile. The root temperature had been presented as follows:

$$T = T_b + a_t \cos^m\left(\frac{\pi y}{2\delta'}\right) \qquad \text{....(2.3)}$$

The separation of variable procedure had been used to solve the two-dimensional conduction equation (differential equation). A fin justification criterion was used to discuss fin effectiveness. The results were (1) the heat lost from the fin decreased as ***m*** increased; (2) tip Biot number was not an important factor in heat lost for large Bi_{top} and Bi_{bottom} and (3) as "**a"** increased (m constant) the heat lost increased almost linearly.

Kang and ***Look*** [36] **(1997)** made a comparison of the heat loss from convecting trapezoidal fins of various slopes (triangular to rectangular). The separation of variable method was used to produce accurate solutions to the two-dimensional conduction equation and Fourier law for $Bi \leq 0.1$. The resulting relationship between the non-dimensional fin length and the slop of the fin's lateral surface for an equal amount of heat loss for given values of Biot numbers

was also demonstrated. The fin root temperature and the fin's surrounding convection coefficient were assumed to be constant.

Kang and ***Look*** [37] **(1999)** used four different methods to analyze the performance of a trapezoidal fin. These four methods were one- and two-dimensional finite difference and two-dimensional modified finite difference method. Comparisons of the heat loss from fins as a function of non-dimensional fin length and Biot number were made. They had assumed that the base temperature, surrounding convection coefficient and the fin thermal conductivity were fixed.

2.4 Fin Arrays

Suryanarayana [12] **(1977)** studied the errors in one-dimensional solution for array of rectangular fins with insulated tip. He had found out that the error increases with an increase of the wall thickness, fin length, and Biot number.

Kraus et al. [38] **(1978)** presented the conditions of heat flow and temperature excess at the fin array tip which induced conditions of heat flow and temperature excess at the fin base. There is a linear transformation between the aforementioned data at the fin tip and the fin base. They introduced a new technique to treat each fin as lumped parameter (actually, a lumped parameter matrix) and cascade the entire fin in the array via matrix operations.

Snider and ***Kraus*** [39] **(1983)** reported some recent developments by the authors in extended surface analysis and design. The authors developed a new technique for characterizing heat transfer properties of single fins and fins in arrays of extended surface. The use of these technique presented the solutions for several interesting fin problems, namely: a more careful characterization of one-dimensional flow configurations, a method for accommodating continuously distributed heat source along the fin, a perturbation approach for the approximate computation of the parameters, and new insights into the precepts of the optimal fin shape.

Kraus [40] **(1988)** presented a discussion of the design parameters of fin efficiency, fin effectiveness, and the recently proposed fin or array input admittance. After discussing what were believed to be the deficiencies and limitations of the fin efficiency as a design parameter, it has been shown that the use of input admittance overcomes these deficiencies.

Houghton et al. [41] **(1992)** developed a one-dimensional analytical solution to determine the oscillatory heat transfer in a fin assembly comprising equally spaced rectangular fins. They had found out that the instantaneous heat flow rate by convection from the fin-side surfaces oscillated periodically about the mean value, which is the fin assembly steady state heat flow rate.

2.5 Optimum Design of Fin

The optimized dimensions of the fin can be found in either one of two ways: the maximum amount of heat dissipation for a given quantity of weight or the minimum weight for dissipating a given quantity of heat. Some optimization works in extended surface were discussed in this section.

2.5.1 Least Material Method

The minimum mass fins are only of academic interest since the resulting profiles are very complex and thus costly to fabricate. However, they serve as a measure of comparison for other optimum fins with much simpler cross-sections.

Schmidt [42] **(1926)** investigated straight and annular fins from the standpoint of least-material requirements. For conductive- convective boundary condition, he proposed the first optimal fin solution by assuming that the temperature profile is a linear function of distance from the root of the fin. Practical results for the optimum dimensions for straight and triangular fins were presented in this paper. Schmidt also found the optimum dimensions for the impractical straight and annular fins of least material, and recommended using least-material annular fin for approximating the behavior of annular triangular

fin. He also showed how the thickness of each type of fin must vary to produce this result. For constant convective heat transfer coefficient, the resulting optimal profile was a concave parabola.

The temperature gradient in conical and cylindrical spines was determined by ***Focke*** [43] **(1942)**. Focke, like ***Schmidt*** [42], showed how the spine thickness must vary in order to keep the material requirement to a minimum. He found that the result was impractical and proceeded to determine the optimum cylindrical- and conical-spine dimensions.

The optimization problem, which was solved by ***Schmidt*** [42], was confirmed by ***Duffin*** [44] **(1959)**. He also assumed that the minimum weight fin had a linear temperature distribution along its length, and included the length of arc assumption, (i.e. disregarding the length of arc).

Ahmadi and ***Razani*** [45] **(1973)** solved the problems of minimizing the volume of purely conducting and conducting-convecting fins. Exact solutions were obtained for the corresponding cross-sectional areas and the temperature distributions. An approximate solution was also given for a convecting-radiating fin.

Maday [46] **(1974)** used the minimum principle to obtain the minimum weight one-dimensional cooling fin. It has included the exact representation for arc-length in the convection calculation and performs the optimum one-dimensional straight fin to be shorter while containing a little less material than the parabolic profile.

Dhar and ***Arora*** [47] **(1976)** described methods of carrying out minimum weight design of finned surface of various types. For each type of surface (flat, cylindrical, etc.) two cases were considered. A method was described by which it was possible to obtain the optimum surface profile of fins required to dissipate a certain amount of heat from the given surface, where there is no restriction on the fin height. This analysis was extended for the case when the fin height is given.

Schnurr et al. [48] **(1976)** described the non-linear optimization approach to determine the minimum weight design for radiating fin arrays used in space applications. Straight and circular fins of rectangular and triangular profile were considered. The heat transfer analysis including fin to fin and fin to base radiative interactions had been considered.

Bar-Cohen [49] **(1979)** calculated the optimum thickness for array of rectangular fins cooled by natural convection. He showed that the maximum heat dissipation in air was obtained when the fin thickness was approximately equal to the optimum fin spacing. The heat transfer from the area between fins was neglected in this analysis.

Razelos and ***Imre*** [50] **(1980)** presented the solution of the minimum mass convective fins (circular fin of trapezoidal profile) with variable thermal conductivity and heat transfer coefficients. They presented relationships of optimum volume, width, and height for each type in order to aid design procedures.

According to ***Schmidt*** [42] and ***Duffin*** [44] the temperature at the tip of the fin is equal to ambient fluid temperature. Later ***Mikk*** [51] **(1980)** re-examined the minimum mass problem for annular fins. His results, which were based on the linear temperature distribution, showed that contrary to the Schmidt-Duffin conclusion, the tip temperature is greater than the ambient temperature except for the limiting case where the annular fin becomes longitudinal. It has also presented a comparison of his results with those of Schmidt, which was based on the dimensionless volume of annular fins with minimum mass in two solutions.

Razelos and ***Imre*** [52] **(1983)** studied the case of annular fins with a trapezoidal profile with only convective heat dissipation. They dealt with optimum design (least material) of annular fin exclusively but allowed for a variable heat transfer coefficient and thermal conductivity. They showed that considering the thermal conductivity as constant, the optimum base thickness and

volume of the fin are inversely proportional to the thermal conductivity of the material of the fin, while the optimum length is independent of the properties of the material used.

Elias [6] **(1998)** proposed a new performance parameter to obtain the optimum dimension for the four different shapes of annular fin, namely, constant thickness, constant area for heat flow (*hyperbolic*), triangular, and parabolic fins. This new parameter was defined as the product of the fin efficiency and fin effectiveness and was named the " *Fin Length Optimization Parameter*". The optimization procedure worked under the assumptions of one-dimensional heat flow, constant thermal properties, and insulated tip including the effect of curvature. The concept and behavior of this parameter were studied with regard to the different variables that affect fin performance, namely, material thermal conductivity, surface heat transfer coefficient, fin base thickness, and fin length.

Khan and ***Zubair*** [53] **(1999)** obtained the optimal dimensions of convective-radiating circular fin with variable profile, heat transfer coefficient and thermal conductivity, as well as internal heat generation. It has been found that a (quadratic) hyperbolic circular fin with n=2 gives an optimum performance. The effect of radiation on the fin performance was found to be considerable for fins operating at higher base temperatures, whereas the effect of variable thermal conductivity on the optimal dimensions was negligible for the variable profile fin.

Kundu and ***Das*** [54] **(2001)** obtained an analytical solution of the temperature distribution in a concentric annular fin with a step change in thickness (AFST). The optimum design of such fins had been performed using Lagrange multiplier technique considering either the fin volume or the rate of heat transfer as the constraint. It had been demonstrated that the optimum AFSTs transfer more heat compared to the optimum annular disc fins for a given fin volume as well as for given fin volume and fin length.

Razelos and ***Krikkis*** [55] **(2001)** studied the optimum dimensions of rectangular longitudinal radiating fins with radiant interaction between the fin and its base. The basic assumptions were one-dimensional heat conduction and ideal black-surface radiation. The governing differential equation was formulated by means of dimensionless variables and was solved using a variable-step Runge-Kutta algorithm with local exploration in order to carry out the required minimization procedure. The optimum thickness, height, and percent contribution of the fin heat dissipation were presented in dimensionless form in several diagrams that give insight into the operational characteristics of the heat rejection mechanism. It had been found that the results were strongly affected by the surface Biot number. The input data were the material, amount of heat rejected, and tube & fin base temperature.

Krikkis and ***Razelos*** [56] **(2002)** determined the optimum dimensions of longitudinal rectangular and triangular fins with mutual irradiation. The basic assumptions were one-dimensional heat conduction and gray diffuse surface radiation. The governing equations were formulated by means of dimensionless variables and were solved numerically in order to carry out the required minimization procedure. The optimum fin dimensions, thickness and height, were presented in generalized dimensionless form and correlations were provided in order to assist the spacecraft thermal systems designer. The results were analyzed and expressed in explicit correlations. Several diagrams were also included, which gives insight to the operational characteristics of the heat rejection mechanism. Moreover, special attention was given to the error analysis of the numerical methods used.

Razelos and ***Krikkis*** [57] **(2003)** attained the optimum dimensions of trapezoidal profile radiating and convective-radiating circular fins. A step-by-step derivation of the governing equations was given, which were set forth in a non-dimensional form and solved numerically. The analysis was based on the

following simplifying assumptions: one-dimensional conduction, insulated tip, and negligible fin-to-base radiant interaction. The influence of the thermal conductivity, emissivity, and other parameters upon the optimum dimensions had been analyzed. The results were generalized by expressing the optimum bore thickness, tip radius, heat dissipation, and volume in dimensionless form. Simple correlations had been derived that could be employed to readily obtain the optimum fin dimensions for a specified heat transfer rate or fin's weight without the use of any graphs and/or interpolation.

Stewart et al. [58] **(2003)** studied and optimized the geometric design and operating parameters for the finned-tube condenser of a vapor compression residual air-cooling system. An optimization design of ten condensers design parameters use various constraints. These design parameters included fin thickness, fin spacing, tube diameter, tube spacing, coil depth, and frontal area aspect ratio. They concluded that the simplex search method found a design that gives the same COP for 23% less cost.

Furthermore, the study of the optimum design of convecting fins has given in texts (***Kern*** and ***Kraus,* 1972**) [59] which treated different types of longitudinal and annular fins, to determine the shape by minimizing the fin material for a given amount of heat dissipation. (***Jacob,* 1957**) [59], (***Schneider,* 1974**)[5] and (***Eckert*** and ***Drake,* 1972**) [60] also used the least material method to find the optimum dimensions.

2.5.2 Maximum Heat for a Given Volume Method

For a given fin weight, the fin can dissipate various quantities of heat, depending on its shape and geometry. Optimizing the fin, namely finding the shape that would dissipate the maximum heat for a given weight, is an important requirement in fin design.

Karlekar and ***Chao*** [61] **(1963)** developed optimization procedure for achieving maximum heat dissipation from a longitudinal fin system of trapezoidal profile with mutual irradiation. The fins were conceived to be arranged symmetrically around a base cylinder of uniform temperature. The governing equation for the temperature field along the fin was formulated in terms of finite differences. A new dimensionless parameter was proposed to characterize the total dissipation capacity of a fin system with mutual irradiation. Trapezoidal fins, including triangular and rectangular profiles, were investigated for a wide range of emissivities and incident space radiation. Optimum fin number and their properties were determined.

Brown [62] **(1965)** made use of Bessel functions to calculate the optimum dimensions of the most common annular fin shape of constant thickness. In this work, an equation was derived relating the optimum dimensions of uniform annular fin assuming one-dimensional heat flow and insulated tip. Under these conditions, Brown found that for every combination of Biot number and dimensionless fin volume there is an optimum value for the dimensionless fin thickness for which the heat transfer is maximum.

Hrymak et al. [63] **(1985)** conducted a study which utilized a numerical method to discover the optimal shape for a fin subjected to both convection and radiation heat loss. Their formulation was written to solve the problem of maximizing the heat dissipation for a given mass of fin.

Buccini and Soliman [64] **(1986)** investigated the optimization process to the more practical geometry of annular fin array (rather than a single fin), treating the problem more precisely as a two-dimensional problem and eliminating the assumption of insulated fin tip. A numerical (finite difference) approach was used for solving the conduction equation for heat transfer through the cylinder wall and fin. They presented the dimensionless fin thickness using Biot number and dimensionless volume of a single fin as the only independent parameters.

In the study of ***Yang*** [65] **(1988)**, the optimum geometric dimensions of parabolic annular fin with a constant volume, which yield the maximum heat dissipation, were determined. One-dimensional conduction with linear variation of thermal conductivity and power law for variation of the heat transfer coefficient were assumed. The effect of the two pertinent physical parameters, thermal conductivity variation parameter and the index of heat transfer coefficient variation upon the optimum dimensions was also studied and presented in graphical form as design guideline for engineering practice.

Brown's approach [62] was adopted by ***Ullmann and Kalman*** [66] **(1989)**. In this paper, the temperature profile, the efficiency and the optimum dimensions of four different shapes of annular fins (rectangular, triangular, hyperbolic, and parabolic) were determined by numerically solving the differential equations. The result obtained shows that fins with a sharp edge have lower efficiencies and higher quantities of heat dissipation per mass. They showed that the parabolic fin dissipates more heat than the others at the same mass by being a longer fin. They also showed that a heavier fin dissipates more heat at larger values of optimized ***R***, where ($R=r_1/r_o$). The fin-optimized dimensions were presented which enable to design the best fin for any practical use. The one-dimensional and insulated tip assumptions were adopted in this paper.

Look and ***Kang*** [67] **(1992)** produced an optimization procedure for the heat loss from a rectangular fin as a function of the fin's geometry. A two-dimensional rectangular fin with non-uniform root temperature and constant physical properties was considered. The relationship between the fin length for $0.99(q_f / k\theta_b)_{max}$ and the fin's effectiveness had been found.

Al-Hattab et al. [68] **(2000)** studied the optimization of two shapes of fins under radiation conditions. The temperature profile, the efficiency, and the optimum dimensions of rectangular and triangular fins were determined by solving numerically the differential equation describing these fins. The results

showed that the former has higher efficiency and lower quantities of heat dissipation per unit mass of the fin. It has been showed that the triangular fin dissipates more heat than rectangular at the same mass by being a longer fin.

Ali [69] **(2001)** presented the optimum arrangement of two-dimensional rectangular and triangular fin arrays. A finite element technique (*Galerkin method*) was used with a straight element of triangular shape. The performance (effectiveness and overall efficiency) and the normalized heat transfer were evaluated from fin arrays at different conditions (free convection, force convection, radiation, and combined force convection and radiation). The effects of fin tip and periodic and non-periodic base temperature on an optimum arrangement were also examined.

Al-Hattab [70] **(2003)** considered a one-dimensional analysis to study an optimization approach for a rectangular annular fin array. The objective of the steady was to determine an optimum non-equal fin length and equal spacing between the fins. The optimization criterion was based on a maximum performance per the volume of the array. The effect of the change in the base temperature due to the existence of the fin was considered through the calculation of the performance. A compression was made between the results obtained from the optimization procedure based on uniform fin length of the array with that of non-uniform fin length. The results indicated that the optimization procedure based on non-uniform fin length produced higher performance with fewer amounts of materials.

2.6 Literature Conclusions

From the preceding review of literatures, it is clear that most of literatures are based on the following:

- The governing equations were solved either analytically or numerically by finite differences.
- A one-dimensional heat flow.
- A single fin problem or symmetrical fins array.
- An insulated fin tip.
- A uniform base temperature.
- The optimization studies were concerned with either a single fin analysis or with a fin array having identical fin dimensions, thickness, length, and spacing between the fins (i.e. symmetrical fin array).
- The variations of thermal parameters do not affect the solution largely. The heat transfer coefficient depends upon the difference of temperature and varies, therefore, along the fin. Using the average heat transfer coefficients as constant around the fin gives reasonable accuracy for many practical purposes. Also, in general, the thermal conductivity of a material varies with temperature, but the change is relatively small that, in any practical situations, a constant value based on the average temperature of the system will give satisfactory results.
- The effectiveness is not a true indication of fin performance since T_b cannot be expected to remain constant if the fin is removed. The fin efficiency has been used as a design parameter rather than the fin effectiveness. Others showed that the change in the base temperature because the additive of extended surface is very small and can be neglected. Recent investigations of the fins system have used the fin effectiveness as a design parameter rather than the fin efficiency due to economic considerations.

Table (2-1) shows the summary of literature review work.

In the present work, an attempt will be made to investigate a design procedure based on the determination of maximum heat dissipation from a rectangular annular fin array with non-uniform fin length. In order to determine the fin effectiveness more precisely, the effect of the existence of the fin on the fin base temperature (i.e. non-constant base temperature) will be taken into account, which was neglected by many researchers. The steady state problem was solved in two-dimensional analysis using the finite element based on Galerkin's method with triangular elements including heat loss from each fin tip and spacing between fins. Hooke and Jeeves numerical optimization method is used to find the optimum fin length corresponding to maximum heat dissipation for two cases: The first is based on non-equal fin length and equal spacing between fins (FAM) and the second is based on equal fin length and equal spacing between fins (SFM). The optimization criterion is based on a maximum effectiveness per the volume of the array.

Table (2-1) Literature summary.

1- Single Annular Fins

Author	Analysis	Fin Shape & Profile	Assumptions
Harber, [18]	(1-D) Steady State	Str. (Rec., Tri. and Tra.) and Cir. (Rec.)	(k), (h) and (T_b) are constant
Murray, [19]	(1-D) Steady State	Cir. (Rec.)	(k), (h) and (T_b) are constant
Herman, [20]	(1-D) Steady State	Cir. (Rec.)	(k), and (T_b) are constant. (h) is variable
Carrier, [21]	(1-D) Steady State	Str. (Rec.) and Cir.(Rec.)	(k), (h) and (T_b) are constant
Gardner, [22]	(1-D) Steady State	Str. (Rec., Tri. and Pra.) and spines	(k), (h) and (T_b) are constant
Zabronsky, [23]	(1-D) Steady State	Cir.(Rec.)	(k), (h) and (T_b) are constant
Keller, [24]	(1-D) and (2-D) Steady State	Ann. (Rec.)	(k), (h) and (T_b) are constant
Yudin, [25]	(1-D) Steady State	Ann. (Rec.)	(k), and (T_b) are constant. (h) is variable
Lau, [26]	(1-D) and (2-D) Steady State	Ann. (Rec.) and Str. (Rec.)	(k), (h) and (T_b) are constant
Abdul-Rahman, [4]	(1-D) and (2-D) Steady State	Ann. (Rec.)	(k), (h) and (T_b) are constant
Hegs, [27]	(1-D) Steady State	Ann. (Rec.)	(k), and (T_b) are constant. (h) is variable
Unal, [28]	(1-D) Steady State	Str. (Rec.) and Cir. [Rec.]	(k), (T_b) are constant, (h) is constant but not equal
Charters, [29]	(1-D) Steady State	Ann. (Rec.)	(k), (h) and (T_b) are constant with insulated tip
Look, [30]	(1-D) and (2-D) Steady State	Ann. (Rec.)	(k), (h) and (T_b) are constant with insulated tip
Look, [31]	(1-D) and (2-D) Steady State	Ann. (Rec.)	(k), (h) and (T_b) are constant with insulated tip

2-Longitudinal Fins

Author	Analysis	Fin Shape & Profile	Assumptions
Sparrow, [32]	(2-D) Steady State	Str. (Rec.)	(k), (h) are constant with Non-constant (T_b)
Levitsky, [33]	(3-D) Steady State	Str. (Rec.) and Cir. (Rec.)	(k), (h) and (T_b) are constant
Look, [34]	(2-D) Steady State	Str. (Rec.)	(k), (h) are constant with Non-constant (T_b)
Look, [35]	(2-D) Steady State	Str. (Rec.)	(k), (h) are constant with Non-constant (T_b)
Kang, [36]	(2-D) Steady State	Str. (Tri. and Rec.)	(k), (h) and (T_b) are constant
Kang, [37]	(1-D) and (2-D) Steady State	Str. (Tri. and Rec.)	(k), (h) are constant with Non-constant (T_b)

3-Fin Arrays

Author	Analysis	Fin Shape & Profile	Assumptions
Suryanarayana, [12]	(1-D) Steady State	Array of Str. (Rec.)	(k), (h) and (T_b) are constant
Kraus, [38]	(2-D) Steady State	Array of Str. (Rec.)	(k), (h) and (T_b) are constant
Sinder, [39]	(1-D) Steady State	Array of Str. (Rec.)	(k), (h) and (T_b) are constant
Kraus, [40]	(1-D) Steady State	Array of Str. (Rec.)	(k), (h) are constant, (T_b) is variable
Houghton, [41]	(1-D) Unsteady State	Array of Str. (Rec.)	(k), (h) and (T_b) are constant

4- Optimum Design of Fin:

a- Least material method

Author	Analysis	Fin Shape & Profile	Assumptions
Schmidt, [42]	(1-D) Steady State	Cir. and Str. (Rec. and Tri.)	(k), (h) and (T_b) are constant
Duffin, [44]	(1-D) Steady State	General	(k), (h) and (T_b) are constant

Author	Analysis	Fin Shape & Profile	Assumptions
Ahmadi, [45]	(1-D) Steady State	Str. (Rec.)	(k), (h), (T_b) and (ϵ) are constant
Maday, [46]	(1-D) Steady State	General	(k), (h) and (T_b) are constant
Dhar, [47]	(1-D) Steady State	General	(k), (h) and (T_b) are constant
Schnurr, [48]	(1-D) Steady State	Str. and Cir. (Rec. and Tri.) on tube	(k), (h), (T_b) and (ϵ) are constant
Bar-Cohen, [49]	(1-D) Steady State	Str. (Rec.)	(k), (h) and (T_b) are constant
Razelos, [50]	(1-D) Steady State	Rec. (longitudinal or annular) and Cir. spines	(k), and (T_b) are constant. (h) is variable
Mikk, [51]	(1-D) Steady State	Cir. and Str. (Rec. and Tri.)	(k), (h) and (T_b) are constant
Razelos, [52]	(1-D) Steady State	Ann. (Trap.)	(k), and (T_b) are constant. (h) is variable
Elias, [6]	(1-D) Steady State	Ann. (Rec., Tri., Hyp., and Par.)	(k), (h) and (T_b) are constant
Khan, [53]	(1-D) Steady State	General	(k), (h) are variable and (T_b) is constant
Kundu, [54]	(1-D) Steady State	Concentric Ann.	(k), (h) and (T_b) are constant
Razelos, [55]	(1-D) Steady State	Str. (Rec.)	(k), (h) and (T_b) are constant
Krikkis, [56]	(1-D) Steady State	Str. (Rec. and Tri.)	(k), (h) and (T_b) are constant
Razelos, [57]	(1-D) Steady State	Cir. (Trap.)	(k), (h) and (T_b) are constant
Sterwart, [58]	(1-D) Steady State	Condenser	(k), (h) and (T_b) are constant

b- Maximum Heat for a Given Volume Method

Author	Analysis	Fin Shape & Profile	Assumptions
Karlekar, [61]	(1-D) Steady State	Str. (Tra.) on tube	(k), (T_b) and (ϵ) are constant
Brown, [62]	(1-D) Steady State	Ann. (Rec.)	(k), (h) and (T_b) are constant
Hymark, [63]	(2-D) Steady State	Str. (general)	(k), (h), (T_b) and (ϵ) are constant
Buccini, [64]	(2-D) Steady State	Array of Ann. (Rec.)	(k), (h) and (T_b) are constant

Author	Analysis	Fin Shape & Profile	Assumptions
Yang, [65]	(1-D) Steady State	Ann. (Rec.)	(T_b) is constant, (k), and (h) are variable
Ullmann, [66]	(1-D) Steady State	Ann. (Rec., Tri., Hyp., and Par.)	(k), (h) and (T_b) are constant
Look, [67]	(2-D) Steady State	Str. (Rec.)	(k), and (h) are constant, and (T_b) is not constant
Al-Hattab, [68]	(1-D) Steady State	Str. (Rec. and Tri.)	(k), (T_b) and (ϵ) are constant
Ali, [69]	(2-D) Steady State	Str. (Rec. and Tri.)	(k), is constant, (h) and (T_b) is not constant
Al-Hattab, [70]	(1-D) Steady State	Ann. (Rec.)	(k), and (h) are constant, and (T_b) is not constant

CHAPTER THREE

3

MATHEMATICAL AND NUMERICAL ANALYSIS

3.1 A General Conduction Analysis

As engineers, a primary interesting in knowing the extent to which particular extended surface or fin arrangement could improve heat transfer from a surface to the surrounding fluid. To determine the heat transfer rate associated with a fin, the temperature distribution along the fin should be obtained at first.

In order to set up the relevant governing equation, the general conservation principle can be used which states the following:

heat in + heat generation = heat out + change in internal energy **….(3.1)**

The analysis above is simplified if certain assumptions are made; for steady state conduction without heat generation the conservation equation is reduced to

heat in – heat out = 0 **….(3.2)**

3.2 Assumptions

Important to the analysis of any fin geometry are the constraints or assumptions that are employed to define and limit the problem and, of course, to simplify its solution. The present analysis is based upon the following assumptions, which are common to most of the previous investigations, (***Kraus, 1988***) [40]:

1-The heat flow and temperature distribution throughout the fin are independent of time.

2-The fins and the wall material are homogenous and isotropic, i.e., the thermal conductivity of the fin arrays, k, and the density, ρ, are constant (their dependence on the temperature and position is negligible).

3-Heat transfer coefficient at the wall and over fin surfaces is constant.

4-The base temperature is either constant or it varies periodically with distance while the temperature of the surrounding fluid is uniform.

5-The radiation from the surfaces of fin array was neglected.

6-There is a perfect contact between the wall and the fins.

3.3 Fin System

Consider symmetrical annular fin array shown in figure (3-1). The array comprises of **(n_f)** of equally spaced rectangular fin attached to the cylinder wall(*pipe*).The quantities r_o,r_1,ℓ,H,and s represent the inner radius of pipe, outer radius of pipe, initial fin length, the height of pipe, and spacing between fins, respectively. All the dimensions above remain constant except fin's length according to the optimization procedure; i.e. the symmetrical annular fin array will change to unsymmetrical annular fin array.

3.4 The Dimensionless Quantities

The dimensionless form is often more convenient to express the quantities in a form where each term is dimensionless. It is developed to simplify the solution of many engineering problems and to avoid larger quantities in calculation. The non-dimensional groups in this work will be smaller in number than the original number of variables and parameters. This simplifies the mathematics and presentation of results. All spatial dimensions are normalized

with respect to the outer radius of the pipe **(r_1)** as shown in the following equation:

$$\left.\begin{aligned} r=\frac{R}{r_1},\ \ z=\frac{Z}{r_1},\ L=\frac{\ell}{r_1},\ Le=\frac{H}{r_1},\ \Gamma=\frac{\delta}{r_1} \\ Bw=\frac{bw}{r_1},\ \ r_{in}=\frac{r_\circ}{r_1},\ \ r_{out}=1,\quad \beta=\frac{r_2}{r_1} \end{aligned}\right\} \qquad \text{....(3.3)}$$

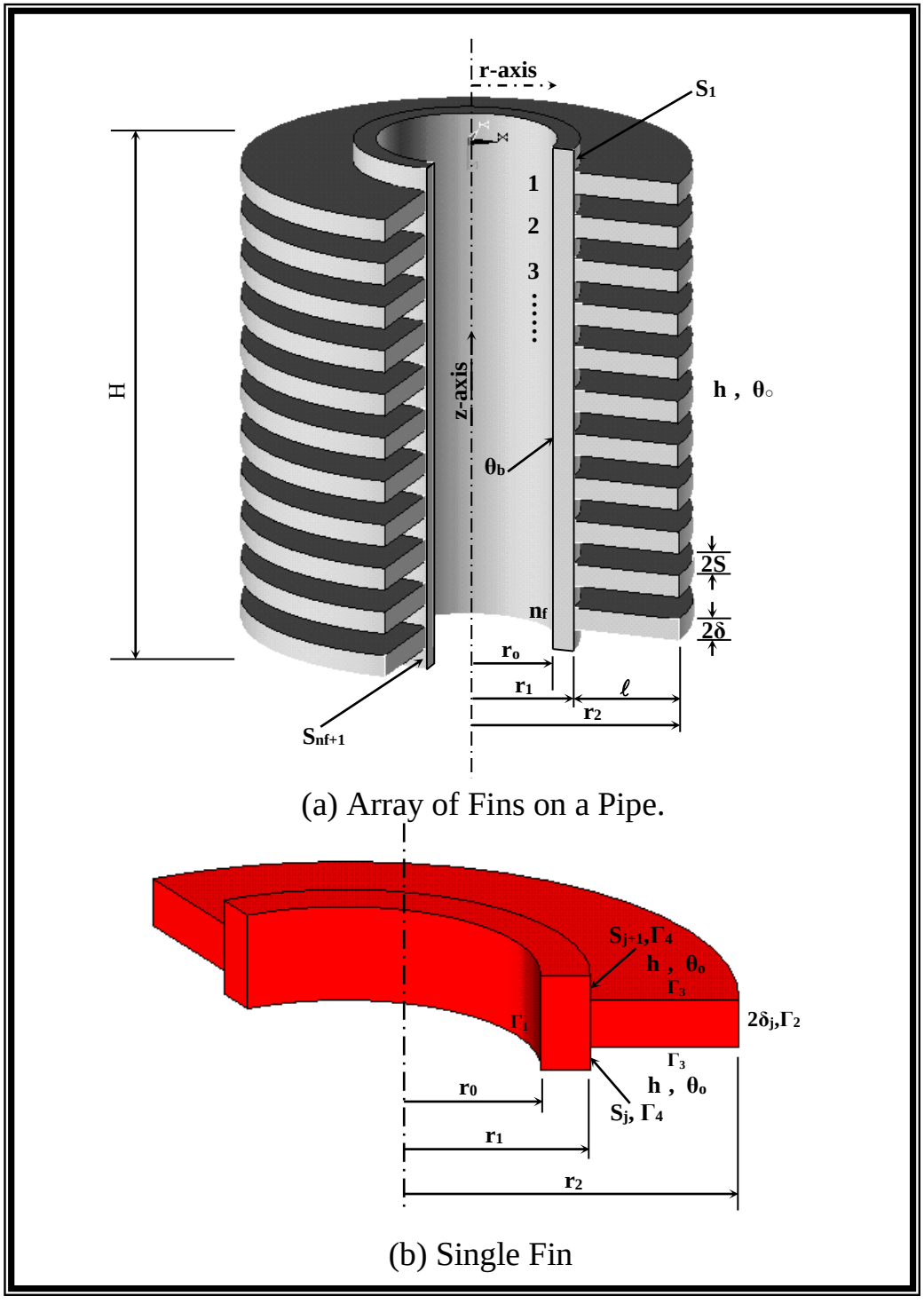

Figure (3-1) Symmetrical Annular Fin Array (Non-optimized).

The temperature is normalized in terms of fin base temperature **(θ_b)** as follows:

$$\theta = T - T_f \ , \theta_b = T_b - T_f \qquad \textbf{….(3.4)}$$

$$\Phi = \frac{\theta}{\theta_b} \qquad \textbf{….(3.5)}$$

3.5 Axi-symmetric Field Problem

There is a group of three-dimensional field problems that can be solved using two-dimensional elements. These problems possess symmetry about an axis of rotation and are known as ***axi-symmetric problems***. The boundary condition as well as the region geometry must be independent of the circumferential direction. An axi-symmetric conduction heat transfer which is independent of (θ_c) is considered in the present work.

3.5.1 Governing Differential Equation

The steady state conduction heat transfer of annular fin array to the surrounding fluid in cylindrical coordinate **(*r,z*)** is formulated by applying the energy balance on the differential element **(*dr,dz*)** as shown in Figure (3-2), taking into account the assumptions of the problem and using the principle of equation(3.2). An axi-symmetric problem in the present analysis is independent of **(θ_c)**, thus the governing equation is:

$$\frac{\partial^2 \Phi}{\partial r^2} + \frac{1}{r}\frac{\partial \Phi}{\partial r} + \frac{\partial^2 \Phi}{\partial z^2} = 0 \qquad \textbf{….(3.6)}$$

which can be written as

$$\frac{1}{r}\left[\frac{\partial}{\partial r}\left(r\frac{\partial \Phi}{\partial r}\right)\right] + \frac{\partial^2 \Phi}{\partial z^2} = 0 \qquad \textbf{….(3.7)}$$

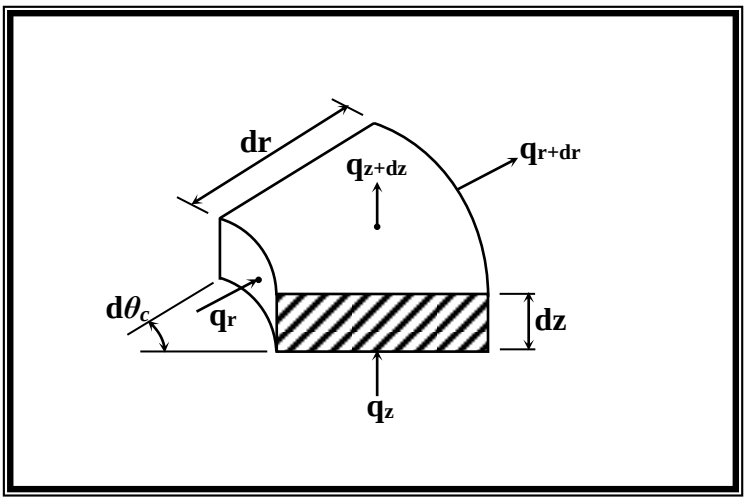

Figure (3-2) Energy Balance on Differential Element (dr,dz)

3.5.2 Boundary Conditions

Most physical problems have a mixture of boundary conditions. The values of Φ are specified on a part of the boundary while the values related to the derivatives $\partial\Phi/\partial r$ and $\partial\Phi/\partial z$ are specified on other parts of the boundary.

Assume Γ_1, Γ_2, Γ_3, and Γ_4 are the parts of the element boundary as shown in Figure (3-1 b).

At Γ_1

The actual base temperature of the fin is not really constant, (***Al-Hattab, 2003***) [70] as is usually assumed in analytical work, so

$$\Phi = 1 + b_t \sin^m\left(\frac{\pi z}{2H}\right) \qquad \text{....(3.8)}$$

At Γ_2

$$\frac{\partial\Phi}{\partial r} = Bi\Phi \qquad \text{....(3.9)}$$

At Γ_3

$$\frac{\partial\Phi}{\partial z} = Bi\Phi \qquad \text{....(3.10)}$$

At Γ_4

$$\frac{\partial \Phi}{\partial r} = Bi\Phi \qquad \text{....(3.11)}$$

The Biot number ***(Bi)*** is defined as the ratio of internal conduction resistance to the surface convection resistance. It is expressed as,

$$Bi = \frac{R_{cond.}}{R_{conv.}} = \frac{L_c/kA}{1/hA} = \frac{hL_c}{k} = \frac{h\,r_1}{k} \qquad \text{....(3.12)}$$

3.6 Finite Element Solution

The ***finite element*** is a numerical procedure for obtaining solutions to many of the problems encountered in engineering analysis. It has two characteristics distinguishing it from other numerical procedures, (***Bathe, 1996***)[71]:

1.The method utilizes an integral formulation to generate a system of algebraic equations.

2. The method uses continuous piecewise smooth functions from approximating the unknown quantity or quantities.

The most popular finite element groups are: (1) the variational method, and (2) the weighted residual method which is divided into three ways:

A- Sub domain method.

B- Collocation method.

C- Galerkin's method.

In the present analysis, ***Galerkin's method*** is used to solve the governing equation of (3.7) to find the temperature distribution in annular fin array.

The finite element method can be subdivided into five basic steps. These steps are listed here and illustrated in the next sections, (***Lewis et al, 1996***) [72]:

1-Discretize the region. This includes locating and numbering the node points as well as specifying their coordinates values.

2-Specify the approximation equation. The order of approximation, linear or quadratic, must be specified and the equations must be written in terms of the unknown nodal values. An equation is written for each element.

3-Develop the system of equations. When using Galerkin's method, the weighting function for each unknown nodal value is defined and weighted residual integrals are evaluated.

4-Solve the system of equations.

5-Calculate the quantities of interest.

3.6.1 Axi-symmetric Elements

The ***axi-symmetric element*** is obtained by rotating a two-dimensional element about the *z*-axis to obtain the torus. The idea is illustrated with the triangular element as shown in Figure (3-3). The problem is to solve a two-dimensional element with triangular shape.

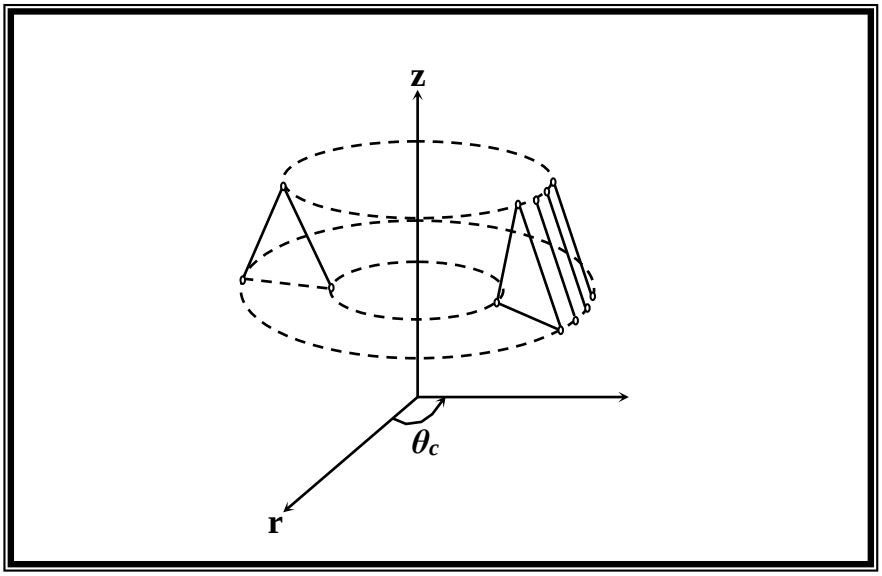

Figure (3-3) The Axi-symmetric Triangular Element, Ref.[73].

The linear triangular element shown in Figure (3-4 a) has straight sides and three nodes, one at each corner. A consistent labeling of the nodes is quite necessity and the labeling in this work proceeds counterclockwise from node ***i***, which is arbitrarily specified. The nodal values of **Φ** are $\Phi_i, \Phi_j,$ and Φ_k whereas the nodal coordinates are (R_i, Z_i) , (R_j, Z_j) , and (R_k, Z_k). A single triangular element in *r-z* plan is shown in Figure (3-4 b).

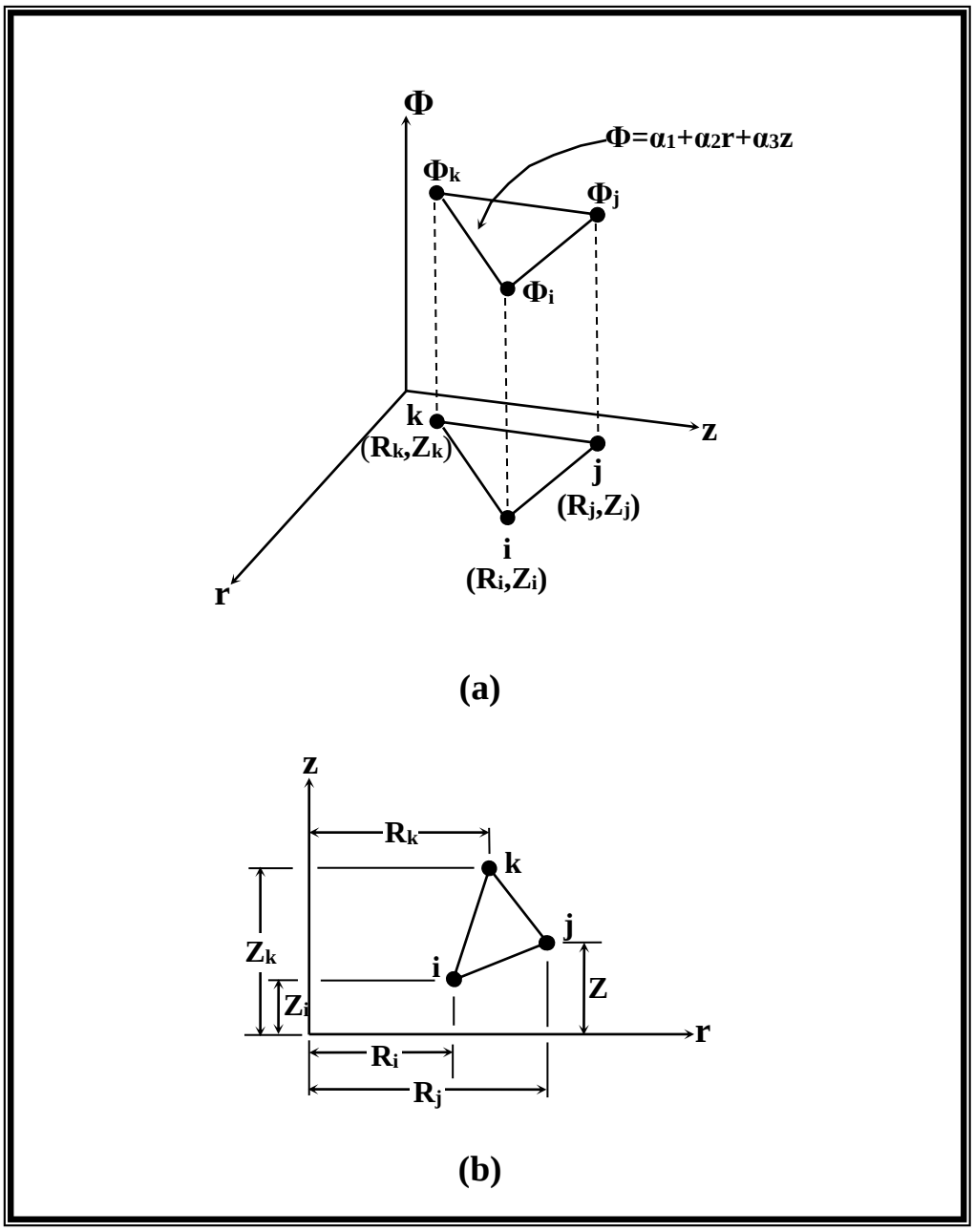

Figure (3-4) (a) Triangular Element, (b) The Axi-symmetric Triangular Element in r-z Plan, Ref.[73].

3.6.2 Mesh Generation

The basic idea of mesh generation scheme is to generate element connectivity data and nodal coordinate data by reading the input data for a few key points.

Consider a single fin, the region is divided into a number of triangular elements referred to as **(*Ne*)** as shown in Figure (3-5 a). Note that the total number of elements for the region of **(n_f)** fins is:

$$Ne = n_f \left[(ne)_r \cdot \frac{(ne)_z}{2} + 4 \right] \qquad \text{....(3.12)}$$

where, $(ne)_r$ and $(ne)_z$ are the number of elements in *r-direction* and *z-direction*, respectively.

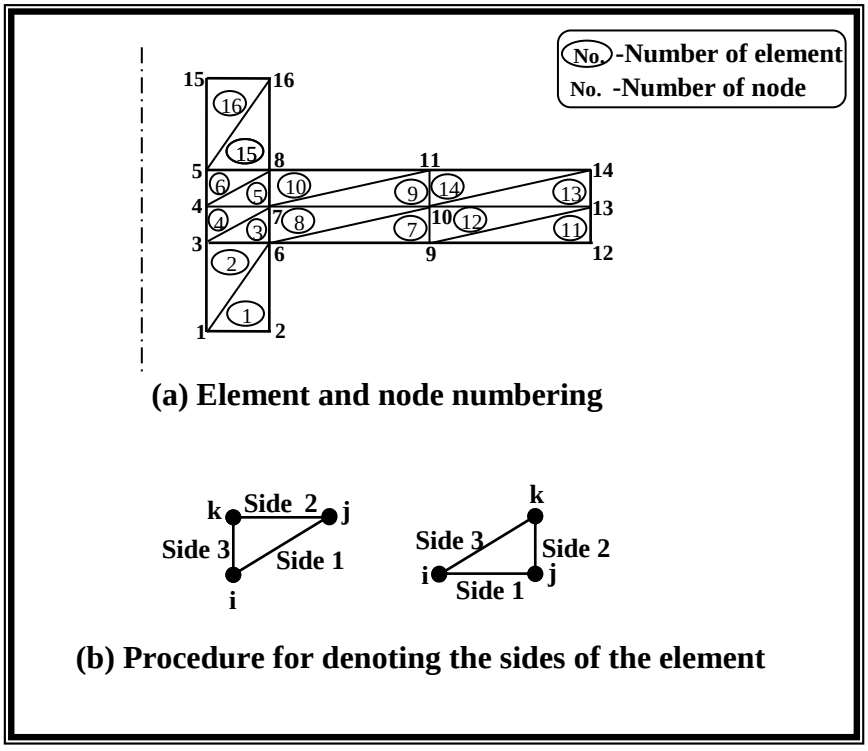

Figure (3-5) Mesh Generation (Single Fin).

Since, the node numbering will be carried out in ***r*-direction** first and increased in the ***z*-direction** next, the total number of nodes (points) in the r and z directions is:

$$\left(n_p\right)_r = 1 + \frac{(ne)_r}{2} \qquad \text{....(3.14)}$$

$$\left(n_p\right)_z = (ne)_z - 1 \qquad \text{....(3.15)}$$

The total number of points ***(n_p)*** over fin array is

$$n_p = n_f \left[\left(n_p\right)_r \cdot \left(n_p\right)_z + 4\right] - 2\left(n_f - 1\right) \qquad \text{....(3.16)}$$

For each element, there are three nodes, each node has a numerical value referred to as ***nel(i, j)***, where **(*i*)** is the number of element while **(*j*)** is the number of node.

The numerical values for the three nodes in **element (1)** are calculated as

$$\left.\begin{aligned} nel(1,1) &= 1 \\ nel(1,2) &= 2 \\ nel(1,3) &= 4 + (ne)_z \end{aligned}\right\} \qquad \text{....(3.17)}$$

and for **element (2)** are

$$\left.\begin{aligned} nel(2,1) &= 1 \\ nel(2,2) &= 4 + (ne)_z \\ nel(2,3) &= 3 \end{aligned}\right\} \qquad \text{....(3.18)}$$

Since the numerical values for the nodes of elements inside the fin region are considered as follows:

For the ***odd*** number of element (***i***)

$$\left.\begin{aligned} nel(i,1) &= c \\ nel(i,2) &= c + (ne)_z \\ nel(i,3) &= c + [(ne)_z + 1] \times [nr + 1] + 1 \end{aligned}\right\} \quad \text{....(3.19)}$$

For the ***even*** number of element (***i***)

$$\left.\begin{aligned} nel(i,1) &= c \\ nel(i,2) &= c + [(ne)_z + 1](nr + 1) + 1 \\ nel(i,3) &= (f - 1)(nr + 1)[(ne)_z + 1] + 3 \end{aligned}\right\} \quad \text{....(3.20)}$$

where **(*f*)** represents the local number of fin, while **(*c*)** and **(*nr*)** are

$$c = [(ne)_z + 1](f - 1) + nr[(ne)_z + 1](f - 2) + 2 \quad \text{....(3.21)}$$

$$nr = (ne)_r + 1 \quad \text{....(3.22)}$$

The numerical values of nodes for the last two elements are

$$\left.\begin{aligned} nel(Ne-1,1) &= c_1 \\ nel(Ne-1,2) &= c_1 + (ne)_z + 1 \\ nel(Ne-1,3) &= c_1 + (ne)_z + 1 + (ne)_r[(ne)_z + 1] + 2 \end{aligned}\right\} \quad \text{....(3.23)}$$

$$\left.\begin{aligned} nel(Ne,1) &= c_1 \\ nel(Ne-1,2) &= c_1 + (ne)_z + 1 + (ne)_r[(ne)_z + 1] + 2 \\ nel(Ne-1,3) &= nel(Ne,1) - 1 \end{aligned}\right\} \quad \text{....(3.24)}$$

where

$$c_1 = n_f[(ne)_z + 1] + nr[(ne) + 1](n_f - 1) + 2 \quad \text{....(3.25)}$$

The ***r*** and ***z*** coordinates for each node are read into ***r(i)*** and ***z(i)*** respectively where ***(i)*** is referred to the number of point ***(n_p)***. For fin region, **(d*r*)** and **(d*z*)** are given as

$$\left.\begin{aligned} dr &= \frac{\ell}{(ne)_r} \\ dz &= \frac{2\delta}{(ne)_z} \end{aligned}\right\} \qquad \text{....(3.26)}$$

This scheme gives a minimum value of ***bandwidth***; the bandwidth ***(NBW)*** is given by

$$NBW = max\left[BW^{(e)}\right]+1 \qquad \text{....(3.27)}$$

where, $\boldsymbol{BW^{(e)}}$ is the difference between the largest and smallest node numbers in an element. The largest values of $\boldsymbol{BW^{(e)}}$ are chosen to represent all nodal values.

The derivative boundary conditions occur on one or more sides of an element. The sides have been numbered to facilitate the input; these numbers are shown in Figure (3-5 b). The number of derivative boundary condition ***(NDBC)*** is calculated as

$$NDBC = n_f\left[(ne)_r + \frac{(ne)_z}{2}\right] \qquad \text{....(3.28)}$$

Then, the two-dimensional finite element mesh in the present analysis is illustrated in Figure (3-6).

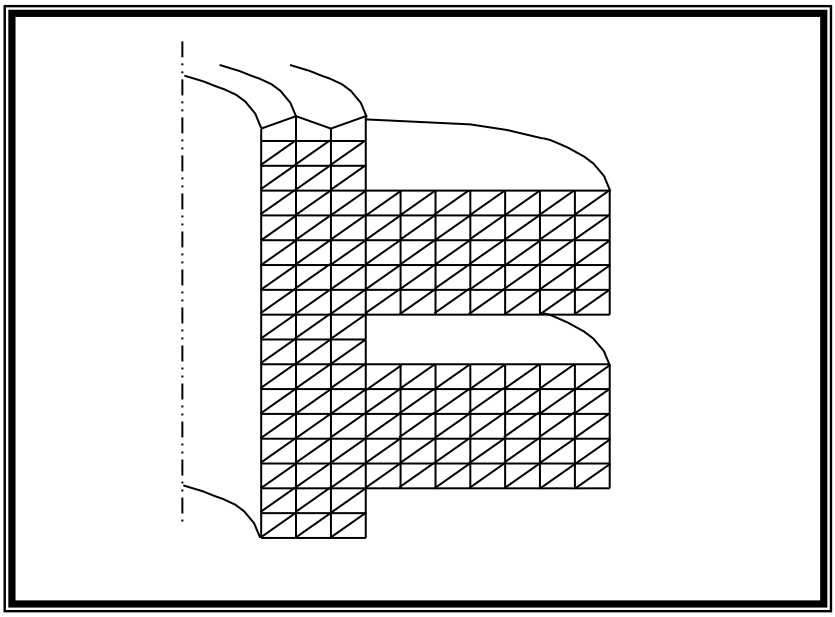

Figure (3-6) Finite Element Mesh.

3.6.3 The Element Equation

The interpolation polynomial is, (***Segerlind, 1984***) [73]

$$\Phi = \alpha_1 + \alpha_2 r + \alpha_3 z \qquad \text{....(3.29)}$$

with the nodal conditions

$$\left.\begin{aligned} &\Phi = \Phi_i \ \ at \ \ r = R_i \ , z = Z_i \\ &\Phi = \Phi_j \ \ at \ r = R_j \ , z = Z_j \\ &\Phi = \Phi_k \ \ at \ r = R_k \ , z = Z_k \end{aligned}\right\} \qquad \text{....(3.30)}$$

The substitution of these conditions into equation (3.29) produces the system of equations

$$\left.\begin{aligned} \Phi_i &= \alpha_1 + \alpha_2 R_i + \alpha_3 Z_i \\ \Phi_j &= \alpha_1 + \alpha_2 R_j + \alpha_3 Z_j \\ \Phi_k &= \alpha_1 + \alpha_2 R_k + \alpha_3 Z_k \end{aligned}\right\} \qquad \text{....(3.31)}$$

which yields

$$\left.\begin{aligned} \alpha_1 &= \frac{1}{2A}\left[\left(R_j Z_k - R_k Z_j\right)\Phi_i + \left(R_k Z_i - R_i Z_k\right)\Phi_j + \left(R_i Z_j - R_j Z_i\right)\Phi_k\right] \\ \alpha_2 &= \frac{1}{2A}\left[\left(Z_j - Z_k\right)\Phi_i + \left(Z_k - Z_i\right)\Phi_j + \left(Z_i - Z_j\right)\Phi_k\right] \\ \alpha_3 &= \frac{1}{2A}\left[\left(R_k - R_j\right)\Phi_i + \left(R_i - R_k\right)\Phi_j + \left(R_j - R_i\right)\Phi_k\right] \end{aligned}\right\} \qquad \text{....(3.32)}$$

where the determinate

$$\begin{vmatrix} 1 & R_i & Z_i \\ 1 & R_j & Z_j \\ 1 & R_k & Z_k \end{vmatrix} = 2A \qquad \text{....(3.33)}$$

and ***A*** is the area of the triangular element.

Substituting for $\boldsymbol{\alpha_1}$, $\boldsymbol{\alpha_2}$, and $\boldsymbol{\alpha_3}$ in equation (3.29) and rearranging produces an equation for $\boldsymbol{\Phi}$ in terms of three shape functions and $\boldsymbol{\Phi_i}$, $\boldsymbol{\Phi_j}$, and $\boldsymbol{\Phi_k}$ that is

$$\Phi = N_i \Phi_i + N_j \Phi_j + N_k \Phi_k \qquad \text{....(3.34)}$$

and also as

$$\Phi = \begin{bmatrix} N_i & N_j & N_k \end{bmatrix} \begin{Bmatrix} \Phi_i \\ \Phi_j \\ \Phi_k \end{Bmatrix} = [N]\{\Phi\} \quad \text{....(3.35)}$$

where

$$N_i = \frac{1}{2A}\left[a_i + b_i r + c_i z\right] \quad \text{....(3.36)}$$

$$N_j = \frac{1}{2A}\left[a_j + b_j r + c_j z\right] \quad \text{....(3.37)}$$

$$N_k = \frac{1}{2A}\left[a_k + b_k r + c_k z\right] \quad \text{....(3.38)}$$

and

$$\left.\begin{aligned} a_i &= R_j Z_k - R_k Z_j, b_i = Z_j - Z_k \text{ and } c_i = R_k - R_j \\ a_j &= R_k Z_i - R_i Z_k, b_j = Z_k - Z_i \text{ and } c_j = R_i - R_k \\ a_k &= R_i Z_j - R_j Z_i, b_k = Z_i - Z_j \text{ and } c_k = R_j - R_i \end{aligned}\right\} \quad \text{....(3.39)}$$

$$[N] = \begin{bmatrix} N_i & N_j & N_k \end{bmatrix} \quad \text{....(3.40)}$$

then

$$[N]^T = \begin{bmatrix} N_i \\ N_j \\ N_k \end{bmatrix} \quad \text{....(3.41)}$$

Note that $N_i+N_j+N_k=1$ at any point.

3.6.4 Galerkin's Method

The implementation of Galerkin's finite element method can be subdivided into three steps, (***Chaudruptla*** and ***Belegundu, 1997***) [74]:

1-Establishing the element interpolation properties.

2-Evaluating the element matrices.

3-Solving an actual problem.

The weighted residual integral for an axi-symmetric field problem is the volume integral

$$\left\{R^{(e)}\right\} = -\int_v [N]^T \left(\frac{1}{r}\frac{\partial}{\partial r}\left(r\frac{\partial \Phi}{\partial r}\right) + \frac{\partial^2 \Phi}{\partial z^2}\right) dv \qquad \text{....(3.42)}$$

where

{$R^{(e)}$}-is the residual column vector. Each component of a column vector **{*R*}** represents a residual equation. The vector is

$$\{R\} = \begin{Bmatrix} R_1 \\ R_2 \\ R_3 \\ \vdots \\ R_{\xi-1} \\ R_{\xi} \end{Bmatrix} \qquad \text{....(3.43)}$$

For example, $\boldsymbol{R_{\xi}^{(e)}}$ is the contribution of element (***e***) to the residual equation for node $\boldsymbol{\xi}$.

The derivative terms in equation (3.42) must be transformed into lower-order forms using the product rule for differentiation and Gauss's theorem, (***Segerlind, 1984***) [73].

The second-derivative terms in equation (3.42) can be replaced by applying the product rule for differentiation, which gives

$$\frac{\partial}{\partial z}\left([N]^T\right)\frac{\partial \Phi}{\partial z} = [N]^T \frac{\partial^2 \Phi}{\partial z^2} + \frac{\partial [N]^T}{\partial z}\frac{\partial \Phi}{\partial z} \qquad \text{....(3.44)}$$

Rearranging gives

$$[N]^T \frac{\partial^2 \Phi}{\partial z^2} = \frac{\partial}{\partial z}\left([N]^T \frac{\partial \Phi}{\partial z}\right) - \frac{\partial [N]^T}{\partial z}\frac{\partial \Phi}{\partial z} \qquad \textbf{….(3.45)}$$

The first term in equation (3.42) is replaced once it is determined that

$$\frac{1}{r}\frac{\partial}{\partial r}\left([N]^T r \frac{\partial \Phi}{\partial r}\right) = \frac{1}{r}\left(\frac{\partial [N]^T}{\partial r} r \frac{\partial \Phi}{\partial r}\right) + \frac{1}{r}[N]^T \frac{\partial}{\partial r}\left(r \frac{\partial \Phi}{\partial r}\right) \qquad \textbf{….(3.46)}$$

Rearranging yields

$$[N]^T\left(\frac{1}{r}\frac{\partial}{\partial r}\left(r \frac{\partial \Phi}{\partial r}\right)\right) = \frac{1}{r}\frac{\partial}{\partial r}\left([N]^T r \frac{\partial \Phi}{\partial r}\right) - \frac{\partial [N]^T}{\partial r}\frac{\partial \Phi}{\partial r} \qquad \textbf{….(3.47)}$$

The substitution of equation (3.45) and equation (3.47) into equation (3.42) is

$$\begin{aligned}\left\{R^{(e)}\right\} = &\int_v \left(\frac{\partial [N]^T}{\partial r}\frac{\partial \Phi}{\partial r} + \frac{\partial [N]^T}{\partial z}\frac{\partial \Phi}{\partial z}\right) dv \\ &- \int_v \left(\frac{1}{r}\frac{\partial}{\partial r}\left([N]^T r \frac{\partial \Phi}{\partial r}\right) + \frac{\partial}{\partial z}\left([N]^T \frac{\partial \Phi}{\partial z}\right)\right) dv\end{aligned} \qquad \textbf{….(3.48)}$$

The second volume integral can be transformed into a surface integral using ***Gauss's theorem***. The result is

$$\int_\Gamma \left(\frac{1}{r}\left([N]^T r \frac{\partial \Phi}{\partial r}\right)\cos\Psi + [N]^T \frac{\partial \Phi}{\partial z}\sin\Psi\right) d\Gamma \qquad \textbf{….(3.49)}$$

which simplifies to

$$\int_\Gamma [N]^T \left(\frac{\partial \Phi}{\partial r} cos\Psi + \frac{\partial \Phi}{\partial z} sin\Psi\right) d\Gamma \qquad \textbf{….(3.50)}$$

where, (**Ψ**) is the angle to the outward normal and (**Γ**) is the element boundary. The boundary surface is illustrated in Figure (3-7).

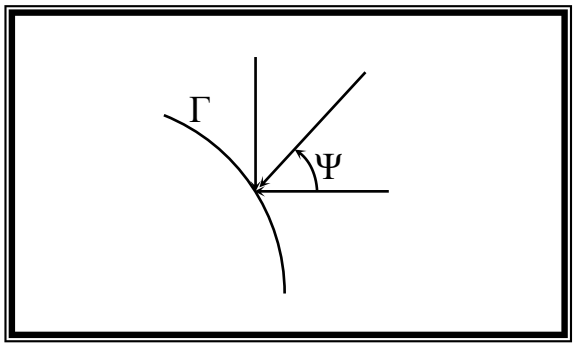

Figure (3-7) Boundary Surface.

The complete residual integrals are

$$\{R^{(e)}\}=\int_v\left(\frac{\partial[N]^T}{\partial r}\frac{\partial\Phi}{\partial r}+\frac{\partial[N]^T}{\partial z}\frac{\partial\Phi}{\partial z}\right)dv - \int_\Gamma[N]^T\left(\frac{\partial\Phi}{\partial r}\cos\Psi+\frac{\partial\Phi}{\partial z}\sin\Psi\right)d\Gamma \quad \text{....(3.51)}$$

Equation (3.51) is close to the desired form. It can be put in a final form by substituting for **Φ** using the relationship

$$\Phi^{(e)}=[N]\{\Phi^{(e)}\} \quad \text{....(3.52)}$$

By using equation (3.52), $\partial\Phi/\partial r$ and $\partial\Phi/\partial z$ in the first integral of equation (3.51) can be replaced by

$$\frac{\partial\Phi}{\partial r}=\frac{\partial[N]}{\partial r}\{\Phi^{(e)}\} \;\; and \;\; \frac{\partial\Phi}{\partial z}=\frac{\partial[N]}{\partial z}\{\Phi^{(e)}\} \quad \text{....(3.53)}$$

It gives

$$\{R^{(e)}\}=\left(\int_v\left(\frac{\partial[N]^T}{\partial r}\frac{\partial[N]}{\partial r}+\frac{\partial[N]^T}{\partial z}\frac{\partial[N]}{\partial z}\right)dv\right)\{\Phi^{(e)}\} - \int_\Gamma[N]^T\left(\frac{\partial\Phi}{\partial r}\cos\Psi+\frac{\partial\Phi}{\partial z}\sin\Psi\right)d\Gamma \quad \text{....(3.54)}$$

The first integral in equation (3.54) multiplies **{Φ$^{(e)}$}**; thus it is the element stiffness matrix. The surface integral is the interelement requirement for interior element boundaries and the derivative boundary condition for element boundaries on **Γ$_2$, Γ$_3$** and **Γ$_4$**. The general form of **{*R* $^{(e)}$}** is

$$\{R^{(e)}\} = \{I^{(e)}\} + [K_D^{(e)}]\{\Phi^{(e)}\} \qquad \text{....(3.55)}$$

where

$$\{I^{(e)}\} = -\int_{\Gamma} [N]^T \left(\frac{\partial \Phi}{\partial r} cos\Psi + \frac{\partial \Phi}{\partial z} sin\Psi \right) d\Gamma \qquad \text{....(3.56)}$$

$$[K_D^{(e)}] = \int_{v} \left(\frac{\partial [N]^T}{\partial r} \frac{\partial [N]}{\partial r} + \frac{\partial [N]^T}{\partial z} \frac{\partial [N]}{\partial z} \right) dv \qquad \text{....(3.57)}$$

The variable **(Φ)** in equation (3.56) was not replaced because the quantity

$$\frac{\partial \Phi}{\partial r} cos\Psi + \frac{\partial \Phi}{\partial z} sin\Psi \qquad \text{....(3.58)}$$

occurs in the derivative boundary conditions.

The integral in equation (3.57) can be written more compactly by defining the gradient vector.

$$\{gv\} = \begin{Bmatrix} \frac{\partial \Phi}{\partial r} \\ \\ \frac{\partial \Phi}{\partial z} \end{Bmatrix} = \begin{bmatrix} \frac{\partial [N]}{\partial r} \\ \\ \frac{\partial [N]}{\partial z} \end{bmatrix} \{\Phi^{(e)}\} = [B]\{\Phi^{(e)}\} \qquad \text{....(3.59)}$$

The first row of **{gv}** is the derivative of **[*N*]** with respect to **r**; the second row is the derivative of **[*N*]** with respect to **z**. The transposition of **[*B*]** contains two columns and is given by

$$[B]^T = \left[\frac{\partial [N]^T}{\partial r} \frac{\partial [N]^T}{\partial z} \right] \quad \text{....(3.60)}$$

By using equations (3.59), and (3.60), it is easy to verify that

$$\int_v [B]^T [B] dv = \int_v \left(\frac{\partial [N]^T}{\partial r} \frac{\partial [N]}{\partial r} + \frac{\partial [N]^T}{\partial z} \frac{\partial [N]}{\partial z} \right) dv \quad \text{....(3.61)}$$

so that, the stiffness matrix can be written in the compact form

$$\left[K_D^{(e)}\right] = \int_v [B]^T [B] \, dv \quad \text{....(3.62)}$$

3.6.5 Element Matrices

The immediate objective is to evaluate the volume integrals that give $[K_D^{(e)}]$.The contribution of the derivative boundary condition of this integral will be discussed in the next section.

The coefficients in [***B***] are obtained by differentiating the shape function relative to ***r*** and ***z***. This produces the matrix

$$[B] = \frac{1}{2A} \begin{bmatrix} b_i & b_j & b_k \\ c_i & c_j & c_k \end{bmatrix} \quad \text{....(3.63)}$$

Each coefficient in [B] is constant.

$$\left[K_D^{(e)}\right] = \int_v [B]^T [B] dv = [B]^T [B] \int_v dv = [B]^T [B] v \quad \text{....(3.64)}$$

The volume of an area revolved about the *z*-axis is $v = 2\pi r' A$, where r' is the radial distance to the centroid of the area, (***Rockey et al., 1975***) [75]. Therefore, the element stiffness matrix is

$$\left[K_D^{(e)}\right] = 2\pi r' A [B]^T [B] \quad \text{....(3.65)}$$

This matrix product is easily evaluated to give

$$\left[K_D^{(e)}\right]=\frac{2\pi r'}{4A}\begin{bmatrix} b_i^2 & b_ib_j & b_ib_k \\ b_ib_j & b_j^2 & b_jb_k \\ b_ib_k & b_jb_k & b_k^2 \end{bmatrix}+\frac{2\pi r'}{4A}\begin{bmatrix} c_i^2 & c_ic_j & c_ic_k \\ c_ic_j & c_j^2 & c_jc_k \\ c_ic_k & c_jc_k & c_k^2 \end{bmatrix} \quad \text{....(3.66)}$$

where ***A*** is the area of the triangle.

The radial distance to the centroid of a triangular element is

$$r'=\frac{R_i+R_j+R_k}{3} \quad \text{....(3.67)}$$

3.6.6 Interelement Vector

The element matrix in equation (3.66) is valid for interior elements and boundary elements when **Φ(*r,z*)** is specified on the boundary. When the derivative boundary condition (section 3.5.2) is specified, there is an additional contribution to $[K_D^{(e)}]$. This contribution is considered in this section.

The derivative boundary condition appearing in $\{I^{(e)}\}$ matrices is shown schematically in Figure (3-7). In general, the boundary condition can be written as, (***Segerlind, 1984***) [73]:

$$\frac{\partial\Phi}{\partial n}=-\left(\frac{\partial\Phi}{\partial r}\cos\Psi+\frac{\partial\Phi}{\partial z}\sin\Psi\right)=-\mu\Phi_b+s \quad \text{....(3.68)}$$

For force convection heat transfer (*present analysis*):

$$-\frac{\partial\Phi}{\partial n}=Bi\,\Phi_b \quad \text{....(3.69)}$$

where $\partial\Phi/\partial n$ is the derivative normal to the boundary. In each case, Φ_b represents the value of **Φ** on **Γ**, which is unknown.

The inclusion of the boundary condition into the finite element analysis of the heat transfer problem is to be done by using the interelement vector $\{I^{(e)}\}$ given by equation (3.56). Back to equation (3.56)

$$\{I^{(e)}\} = -\int_{\Gamma} [N]^T \left(\frac{\partial \Phi}{\partial r} \cos \Psi + \frac{\partial \Phi}{\partial z} \sin \Psi \right) d\Gamma$$

where the integrals are around the boundary of the element in a counterclockwise direction. The integral in equation (3.56) is the sum of three integrals (*one for each side*). Assuming that $\boldsymbol{\Gamma_{bc}}$ is the surface of the element with the boundary condition, $\boldsymbol{\{I^{(e)}\}}$ will be separated into two components:

$$\{I^{(e)}\} = \{I_{bc}^{(e)}\} + \{I_i^{(e)}\} \qquad \textbf{….(3.70)}$$

where

$$\{I_{bc}^{(e)}\} = -\int_{\Gamma_{bc}} [N]^T \left(\frac{\partial \Phi}{\partial r} \cos \Psi + \frac{\partial \Phi}{\partial z} \sin \Psi \right) d\Gamma \qquad \textbf{….(3.71)}$$

The vector $\boldsymbol{\{I_i^{(e)}\}}$ contains the integrals of equation (3.56), which occur on the element side that doesn't have a boundary condition specified on them. These integrals lead to the interelement requirements that must be satisfied before ***Galerkin's residual*** is zero.

Using the definition for $\boldsymbol{\{I_{bc}^{(e)}\}}$ and substituting the relationship in equation(3.68) and equation (3.69) gives

$$\{I_{bc}^{(e)}\} = \int_{bc} Bi [N]^T \Phi_b \, d\Gamma \qquad \textbf{….(3.72)}$$

The value of $\boldsymbol{\Phi}$ on the boundary, $\boldsymbol{\Phi_b}$, is given the element equation $\Phi^{(e)} = [N]\{\Phi^{(e)}\}$; therefore,

$$\{I_{bc}^{(e)}\} = \left(\int_{\Gamma_{bc}} Bi [N]^T [N] d\Gamma \right) \{\Phi^{(e)}\} \qquad \textbf{….(3.73)}$$

The above integral contributes to $\boldsymbol{[K_D^{(e)}]}$, since it multiplies $\boldsymbol{\{\Phi^{(e)}\}}$, so that equation (3.73) can be defined as

$$\{I_{bc}^{(e)}\} = [K_m^{(e)}]\{\Phi^{(e)}\} \qquad \textbf{….(3.74)}$$

The integral equation (3.73) is surface integral and is calculated as follows

$$\left[K_m^{(e)}\right] = \int_{\Gamma_{bc}} Bi \left[N\right]^T \left[N\right] d\Gamma \qquad \text{....(3.75)}$$

Using the definition of shape function

$$\left.\begin{aligned} \left[K_m^{(e)}\right] &= \int_{\Gamma_{bc}} Bi \begin{Bmatrix} N_i \\ N_j \\ N_k \end{Bmatrix} \begin{bmatrix} N_i & N_j & N_k \end{bmatrix} d\Gamma \\ &= L_{jk} \int_{\Gamma_{bc}} Bi \begin{Bmatrix} L_1 \\ L_2 \\ L_3 \end{Bmatrix} \begin{bmatrix} L_1 & L_2 & L_3 \end{bmatrix} 2\pi r d\ell_2 \end{aligned}\right\} \qquad \text{....(3.76)}$$

The length ratio coordinates result in a simple formula for evaluating an integral involving a product of shape functions. Assuming that the integration is along side (***jk***), the area coordinates reduced to $L_1=0$, $L_2=\ell_1$, and $L_3=\ell_2$ along this side the integral becomes

$$\begin{aligned} \left[K_m^{(e)}\right] &= 2\pi Bi\, L_{jk} \int_0^1 \begin{Bmatrix} 0 \\ \ell_1 \\ \ell_2 \end{Bmatrix} \begin{bmatrix} 0 & \ell_1 & \ell_2 \end{bmatrix} r\, d\ell_2 \\ &= 2\pi Bi\, L_{jk} \int_0^1 \begin{bmatrix} 0 & 0 & 0 \\ 0 & r\ell_1^2 & r\ell_1\ell_2 \\ 0 & r\ell_1\ell_2 & r\ell_2^2 \end{bmatrix} d\ell_2 \end{aligned} \qquad \text{....(3.77)}$$

The radial distance to a point on the boundary is

$$r = N_i R_i + N_j R_j + N_k R_k = \ell_1 R_j + \ell_2 R_k \qquad \text{....(3.78)}$$

since $N_i=0$. Substitution for **(*r*)** in equation (3.77) produces

$$\left[K_m^{(e)}\right] = 2\pi\, Bi\, L_{jk} \int_0^1 \begin{bmatrix} 0 & 0 & 0 \\ 0 & \ell_1^2\left(\ell_1 R_j + \ell_2 R_k\right) & \ell_1\ell_2\left(\ell_1 R_j + \ell_2 R_k\right) \\ 0 & \ell_1\ell_2\left(\ell_1 R_j + \ell_2 R_k\right) & \ell_2^2\left(\ell_1 R_j + \ell_2 R_k\right) \end{bmatrix} d\ell_2 \qquad \text{....(3.79)}$$

The integrals of $\ell_1^2, \ell_1\ell_2, \ell_2^2$ are evaluated using the factorial formula, (***Segerlind, 1984***) [73]:

$$\int_0^1 \ell_1^a \ell_2^b \, d\ell_2 = \frac{\Gamma(a+1)\Gamma(b+1)}{\Gamma(a+b+1+1)} = \frac{a!\,b!}{(a+b+1)!} \qquad \text{....(3.80)}$$

where $\boldsymbol{\Gamma(n+1)=n!}$

$$\left[K_m^{(e)}\right] = \frac{2\pi BiL_{jk}}{12}\begin{bmatrix} 0 & 0 & 0 \\ 0 & (3R_j + R_k) & (R_j + R_k) \\ 0 & (R_j + R_k) & (R_j + 3R_k) \end{bmatrix} \qquad \text{....(3.81)}$$

The other two results for equation (3.75) are

$$\left[K_m^{(e)}\right] = \frac{2\pi BiL_{ij}}{12}\begin{bmatrix} 3(R_i + R_j) & (R_i + R_j) & 0 \\ (R_i + R_j) & (R_i + 3R_j) & 0 \\ 0 & 0 & 0 \end{bmatrix} \qquad \text{....(3.82)}$$

$$\left[K_m^{(e)}\right] = \frac{2\pi BiL_{jk}}{12}\begin{bmatrix} (3R_i + R_k) & 0 & (R_i + R_k) \\ 0 & 0 & 0 \\ (R_i + R_k) & 0 & (R_i + 3R_k) \end{bmatrix} \qquad \text{....(3.83)}$$

for sides **(ij)** and **(ik)**, respectively.

3.6.7 The Complete Residual Equation

The complete residual equation is obtained by substituting for $\boldsymbol{\{I^{(e)}\}}$ in equation (3.55) and is

$$\left\{R^{(e)}\right\} = \left\{I_i^{(e)}\right\} + \left(\left[K_D^{(e)}\right] + \left[K_m^{(e)}\right]\right)\left\{\Phi^{(e)}\right\} - \left\{f^{(e)}\right\} \qquad \text{....(3.84)}$$

Neglecting the interelement requirement $\boldsymbol{\{I_i^{(e)}\}}$ gives

$$\left\{R^{(e)}\right\} = \left[K^{(e)}\right]\left\{\Phi^{(e)}\right\} - \left\{f^{(e)}\right\} \qquad \text{....(3.85)}$$

where

$$\left[K^{(e)}\right] = \left[K_D^{(e)}\right] + \left[K_m^{(e)}\right] \qquad \text{....(3.86)}$$

The contribution of $[K_m^{(e)}]$ occurs only for the elements that are subjected to derivative boundary conditions. Note that for heat conduction without heat generation and with convection boundary condition, the force vector equals to zero $(\{f^{(e)}\}=0)$.

3.7 Temperature Distribution

The actual temperature distribution for annular fin array is found by solving the equation (3.85). The ***Gaussian elimination method*** is used to solve the matrices.

There are three points to keep in mind as the elements are developing. First, the residual equations are always arranged in numerical sequence, that is, $R_1, R_2, \ldots, R_{np-1}, R_{np}$ where there are (n_p) nodal values. Second, the nodal values $\Phi_1, \Phi_2 \ldots \Phi_{np}$ are arranged sequentially within an equation. Third, an equation is developed for each node. The boundary conditions are incorporated after all of the equations have been developed using the method of deletion of rows and columns, (***Reddy, 1984***) [76].

3.8 Total Heat Flow Rate

The total rate through the annular fin is of primary interest. After knowing the temperature profile by solving equation (3.85), the total heat flow from fin array is evaluated by summation of heat transfer from each element. Heat transfer from each element is determined as follows:

$$q_e = h A_e (T_e - T_f) = h A_e \theta_e \qquad \text{....(3.87)}$$

where

A_e =surface area of element subjected to boundary condition.

T_e =average temperature over element surface subjected to boundary condition.

h =heat transfer coefficient over the element surface which is assumed to be equivalent for the finned and prime surface.

$$\theta_e = \left(T_e - T_f\right) \quad \text{....(3.88)}$$

The total heat flow from system of fin array (***finned surface + unfinned surface***) is

$$q_t = \sum_{e=1}^{NDBC} q_e \quad \text{....(3.89)}$$

3.9 Fin Array effectiveness

Recall that fins are used to increase the heat transfer from a surface by increasing the effective surface area. However, the fin itself represents a conduction resistance to heat transfer from the original surface. For this reason, there is no assurance that the heat transfer rate will be increased through the use of fins. An assessment of this matter may be made by evaluating the ***fin array effectiveness*** **(ε_{fa})**.

Fin array effectiveness **(ε_{fa})** is defined as the ratio of the fin heat transfer rate to the heat transfer rate that would exist without the fin (**original area A_o**), (***Gardner, 1945***) [22].

$$\varepsilon_{fa} = \frac{q_t}{q_{nf}} \quad \text{....(3.90)}$$

where q_t is the total heat transfer from the total surface area of fin array associated with both the fins and the exposed portion of the base (*often termed as prime surface*). q_{nf} was calculated as follows

$$q_{nf} = h\,A_o\left(T_b - T_f\right) = h\,A_o\,\theta(r_1) \quad \text{....(3.91)}$$

where

$$A_o = 2\pi r_1 H \quad \text{....(3.92)}$$

Equation (3.90) is also applicable for the single fin.

$$\theta(r_1) = \frac{1 - Bi\ln(r_1) + Bi\ln(r_1)}{1 - Bi\ln(r_o) + Bi\ln(r_1)} \quad \textbf{….(3.93)}$$

Equation (3.93) was derived using one dimension analysis because the faces of the cylinder were assumed to be insulated.

The fin effectiveness is an indication of the usefulness of the presence of the fin itself, which directly depends on the surface resistance of the fin. For this demonstration, ε_{fa} **= 1** will be the lowest possible acceptable fin performance. Note, in practice, this ratio should have a magnitude of 3 or more before a fin is considered to be enhancing the heat transfer regardless of the analysis, (***Ali, 2001***) [69].

CHAPTER FOUR 4

Optimum Design and Computer Program

4.1 Introduction

Optimization means minimization or maximization. There are two broad types of design: a functional design and an optimized design. Design optimization is always based on some criterion such as cost, strength, size, weight, reliability, noise, or performance. Annular fins are used extensively in heat exchange devices to increase the heat transfer. For economic purposes several methods were used to evaluate the best performance of the fin array.

The fin optimization problem, referred to in the literature as the optimum volume or the least material problem, is to find the shape of the fin which would minimize the fin volume for a given amount of heat dissipation for a given volume, or, alternatively, to maximize the heat dissipation for a given volume. The latter method was selected in this study.

The heat dissipation from the fin per unit volume increases by increasing the length of the fin, and decreases after the maximum occurs. This is due to the fact that the increase of the volume is greater than the heat dissipation. The dimensions of the fin where this maximum occurs are the optimized dimensions.

In this chapter, the concept of optimum procedure of heat transfer in the fin array and the computer program used are presented.

4.2 Optimum Design of Annular Fin Array

4.2.1 Hooke and Jeeves Method

Hooke and ***Jeeves*** numerical optimization method, (***Bunday, 1985***) [15], is used to determine the optimum length of each fin in the array. Hook and Jeeves method is classified with the direct search method for the function of ***n*** variables.

In the direct search method for function of n variables, Hooke and Jeeves develop a search which consists of a sequence of exploration steps about a base point, which if succeeded will be followed by pattern moves.

4.2.2 Objective Function

In general, keeping all the dimensions of a fin and the operating conditions constant, the effectiveness is related directly to the length of the fin; increasing the length will increase the effectiveness and the maximum effectiveness occurs at the infinite length of the fin. Therefore the optimization criterion will be based on the maximization of the effectiveness for the definite mass of the array. Hence the objective function of the problem is:

$$\varepsilon_{fopt.} = Max.\left(\frac{\varepsilon_{fa}}{L_t}\right) \qquad \text{....(4.3)}$$

where L_t refers to the dimensionless total lengths of fins

$$L_t = \sum_{j=1}^{N}\left(\beta_j - 1\right) \qquad \text{....(4.4)}$$

4.3 Computer Program

The finite element method involves large systems of linear equations and has limited usefulness if a digital computer is not available. The computer program "**SSHTUAFA**" **(*Steady State Heat Transfer from Unsymmetrical Annular Fin Array*)** which is written as a part of this study will be described in

this section. This program is designed to deal with the convection heat transfer from the fin array, the numerical optimization procedure (***Hooke*** and ***Jeeves*** method) and the finite element formulation.

The input data of the program consist of the number of fins (n_f =10), the number of divisions (elements) in *r*-direction (8 elements for each fin), the number of divisions (elements) in *z*-direction (4 elements for each fin), the inner diameter of tube (r_o=4 cm**)**, the outer diameter of tube (r_1=5 cm**)**, the height of the fin array (H=25 cm), the spacing between fins (2s) which represent a variable values as discussed in Chapter Five, the thermal conductivity (k=186 W/m.K, i.e. the cylinder is constructed of 2024-T6 aluminum alloy as taken by ***Incropera*** [2]), the convection heat transfer coefficient (*h*) is between the range of (10-500 W/m^2.K) hence the fins is cooled by air as discussed by ***Holman*** [3], the base temperature (Φ_b=1) and the environment temperature (Φ_f=0).

The outputs of "**SSHTUAFA"** are:

- Temperature profile of the fin array.
- Normalized heat transfer of the fin arrays.
- Effectiveness of the fin arrays.
- Optimum fins length.

The computer program "**SSHTUAFA"** consists of a main program and seven subroutines, which are coded in ***Quick Basic*** language by PC Pentium-III at 1000 MHz processor compatible computer with 128 MB Ram.

4.3.1 "SSHTUAFA" Program

The main properties of the present computer program will be summarized as follows:

4.3.1.1 Main Program

This part of the computer program controls the reading of the input data, calls different subroutines to perform the calculations and prints the output of the program.

The computational procedure is as follows:

1- The program calculates a number of nodes, elements and derivative boundary conditions.

2- It creates, initializes and solves the **(A)** vector. When using a vector storage, the nodal {**Φ**} are located at the top followed by {***f***} and then columns of [***K***].

3- It calls the different subroutines to perform the specific calculations such as "MESH", "ESMFV", "MSE", "DGSM", and "DGFSSE", which will be discussed briefly in the next section.

4- It calculates the temperature profile, normalized heat transfer and effectiveness of the fin arrays.

5- After all calculations mentioned above, the program computes the value of the objective function for each values of fin length and then repeats the steps (1 – 4) many times (depending on the input values of the fins lengths) to find the optimum effectiveness of the fin array, and the optimum fins length using ***Hooke*** and ***Jeeves*** numerical optimization method. "OFL" and "EXPLORATION" subroutines with the theory discussed in section (4.2.1) will do this optimization procedure.

6- It opens a data file to save the program results in each step of program calculations.

7- It prints the results for each step of calculations.

8- It is possible to repeat this procedure of calculations for another value of spacing between fins.

The flowchart of the main program of "**SSHTUAFA"** is shown in Figure (4-1).

4.3.1.2 Subroutines

The various subroutines in the program are described as follows: -

1- Subroutine "MESH"

Subroutine is used for generating the nodal coordinates, elements, the elements subjected to the boundary conditions by using the procedure discussed in Chapter Three, and then plotting the region depending on the ***r*** and ***z*** coordinates for each element.

2- Subroutine "ESMFV"

This subroutine evaluates the element stiffness matrix and force vector using equations (3.85) and (3.86).

3- Subroutine "MSE"

This subroutine incorporates the specific nodal values into the system of equations using the method of deletion of rows and columns (known values of temperature $\{\Phi\}$).

4- Subroutine "DGSM"

It decomposes the global stiffness matrix [***K***] into an upper triangular form using the method of Gaussian elimination. This subroutine assumes that [***K***] is symmetric and only those elements within the bandwidth and on or above the main diagonal are stored. The programming logic is not easy to follow because the coefficients of [***K***] are stored in a vector rather than a two-dimensional array.

5- Subroutine "DGFSSE"

The subroutine "DGFSSE" is a companion program to "DGSM". This subroutine decomposes the global force vector, {***f***}, and solves the system of equations using back substitutions.

6- Subroutine "OFL"

This subroutine finds the optimum fin length, which gives the maximum effectiveness of the fin array by using ***Hooke*** and ***Jeeves*** numerical optimization method. The procedure above will be repeated until reaching the optimum values.

7- Subroutine "EXPLORATION"

The subroutine **"EXPLORATION"** is a companion program to **" OFL"**. The purpose of this subroutine is to acquire knowledge about the local behavior of the objective function. This knowledge is used to find a likely direction for the pattern move by which it is hoped to obtain an even greater increment in the value of the objective function.

The procedures of subroutines "MESH", "ESF", "MSE", "DGSM", "DGFSSE", "OFL" and "EXPLORATION" are illustrated in the flowcharts listed below.

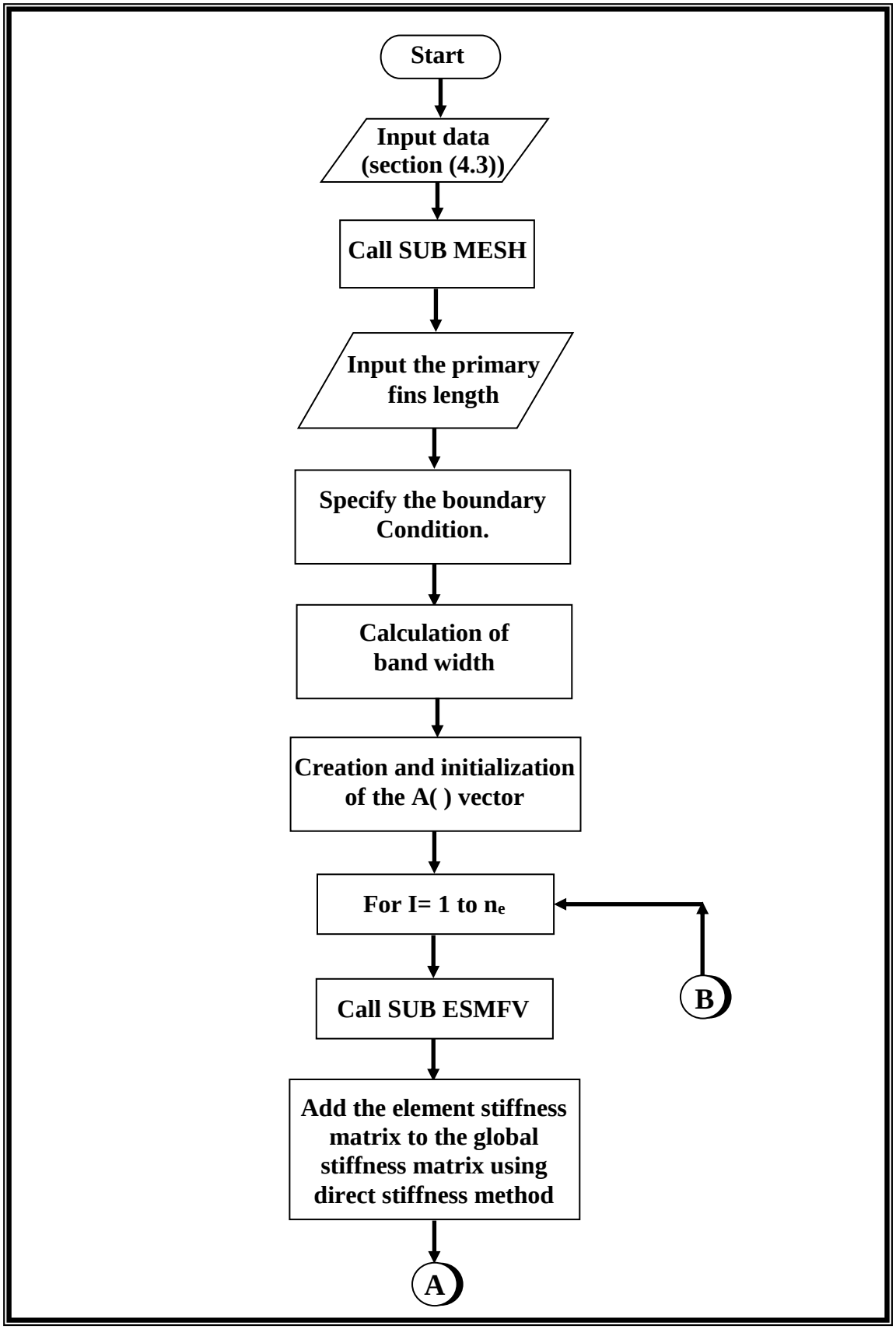

Figure (4-1) Schematic Flowchart of the Main Program.

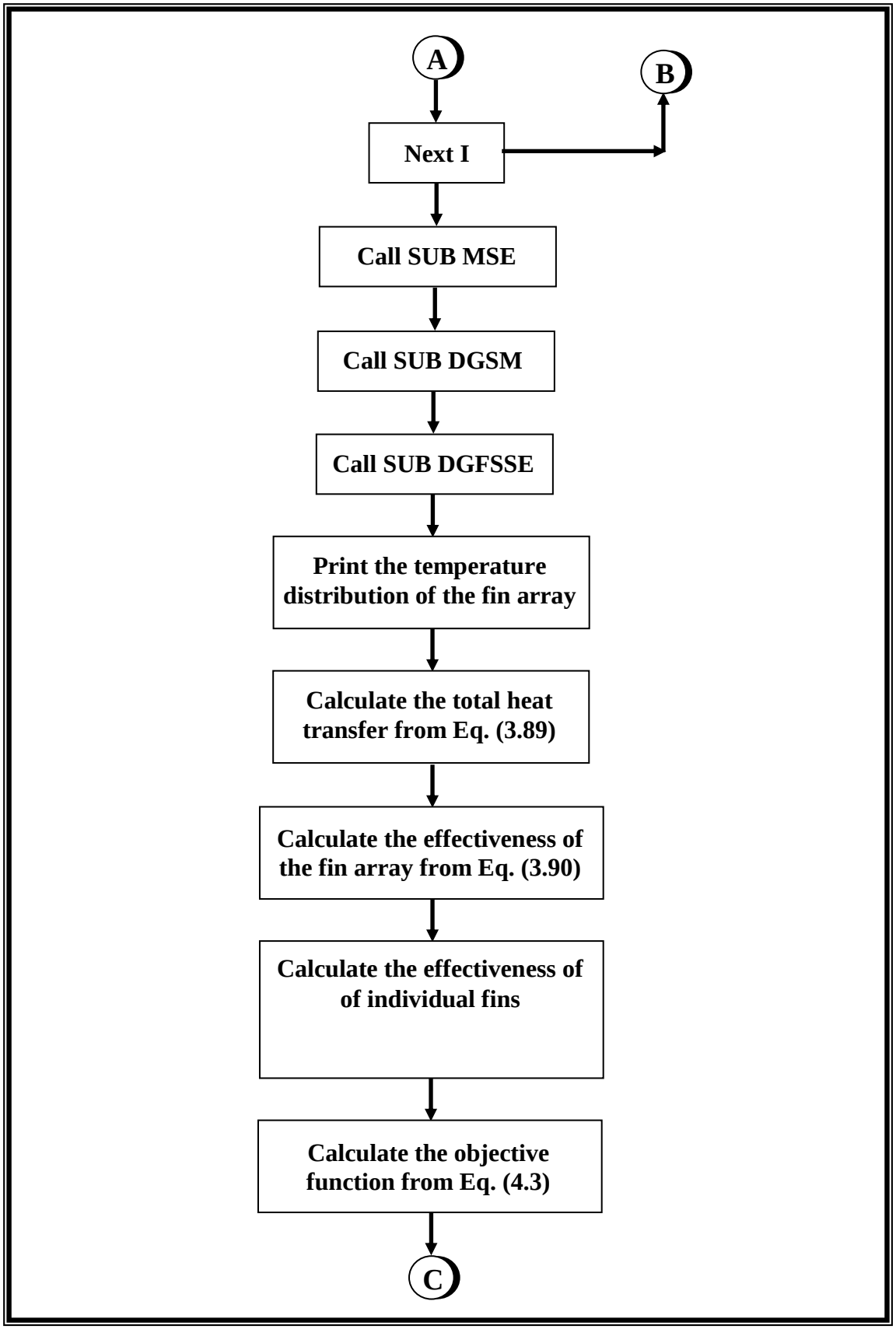

Figure (4-1) Continued.

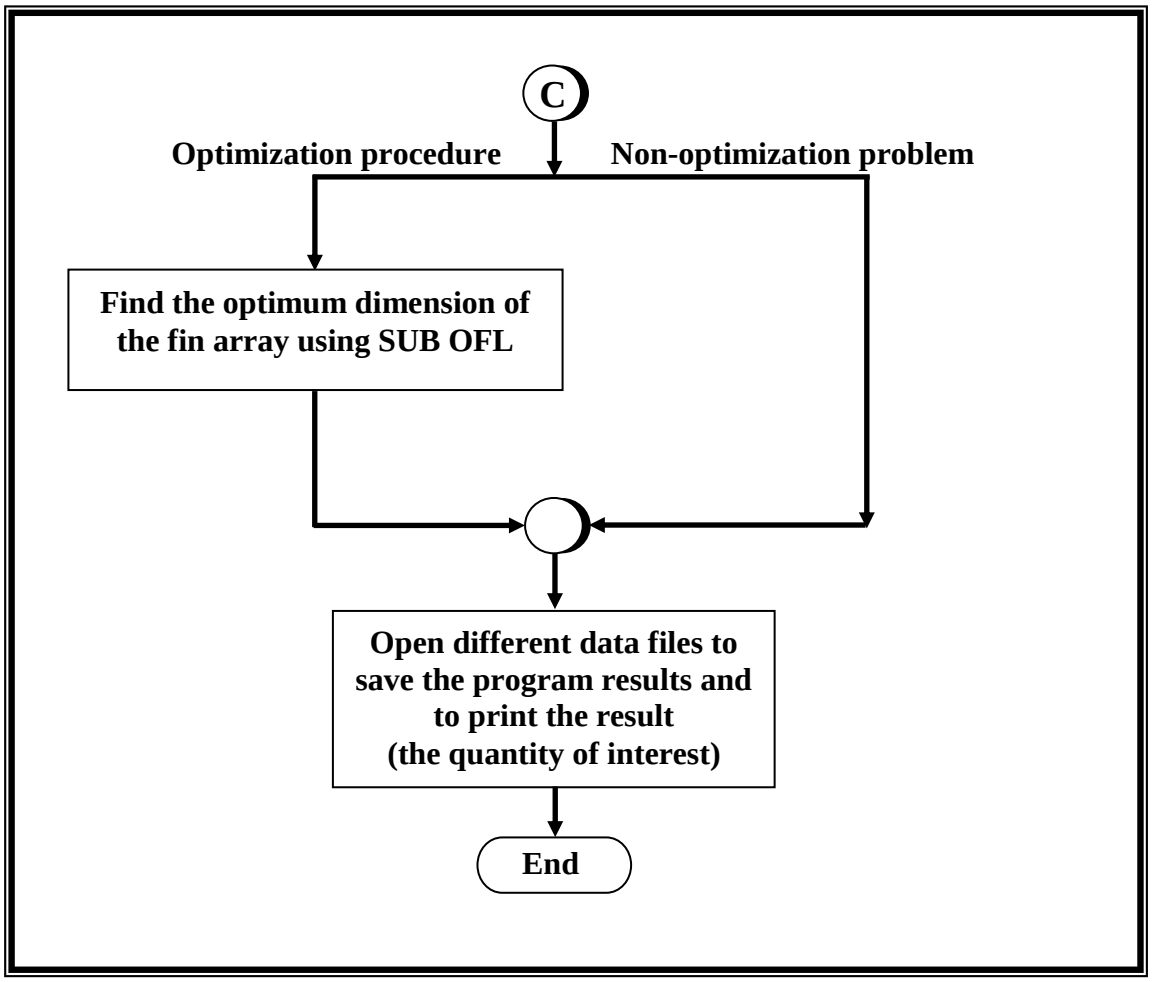

Figure (4-1) Continued.

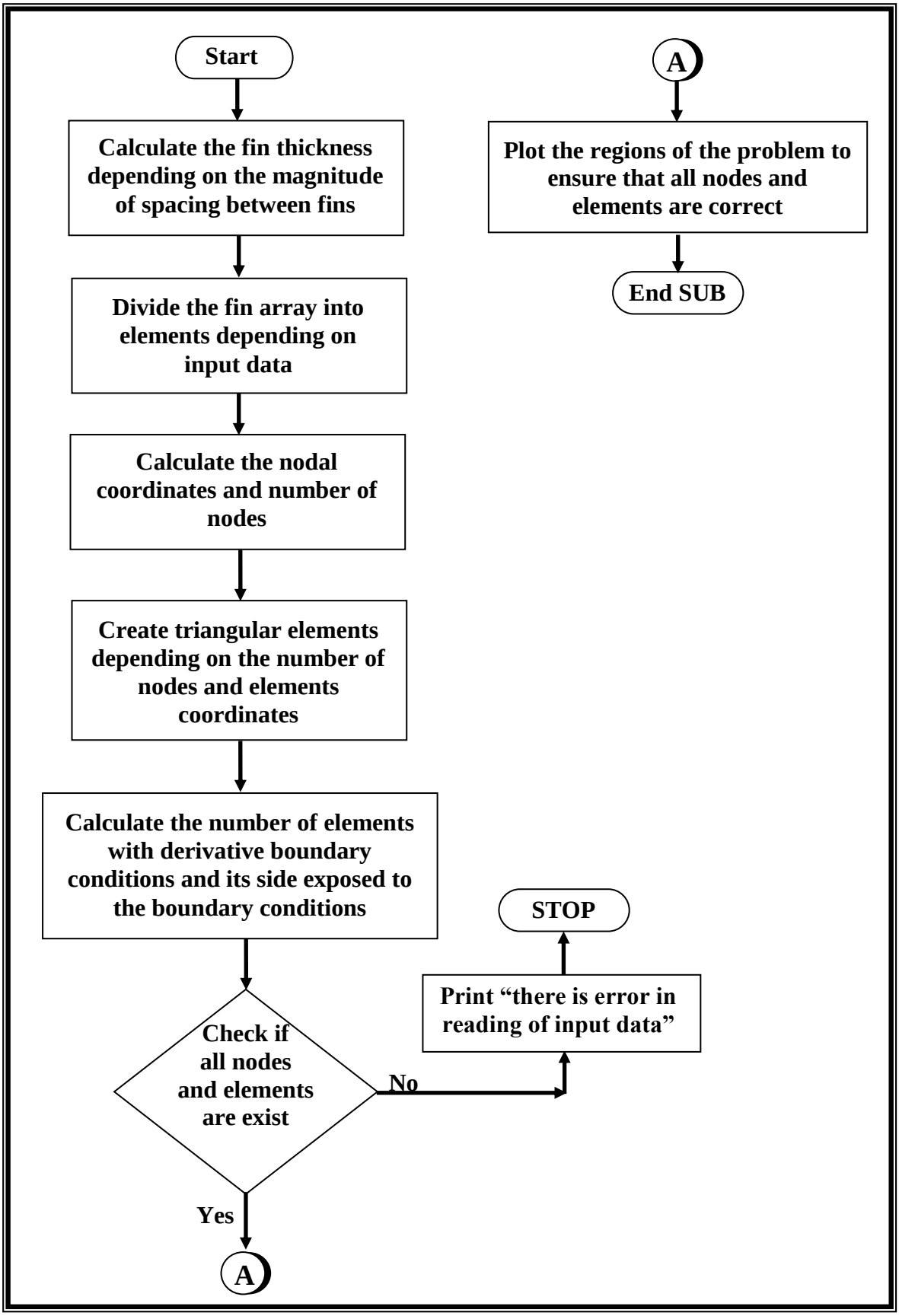

Figure (4-2) MESH SUB.

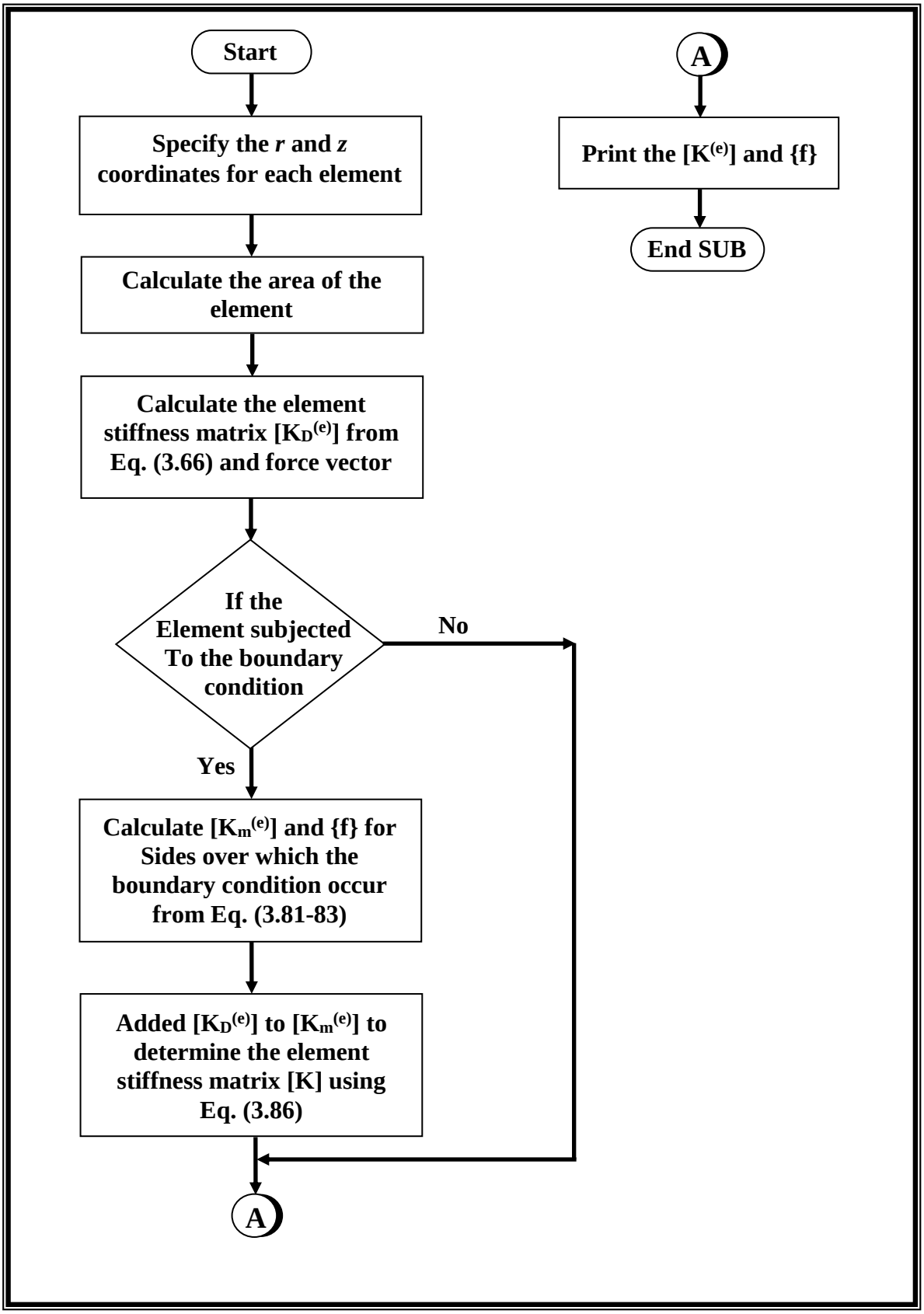

Figure (4-3) ESMFV SUB.

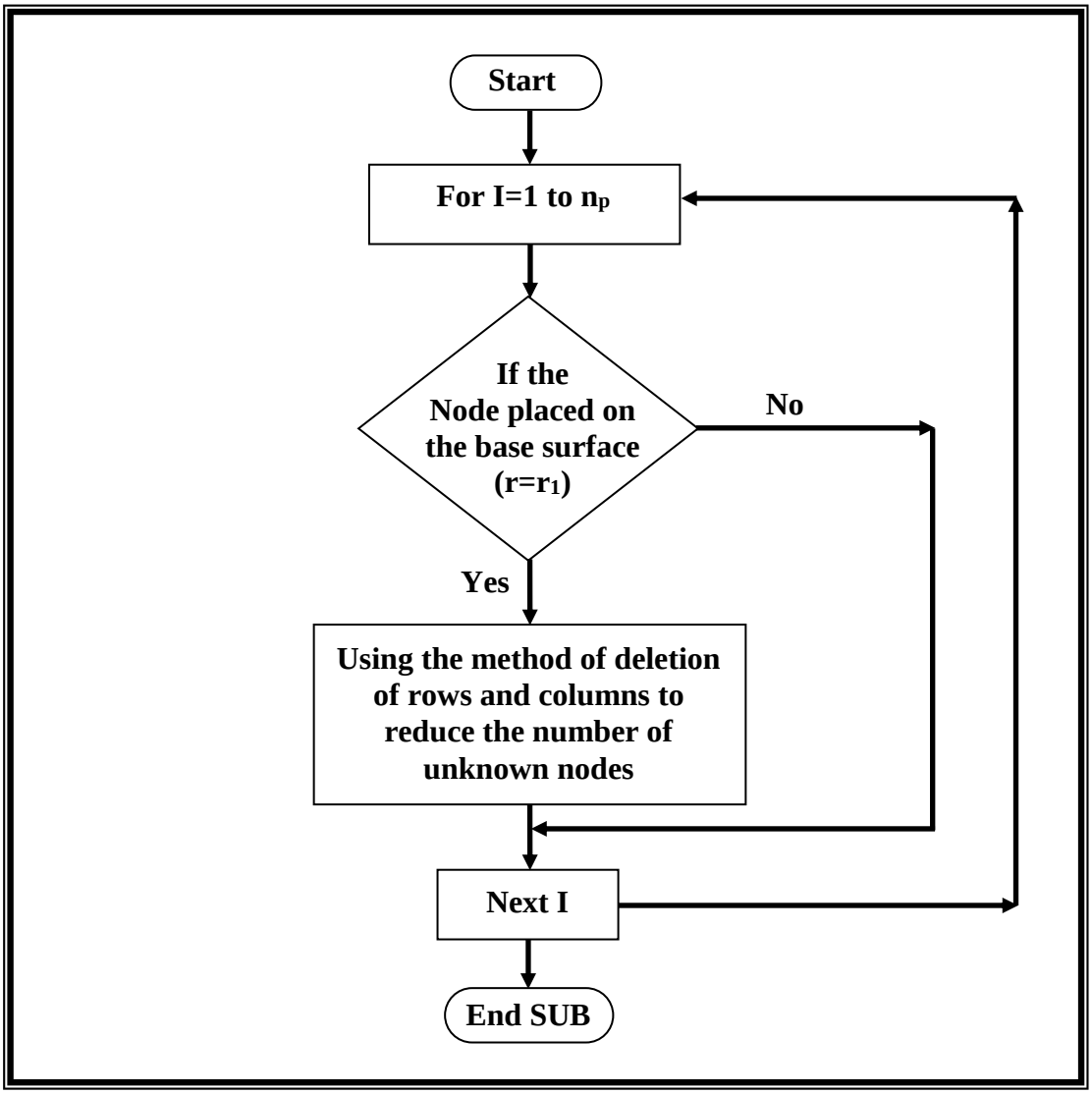

Figure (4-4) MSE SUB.

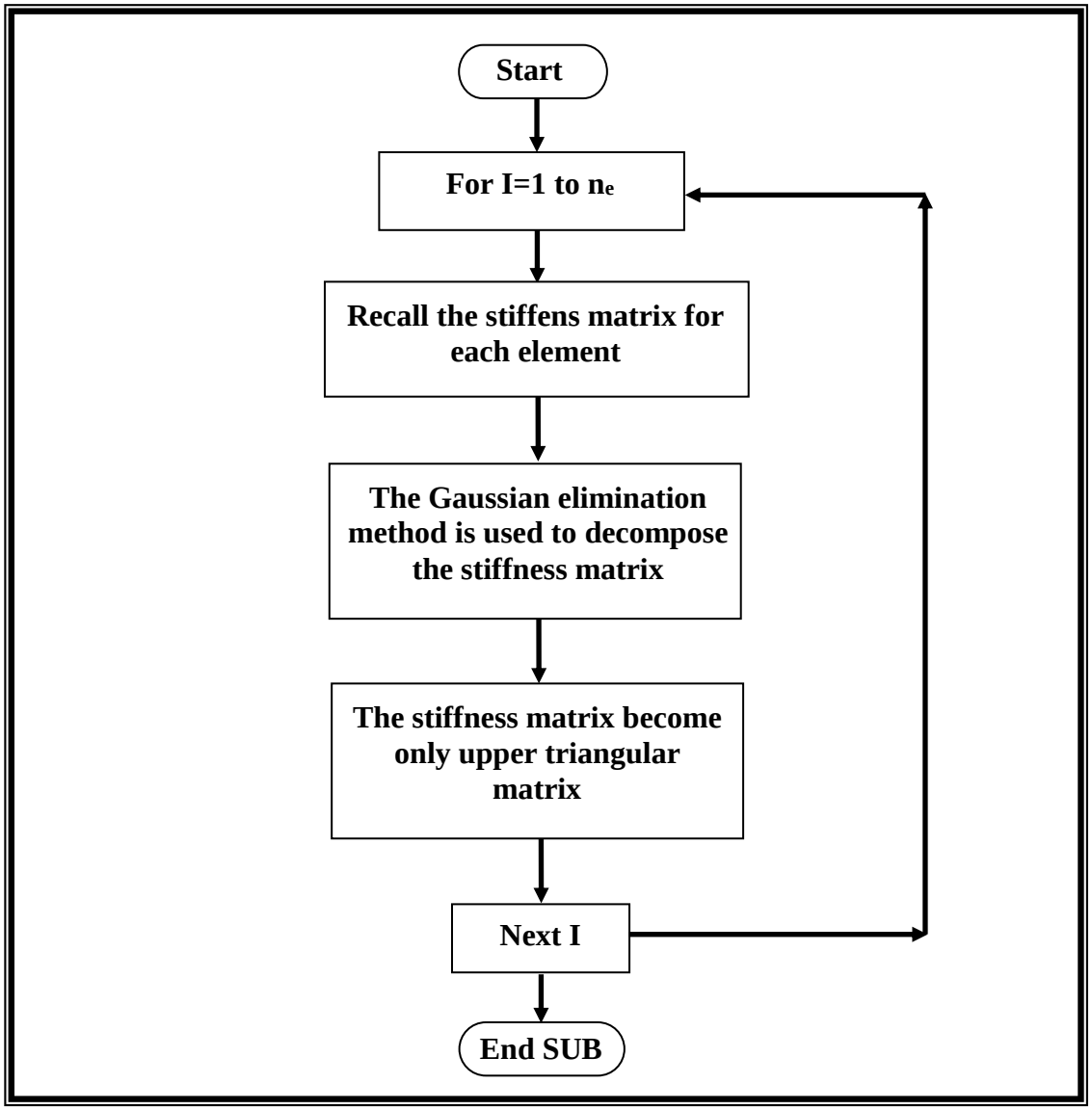

Figure (4-5) DGSM SUB.

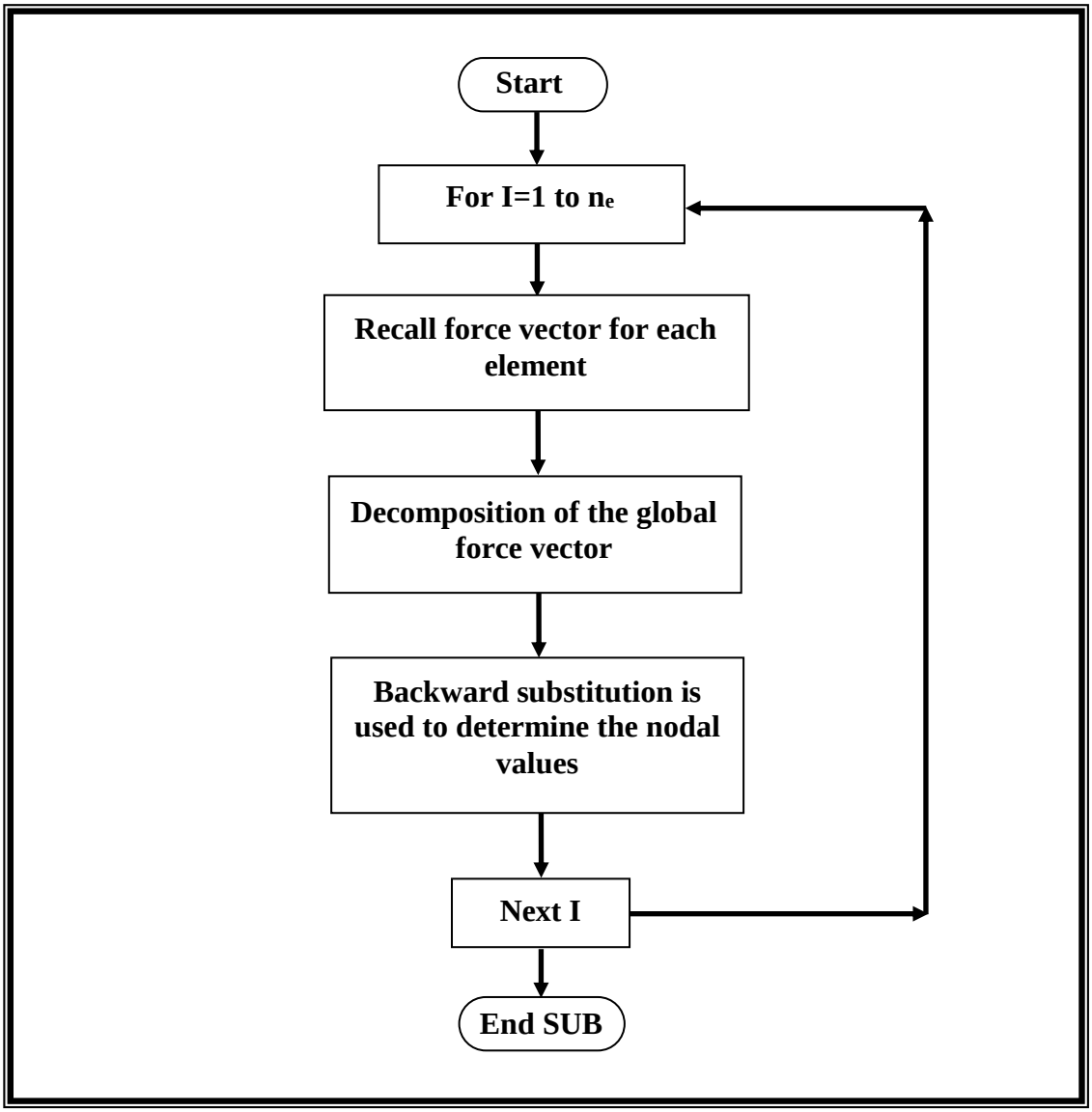

Figure (4-6) DGFSSE SUB.

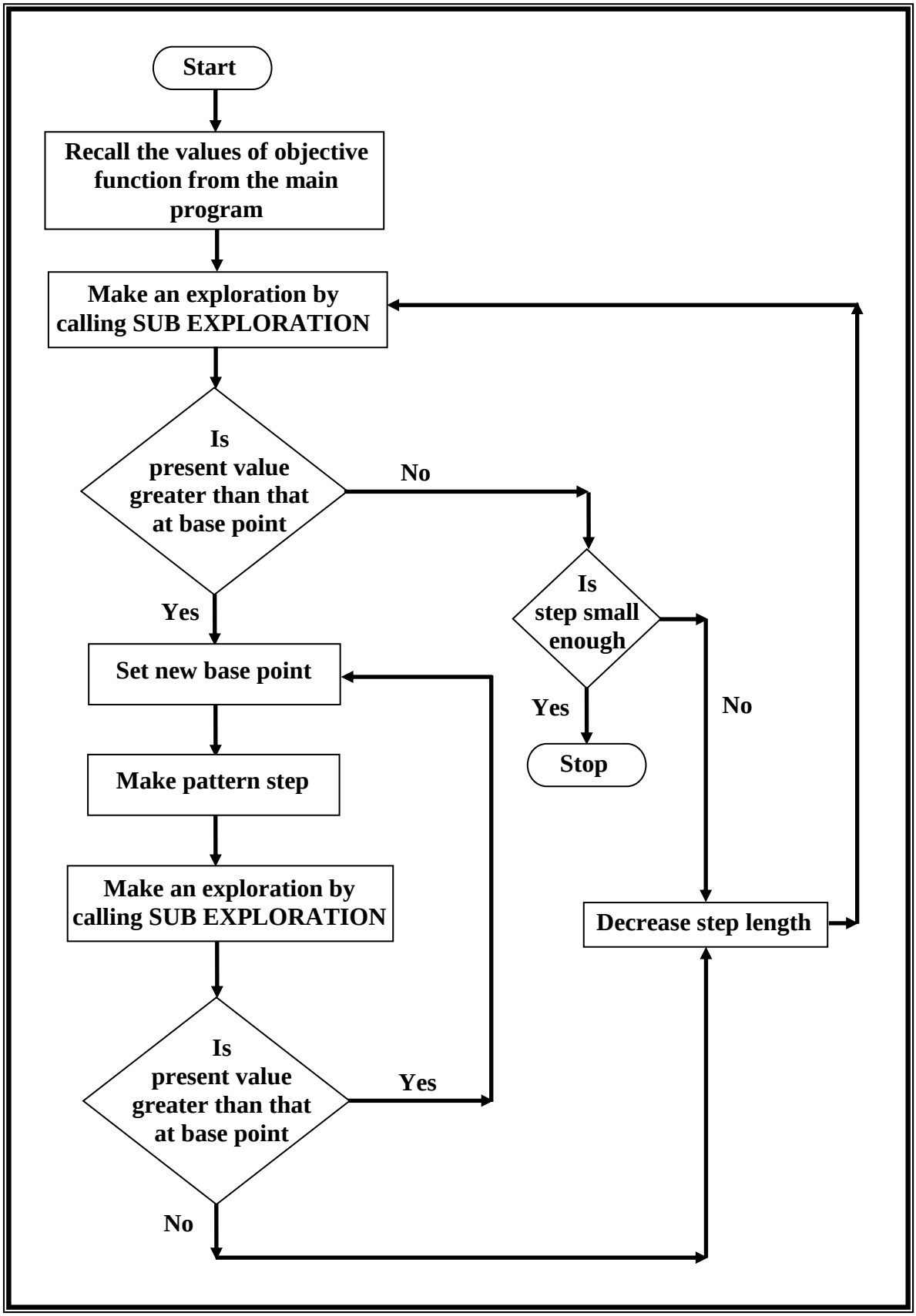

Figure (4-7) OFL SUB.

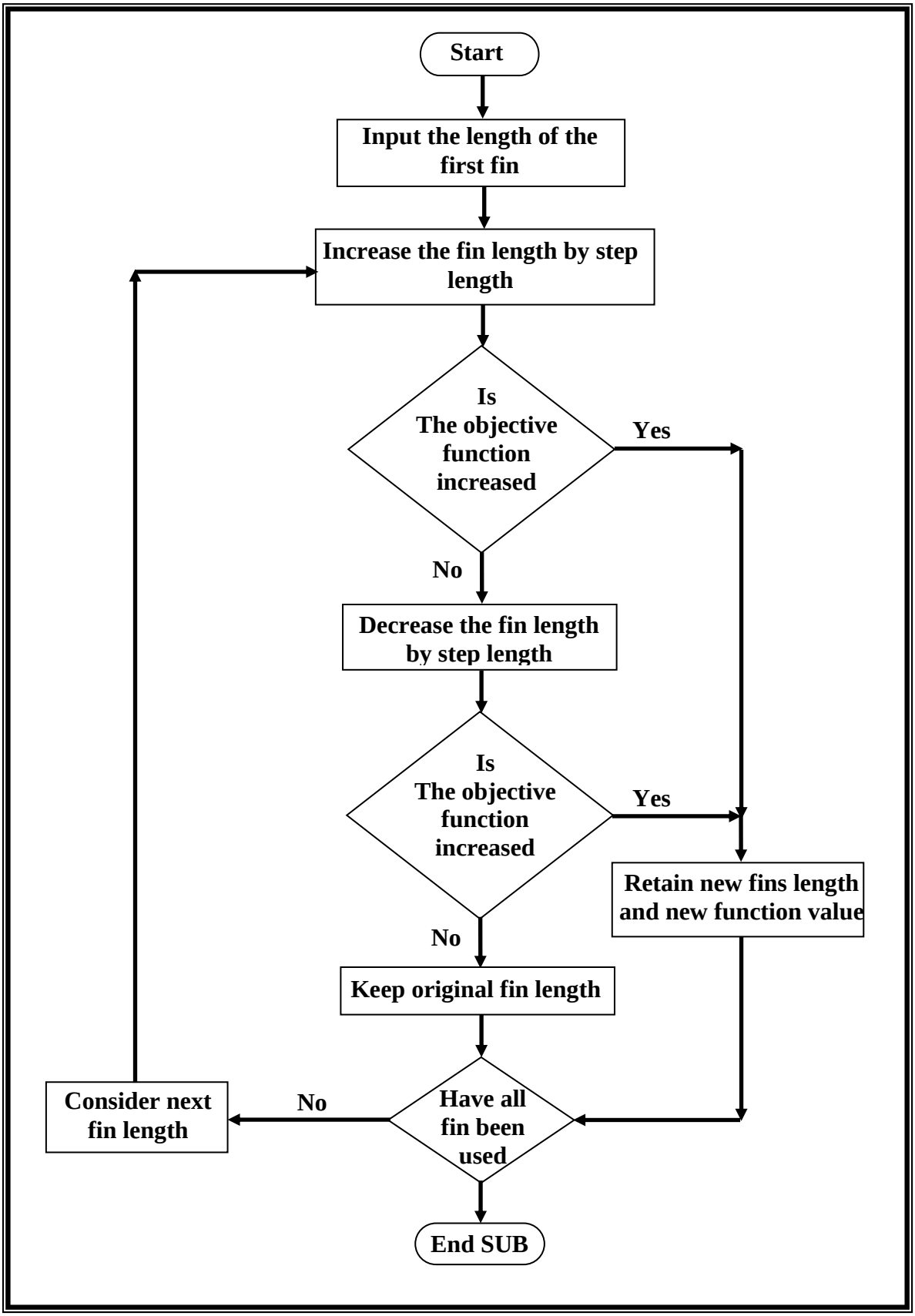

Figure (4-8) EXPLORATION SUB.

CHAPTER FIVE

5

RESULTS AND DISCUSSION

5.1 Introduction

The results of optimum fin length for rectangular annular fin array are presented and discussed in this chapter based on the finite element formulated for the analysis of steady state heat transfer of the annular fin array which are presented in Chapter Three and the aid of the optimization procedure and the computer program described in Chapter Four.

Hooke and Jeeves numerical optimization method is used to find the optimum fin length for two cases: First, single fin method (SFM) based on uniform fin length (equal fin length and equal spacing between fins); Second, fin array method (FAM) based on non-uniform fin length (non-equal fin length and equal spacing between fins).

At first, the designed computer program "**SSHTUAFA**" will be checked by comparing its numerical results with available analytical approaches of other investigators for single and array of annular fin with forced convection heat transfer.

5.2 Validity of the Present Work

In order to check the accuracy of the computer program designed for the model, the centerline temperature profiles of the present work have been compared to the two-dimensional centerline and one-dimensional profiles solved analytically by ***Look*** [30] with the following assumptions:

- Steady state heat transfer.
- Constant base temperature.
- Insulated tip assumption.
- Constant thermophysical properties (h, k).
- Single rectangular annular fin.

A good accuracy in the comparison was found as shown in Figure (5-1) for (Bi=0.05) and Figure (5-2) for (Bi=1). Isothermal contour maps are sketched for the present work for two values of Biot number (0.05) and (1) as shown in figures (5-3) and (5-4) respectively. It is easily seen that as Biot increases, the fin becomes unnecessarily long, hence there is a waste of material. For the above reason, this work was done as an attempt to reduce the waste material to its minimum value.

To check the calculations of heat transfer from the fin array, the effectiveness of single fin solved using the present analysis was compared with the effectiveness of single fin solved analytically in 1-D and 2-D analyses by ***Look*** [30] for different Biot number with the same assumptions mentioned above. Figure (5-5) gives a good agreement obtained in calculating the heat loss form the fin.

Also, in order to check the validity of optimization procedure of the present work, a comparison was made between the optimum fin length of the fin array obtained by the present work (2-D) and the optimum fin length of the same fin array solved analytically by ***Al-Hattab*** [70] (1-D), both with constant base temperature. Figure (5-6) illustrates a good agreement obtained in calculating the optimum fin length.

5.3 Single Fin Effectiveness

Before the discussion of the new approach for the fin array effectiveness, let us illustrate how the base temperature affects single fin effectiveness and its optimum values. In order to demonstrate the existence of the optimum effectiveness of the fin per volume of the fin, consider parameter (Γ=0.2).

Figure (5-7) shows the values of (ε_{fa}/β) for different values of Biot number. In this figure the calculation of the fin heat transfer was considered under the assumption of constant base temperature; the temperature of the outer surface of the pipe (θ_b) remains constant before and after the attachment of the fin at the pipe surface. As shown in Figure (5-7), the effectiveness have optimum (maximum) values at certain values of β. These optimum values increase as Biot number increases.

The fact that the surface temperature of the pipe will be changed after the insertion of the fin is considered for the calculation for fin effectiveness as shown in Figure (5-8).

The results indicate that even though the behavior of (ε_{fa}/β) versus β for different values of Biot number in this case (sinusoidal base temperature) is identical to the former case (constant base temperature assumption), the optimum values of (ε_{fa}/β) and the corresponding optimum β are always less than in the first case. This means that the heat removed and so the effectiveness of the fin decreases due to decreasing the surface temperature after the attachment of the fin.

5.4 Optimum Fin Length Profile

Two methods of calculation were used in this work to determine the optimum fin array effectiveness. In the first method, Single Fin Method (SFM), all fins have the same length which was determine based on the optimization of quantity of heat removed from a single fin per the volume of the fins using equation (4.3) with constant base temperature. In the second method, Fin Array Method (FAM), the effectiveness was determined as in the former method except that it was calculated according to the non-constant base temperature profile (sinusoidal base temparature as in equation (3.8)).

Figure (5-9) shows the optimum fin length profile of the array using SFM and FAM methods for Bi=0.01 and Γ=0.2. It was found that the length of the fins, in the case of FAM, have the lower values near the cold end of the array (z=0) where the length reaches about (0.63) of the length of the fin determined based on the single fin method **(**SFM). Then, the length of the fins in the case of FAM increases towards the hot end of the array (z=H) where the length reaches about (1.13) times the length of the fin determined based on the single fin method (SFM). It was noted that the fifth fin has approximately the same length in the case of SFM. The total length of ten fins in the case of the SFM was higher than that in the case of FAM.

Figure (5-10) shows the optimum fin length profile of the array using SFM and FAM methods for Bi=0.025 and Γ=0.2. It was found that the length of the fins, in the case of FAM, have the lower values near the cold end of the array (z=0) where the length reaches about (0.746) of the length of the fin determined based on single fin method **(**SFM). Then, the length of the fins, in the case of FAM, increases towards the hot end of the array (z=H) where the length reaches about (1.1) times the length of the fin determined based on the single fin method (SFM). It was noted that the fifth fin has approximately the same length in the

case of SFM. The total length of ten fins in case of the SFM was higher than that in the case of FAM.

Figure (5-11) shows the optimum fin length profile of the array using SFM and FAM methods for *Bi*=0.05 and Γ=0.2. It was found that the length of the fins, in the case of FAM, have the lower values near the cold end of the array (z=0) where the length reaches about (0.835) of the length of the fin determined based on single fin method (SFM). Then, the length of the fins, in the case of FAM, increases towards the hot end of the array (z=H) where the length reaches about (1.1) times the length of the fin determined based on the single fin method (SFM). It was noted that the fifth fin has approximately the same length in the case of SFM. The total length of ten fins in case of the SFM was higher than that in the case of FAM.

Figure (5-12) shows the optimum fin length profile of the array using SFM and FAM methods for *Bi*=0.075 and Γ=0.2. It was found that the length of the fins, in the case of FAM, have the lower values near the cold end of the array (z=0) where the length reaches about (0.853) of the length of the fin determined based on single fin method (SFM). Then, the length of the fins, in the case of FAM, increases towards the hot end of the array (z=H) where the length reaches about (1.05) times the length of the fin determined based on the single fin method (SFM). It was noted that the fifth fin has approximately the same length in the case of SFM. The total length of ten fins in case of the SFM was higher than that in the case of FAM.

Figure (5-13) shows the optimum fin length profile of the array using SFM and FAM methods for *Bi*=0.1 and Γ=0.2. It was found that the length of the fins, in the case of FAM, have the lower values near the cold end of the array (z=0) where the length reaches about (0.88) of the length of the fin determined based on single fin method (SFM). Then, the length of the fins, in the case of FAM, increases towards the hot end of the array (z=H) where the length reaches about

(1.05) times the length of the fin determined based on the single fin method (SFM). It was noted that the fifth fin has approximately the same length in the case of SFM. The total length of ten fins in case of the SFM was higher than that in the case of FAM.

Figure (5-14) shows the optimum fin length profile of the array using SFM and FAM methods for *Bi*=0.15 and Γ=0.2. It was found that the length of the fins, in the case of FAM, have the lower values near the cold end of the array (z=0) where the length reaches about (0.91) of the length of the fin determined based on single fin method (SFM). Then, the length of the fins, in the case of FAM, increases towards the hot end of the array (z=H) where the length reaches about (1.027) times the length of the fin determined based on the single fin method (SFM). It was noted that the fifth fin has approximately the same length in the case of SFM. The total length of ten fins in case of the SFM was higher than that in the case of FAM.

It is concluded from Figures (5-9) to (5-14) that as Biot number increases, other parameters remain constants, the length of each fin in the array decreases and so decreases the fin effectiveness.

5.5 Optimum Calculations of the Fin Array

Figure (5-15) illustrates a comparison between the amount of the total heat removed from the fin array (Q_t) versus Biot number at the optimum dimension (length) based on the optimization criteria discussed in Chapter Four using the two methods: SFM and FAM with Γ=0.2. At Biot number less than (0.095), the values of (Q_t) in the case of SFM are slightly higher than in the case of FAM. For Biot number greater than (0.095), the amounts of heat removed from the fin array (Q_t) are identical in the two cases.

The total length of the fin array (L_t) determined at the optimum effectiveness conditions is plotted in Figure (5-16) with Γ=0.2. It was found that, at any value of Biot number, the values of (L_t) in case of FAM are less than the values of (L_t) in the case of SFM. Also, it was found that as Biot number increases the total length of the fin decreases.

Figure (5-17) shows the more interested results of the optimum values of effectiveness ($\varepsilon_{fopt.}$) with Γ=0.2. It was found that the optimum values of the effectiveness in the case of FAM were always higher than the optimum values in the case of SFM. It was shown that for Biot number less than (0.025), the values of ($\varepsilon_{fopt.}$) were almost constant, whereas for Biot number increases beyond this value, a sharp increase in the values of ($\varepsilon_{fopt.}$) was found. This is generally due to the sharp decrease of the total fin length (L_t) in both cases SFM and FAM.

It was found that increasing Biot number would decrease the values of Q_t and L_t.

5.6 Effect of Base Temperature Profile

In order to investigate the effect of the base temperature profile on the heat transfer and the fin length profiles of the array and so the fin array effectiveness and its optimum values; another profile of base temperature was used in this work. The following linear profile is considered with its parameter values (b_t=1):

$$\Phi_b = 1 + b_t \frac{z}{H} \qquad \textbf{….(5.1)}$$

Figure (5-18) shows the profile of fin lengths and its base temperature profile for the two cases (linear and sinusoidal) after re-scaled their values using the following factor:

$$X'_j = \frac{X_j - X_{\min}}{X_{\max} - X_{\min}} \qquad \textbf{….(5.2)}$$

where (X) represents either β_j or Φ_b(j).

The results indicated that the length profile is always different from the base temperature profile. The temperature profiles are most convex than the fin length profile. Also, it was shown that the fin length profiles were approximately identical for both base temperature profiles. It was noted that the mass of array (calculated as L_t) for the case of linear profile is less than for the sinusoidal one.

Figure (5-19) shows the optimum values of the total fins length for the two profiles (linear and sinusoidal) with Γ=0.2 as a function of Biot number (Bi). It was shown that the total fin length was approximately the same for the two cases (linear and sinusoidal) with different values of Biot number (Bi). In general, the total fin length (L_t) decreases when Biot number (Bi) increase.

Figure (5-20) shows the relation between the total heat removed (Q_t) versus Biot number (Bi) with Γ=0.2 for the two cases linear and sinusoidal base temperature profiles. This figure shows that the total heat removed (Q_t) in case of sinusoidal profile is always higher than for the linear profile for different vales Biot number (Bi).

The values of optimum fin array effectiveness per the volume of the array itself ($\varepsilon_{fopt.}$) were shown in figure (5-21) with Γ=0.2. It was found that the values of the effectiveness corresponding to linear profile were always higher than for sinusoidal one.

5.7 Effect of Γ Parameter

Thickness of each fin in the array is an important parameter that affects the fin array effectiveness and its optimum values. For this reason, the total fins length, the total heat removed for the fin array and the optimum fin array effectiveness were plotted for different fins thickness (Γ) with two base temperature profiles (linear and sinusoidal). Recall the definition: ($\Gamma = \frac{\delta}{r_1}$), keeping (r_1) constant and varying the magnitude of half thickness of the fins (δ).

This will lead to varying the spacing between fins. In general increasing (Γ) will increase the value of (δ) and the vice versa.

Optimum values of the total fins length for different values of fins thickness as a function of Biot number (*Bi*) were plotted in figure (5-22) for linear base temperature profile and figure (5-23) for sinusoidal one. It was shown that the total fins length decreases as the Biot increase and approximately the same for the two cases (linear and sinusoidal). In general, increasing the vales of fins thickness or (Γ) will increase the total fin length.

Figures (5-24) and (5-25) show the relation between the total heat removed (Q_t) versus the Biot number (*Bi*) for different fins thickness with linear and sinusoidal base temperature profiles respectively. It was found that as fins thickness or (Γ) increase, the total heat removed increases. In general (Q_t) decrease as Biot number increase for any (Γ). This is due to the sharp decreasing of (L_t) as the Biot increase.

The optimum fin array effectiveness per the volume of the array for different fins thickness and two base temperature profiles (linear and sinusoidal respectively) was shown in figures (5-26) and (5-27). It was concluded that as fins thickness or (Γ) increase, the optimum effectiveness decrease.

For clear representation of the fin array effectiveness per the volume of the array for different values of fins thickness and base temperature profiles, figure (5-28) was plotted. This figure shows the effect of the Biot number (*Bi*), fins thickness and the base temperature profiles on the fin array effectiveness.

In order to investigate the effect of number of fins, figures (5-29) and (5-30) were plotted. Keeping fins thickness (δ) or (Γ) and the height of engine wall (H) constant, the increase in fin number will reduce the spacing between fins.

Figure (5-29) shows the optimum values of the total fins length as a function of Biot number (*Bi*) for sinusoidal base temperature with Γ=0.2 and different number of fins. In general, increasing the number of fins will increase the optimum values of total fins length at any Biot number (*Bi*).

Figure (5-30) shows the relation between the total heat removed (Q_t) versus Biot number (*Bi*) with Γ=0.2 and sinusoidal base temperature and different number of fins. It was shown that increasing number of fins would increase the optimum total heat removed from the fin array at any Biot number (*Bi*). This is due to the increase in the convecting area with the increase of fins number.

CHAPTER SIX

6

CONCLUSIONS AND SUGGESTIONS

6.1 Conclusions

Based on the results obtained from the computer program, which is presented in Chapter Four, and the discussions of the results in Chapter Five, the following conclusions can be drawn:

1- Taken into account the change of the base temperature due to the existence of a fin, the effectiveness and the optimum dimension (length) of the fin are less than in the case of constant base temperature assumption. This means that the heat removed and so the effectiveness of the fin decreases due to decreasing the surface temperature after the attachment of the fin.

2- The profile of the fin length of the array in general depends on the profile of root temperature at the wall of the pipe. It was also noted that the mass of the array (calculated as L_t) for the case of linear profile was less than for the sinusoidal one.

3- The design procedure based on the fin array method (FAM) of optimization produces higher effectiveness and heat removed for the same amount of materials (calculated as L_t).

4- The optimum values of the total heat removed (Q_t) in the case of sinusoidal base temperature were higher than in the case of linear one, whereas the optimum (L_t) was approximately the same. Even though, for small values of Biot number the optimum effectiveness (ε_{fopt}) has the same values in both cases except for Biot number greater than 0.075.

5- As Biot number increases, other parameters remain constant, the length of the fin array decreases.

6- It is found that increasing the Biot number will decrease the values of the total heat removed (Q_t) and total fins length (L_t).

7- As Γ decrease, the total fins length (L_t) and the total heat removed from the fin array (Q_t) decrease while the optimum effectiveness (ε_{fopt}) increase.

6.2 Suggestions for Further Work

The following recommendations are suggested for further work:

1- Three-dimensional analysis could be investigated.

2- Other fins profile can be solved using this analysis such as parabolic, hyperbolic and triangular profiles.

3- Using the same analysis to find the optimum spacing between fins with a new objective function including the effects of fin length and the spacing between fins on the fin array effectiveness.

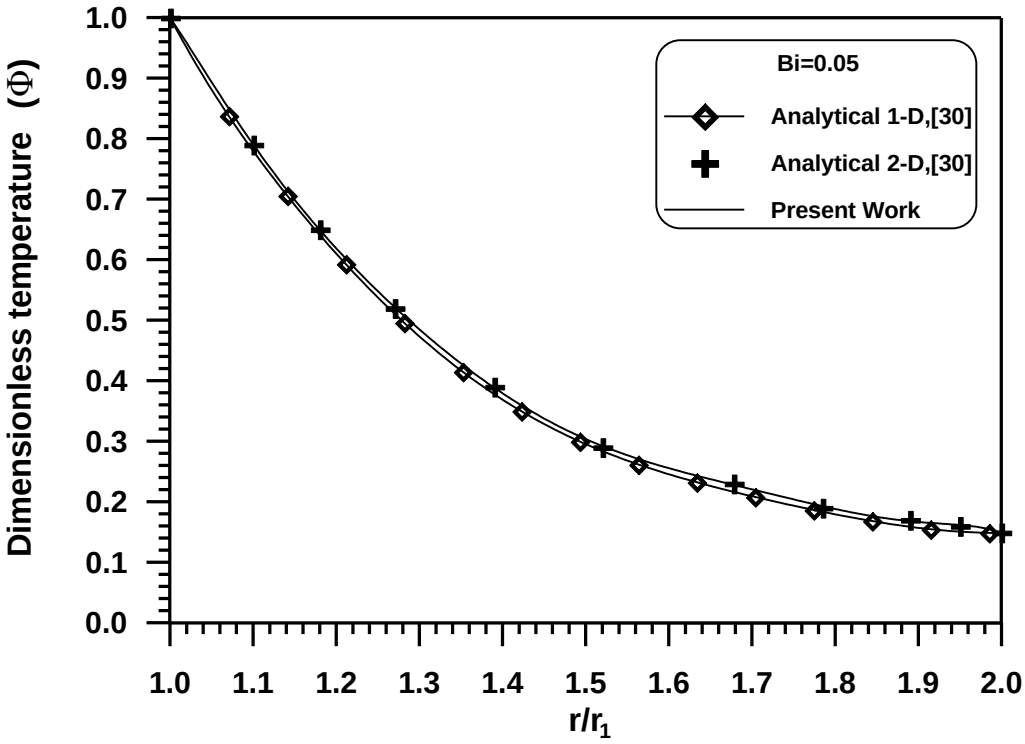

Figure (5-1) A Comparison of 1-D and Centerline 2-D Non-dimensional Temperature for Bi=0.05.

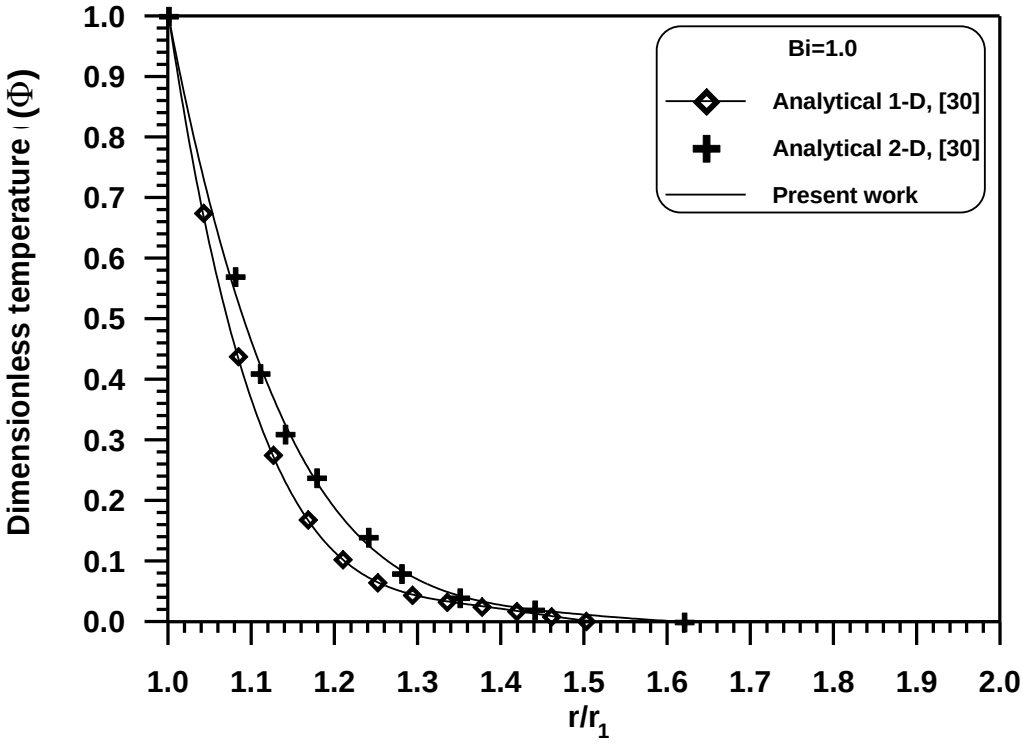

Figure (5-2) Comparison of 1-D and Centerline 2-D Non-dimensional Temperature for Bi=0.1.

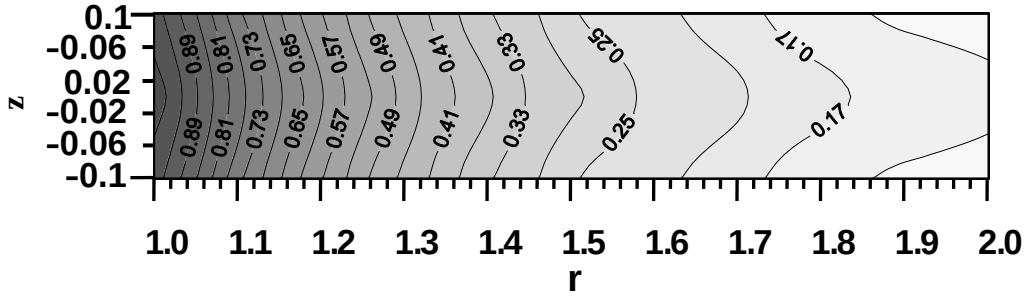

Figure (5-3) Isothermal Contour Map (Variation with Z) Superposed on the Fin Geometry of Ref. [30] for Bi= 0.05.

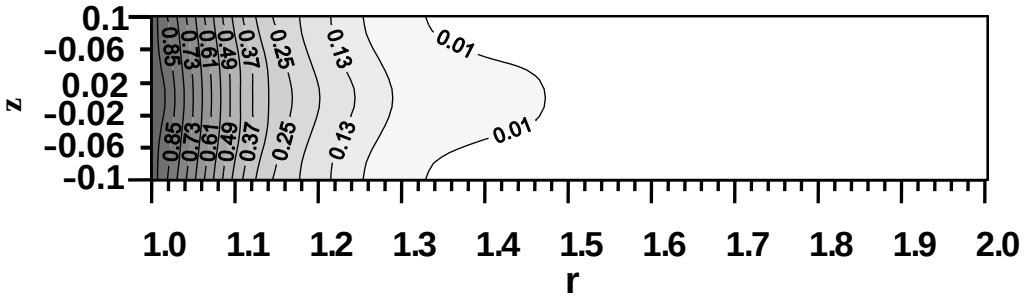

Figure (5-4) Isothermal Contour Map (Variation with Z) Superposed on the Fin Geometry of Ref. [30] for Bi= 1.

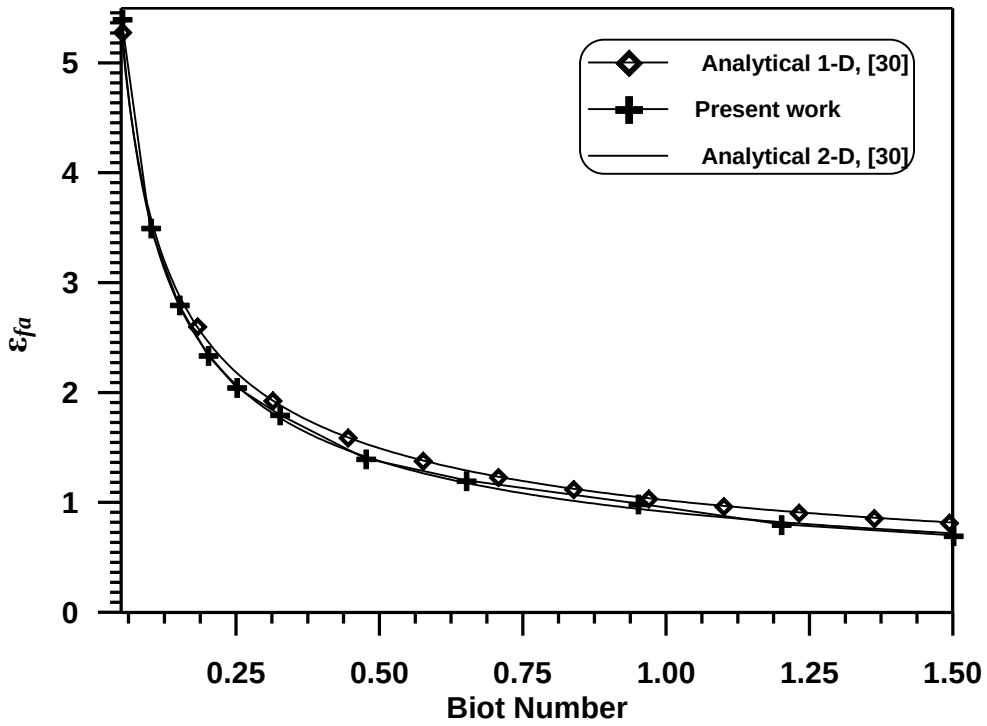

Figure (5-5) Comparison of the Effectiveness between the Present Study and An Analytical Solution for Single Fin.

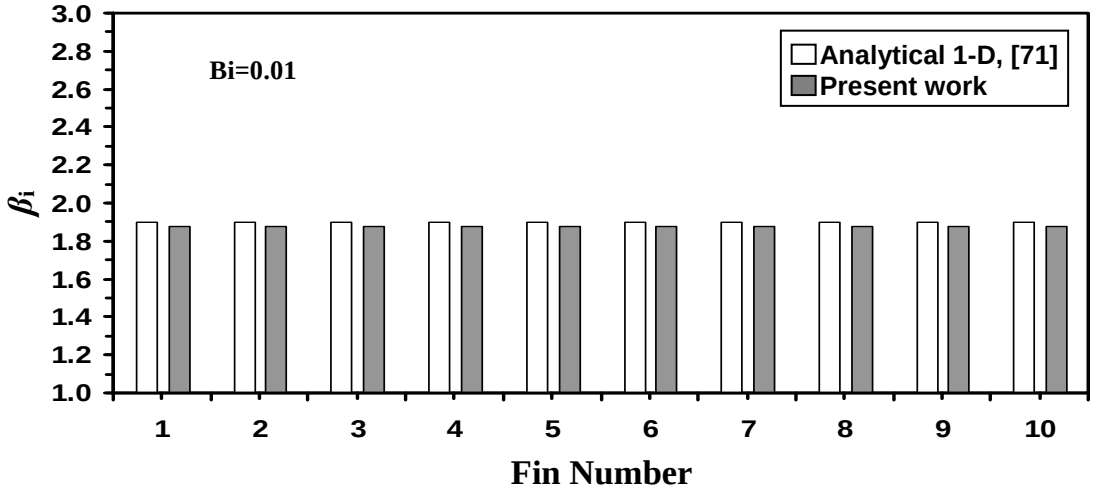

Figure (5-6) Comparison between the Optimum Dimensions (Fin Length) of 1-D, Ref. [71] and 2-D (Present Work) for Constant Base Temperature.

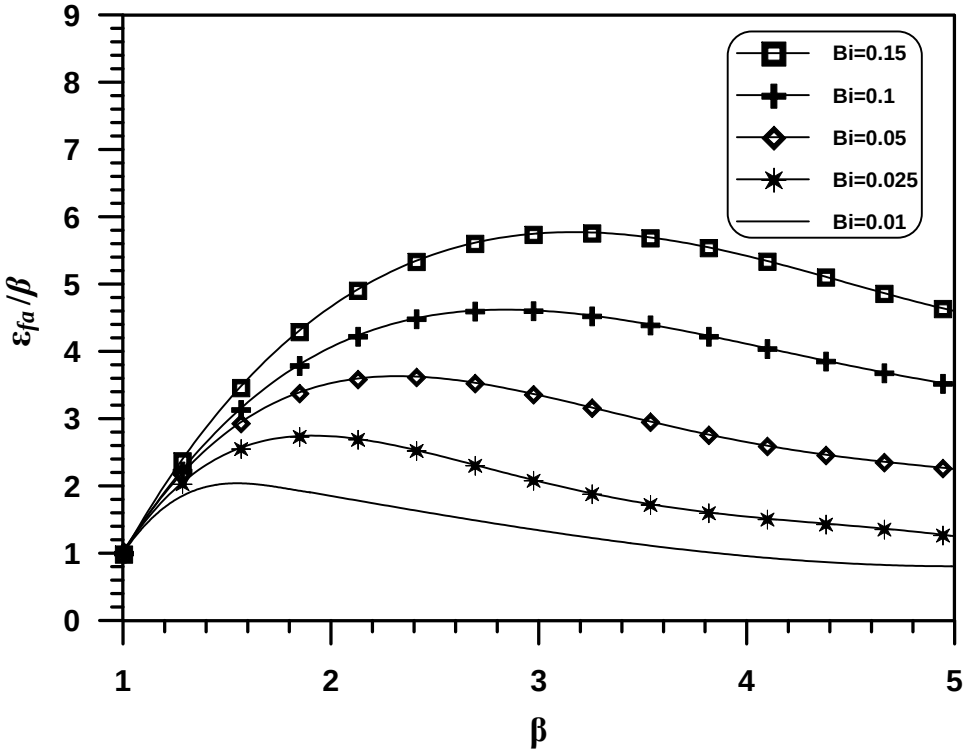

Figure (5-7) Optimum Effectiveness per Fin Volume (ε_{fa}/β) Based on Constant Base Temperature.

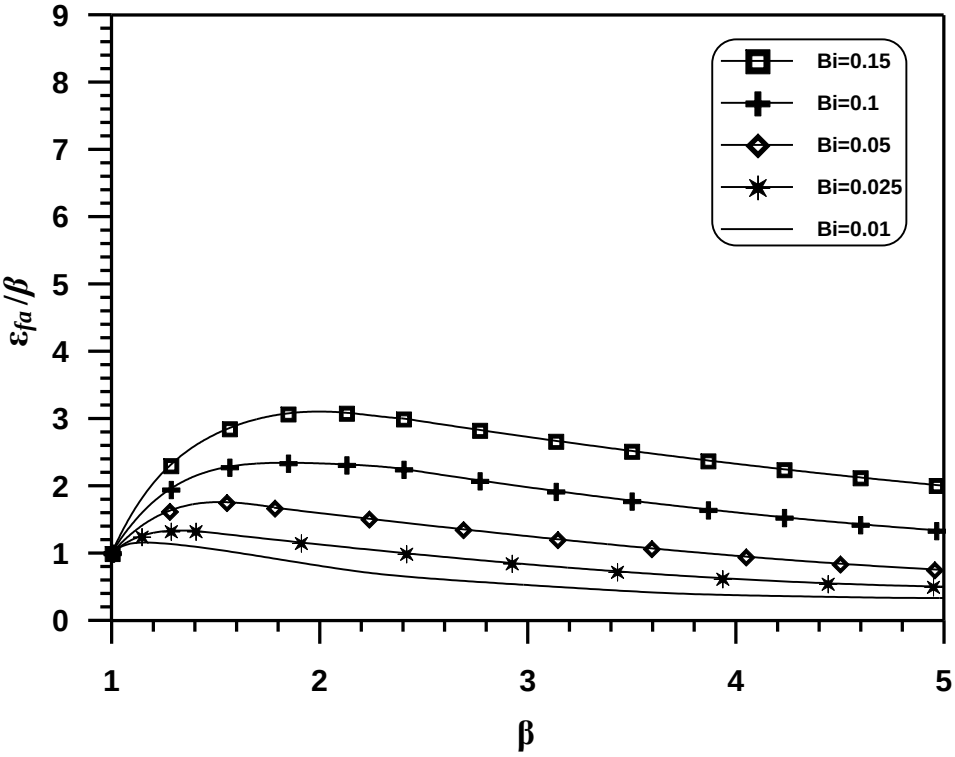

Figure (5-8) Optimum effectiveness per Fin Volume (ε_{fa}/β) Based on Non-constant Base Temperature.

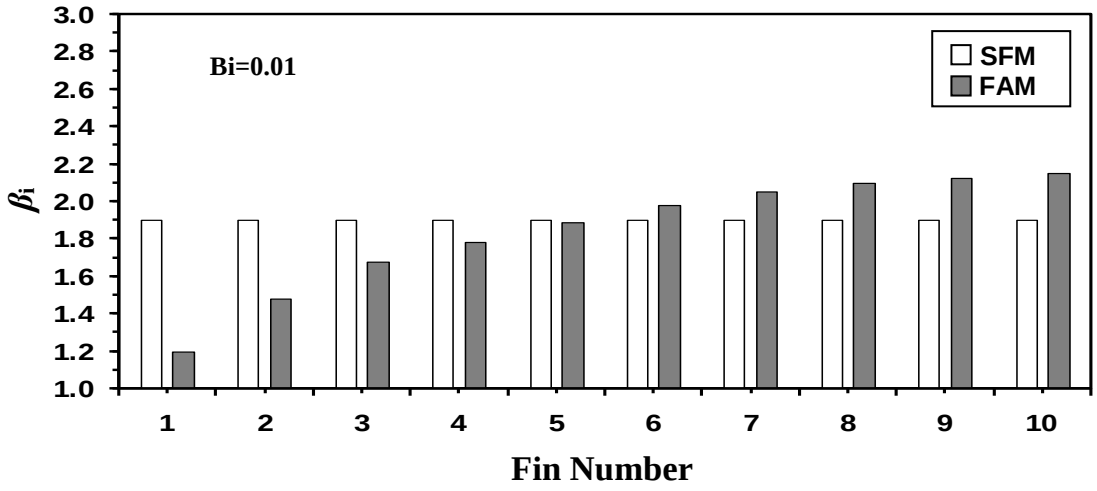

Figure (5-9) Optimum Fin Length for Bi=0.01.

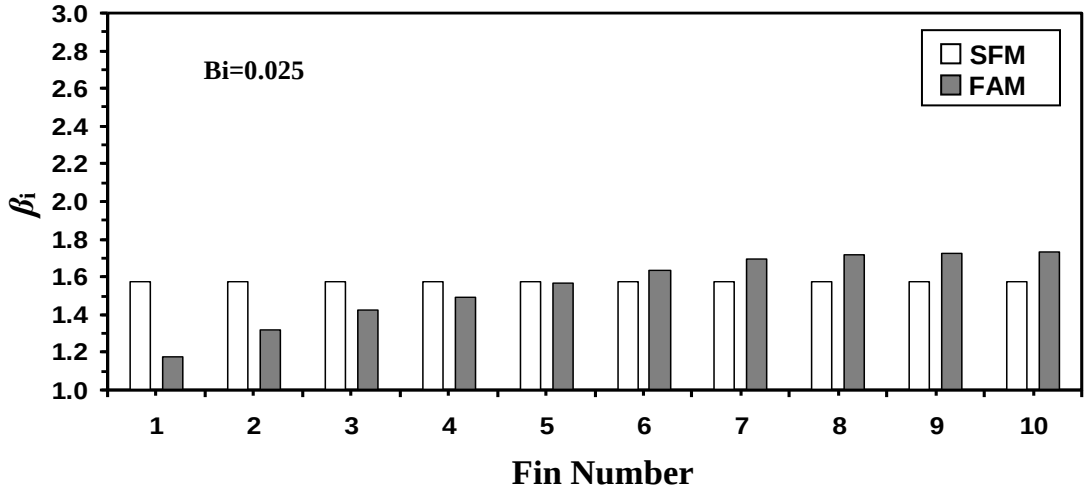

Figure (5-10) Optimum Fin Length for Bi=0.025.

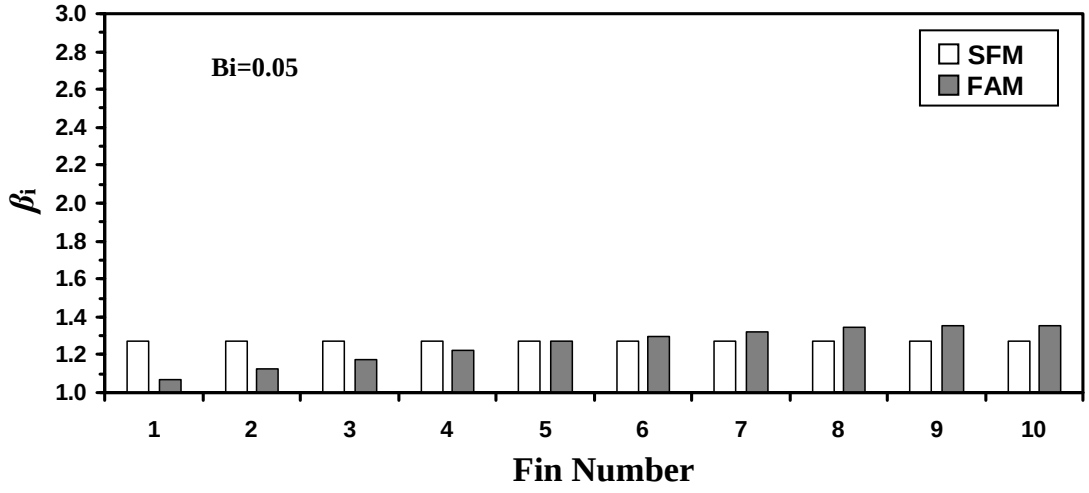

Figure (5-11) Optimum Fin Length for Bi=0.05.

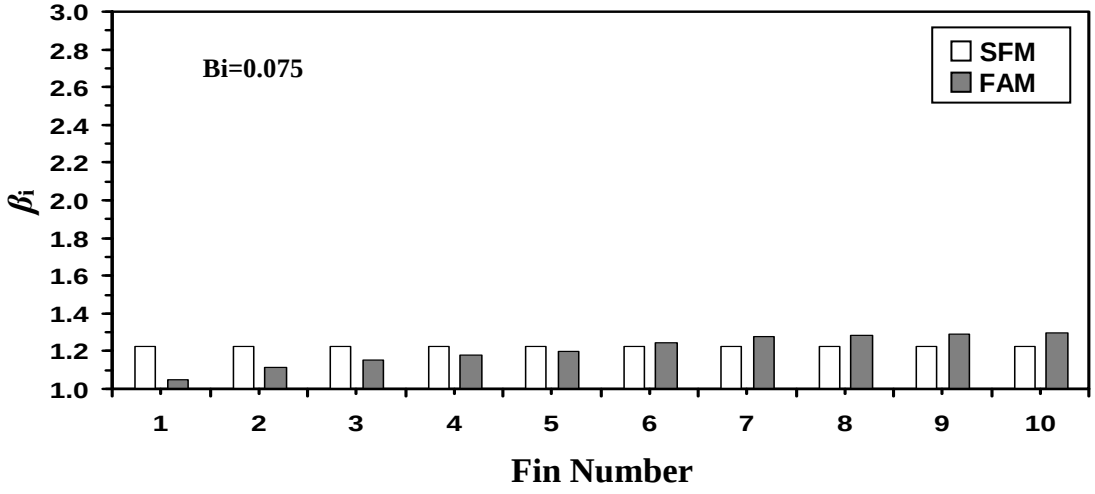

Figure (5-12) Optimum Fin Length for Bi=0.075.

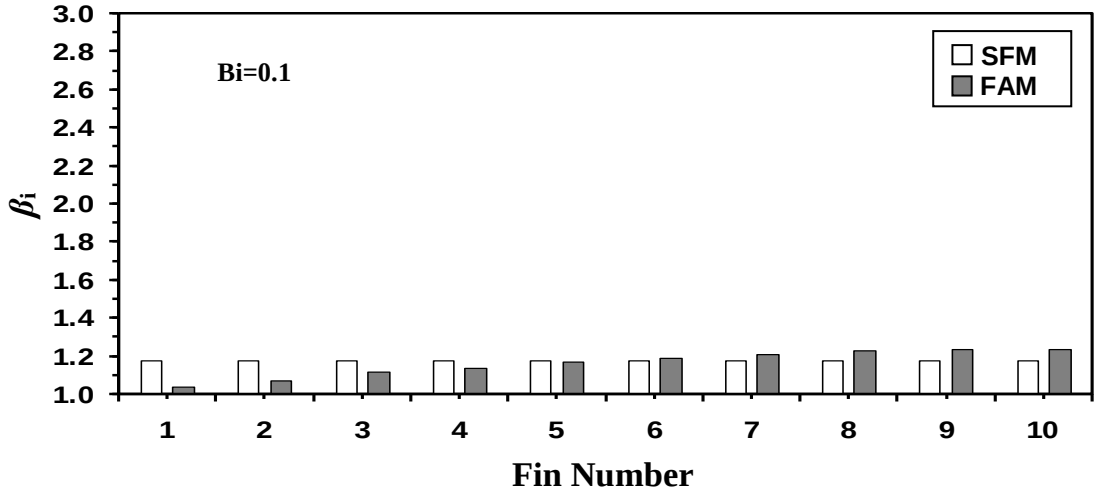

Figure (5-13) Optimum Fin Length for Bi=0.1.

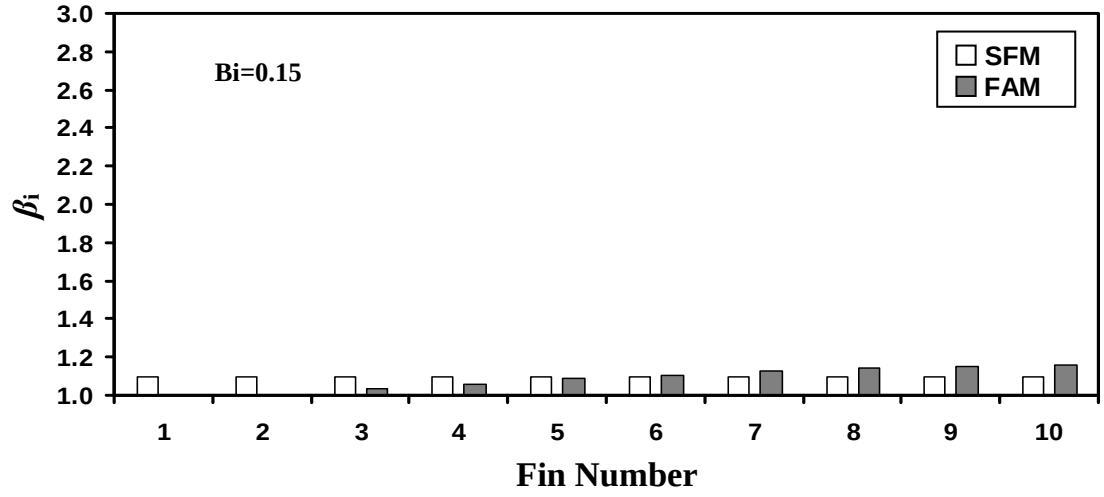

Figure (5-14) Optimum Fin Length for Bi=0.15.

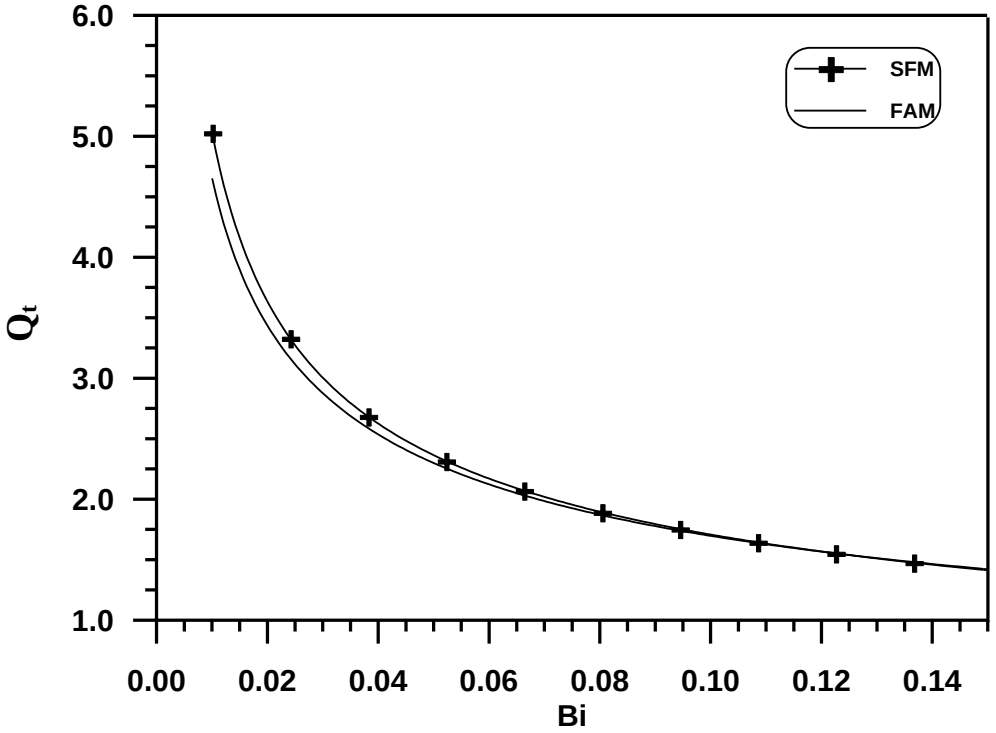

Figure (5-15) Total Heat Removed (Q_t) versus Biot Number (Bi) for FAM and SFM.

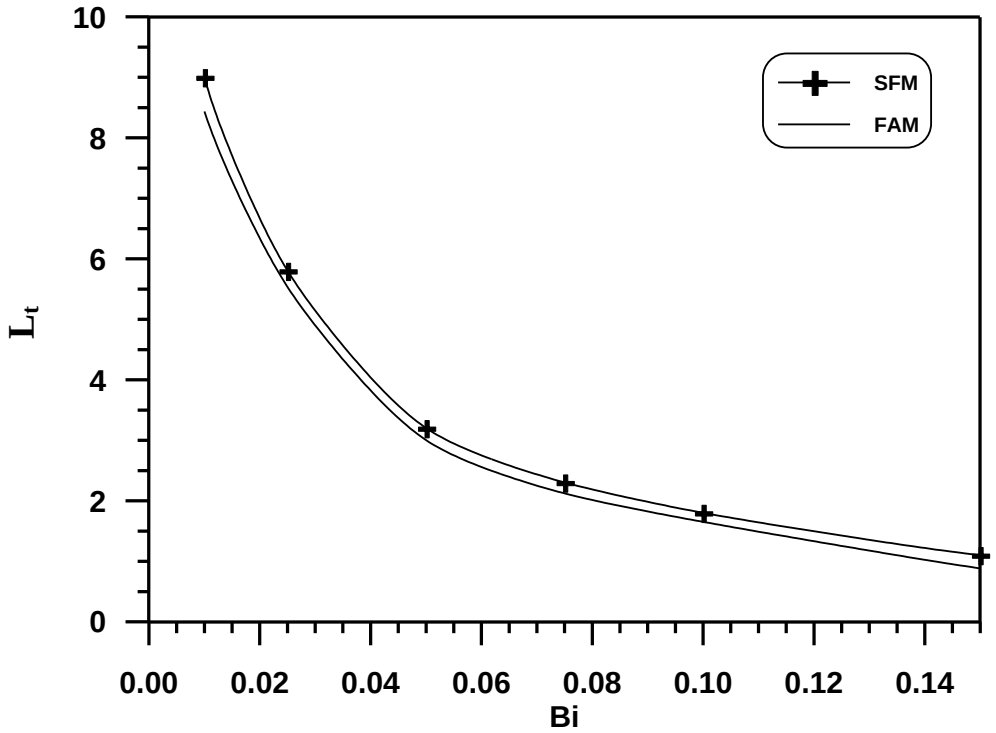

Figure (5-16) Total Length (L_t) versus Biot Number (Bi) for FAM and SFM.

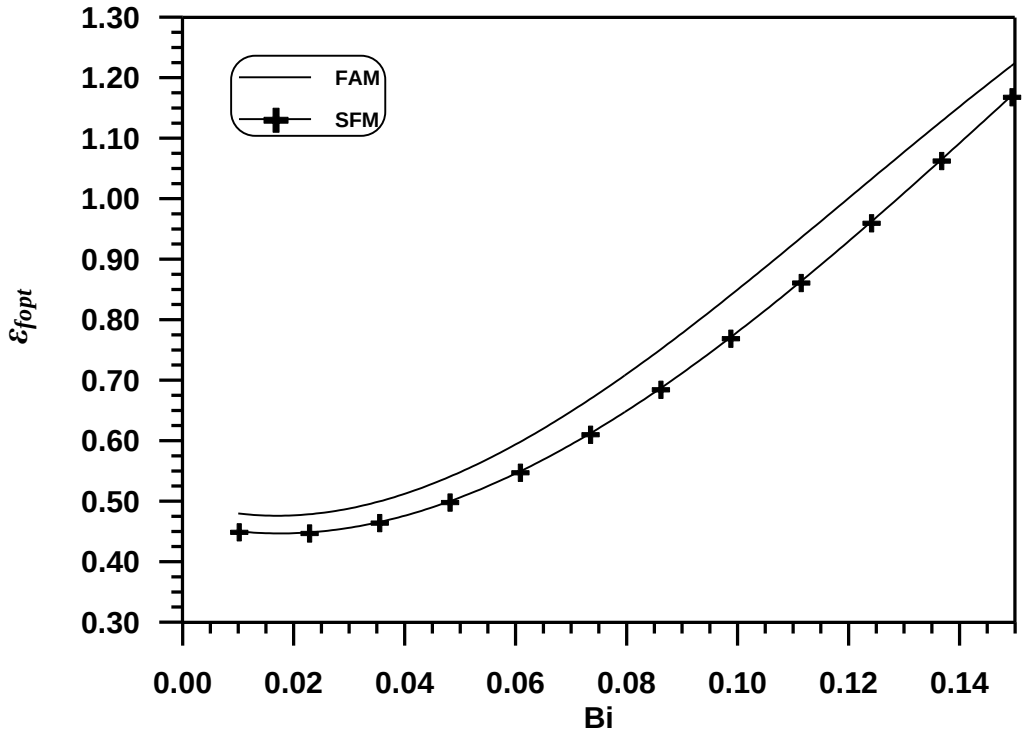

Figure (5-17) Optimum Performance (ε_{fopt}) versus Biot Number (Bi) for FAM and SFM.

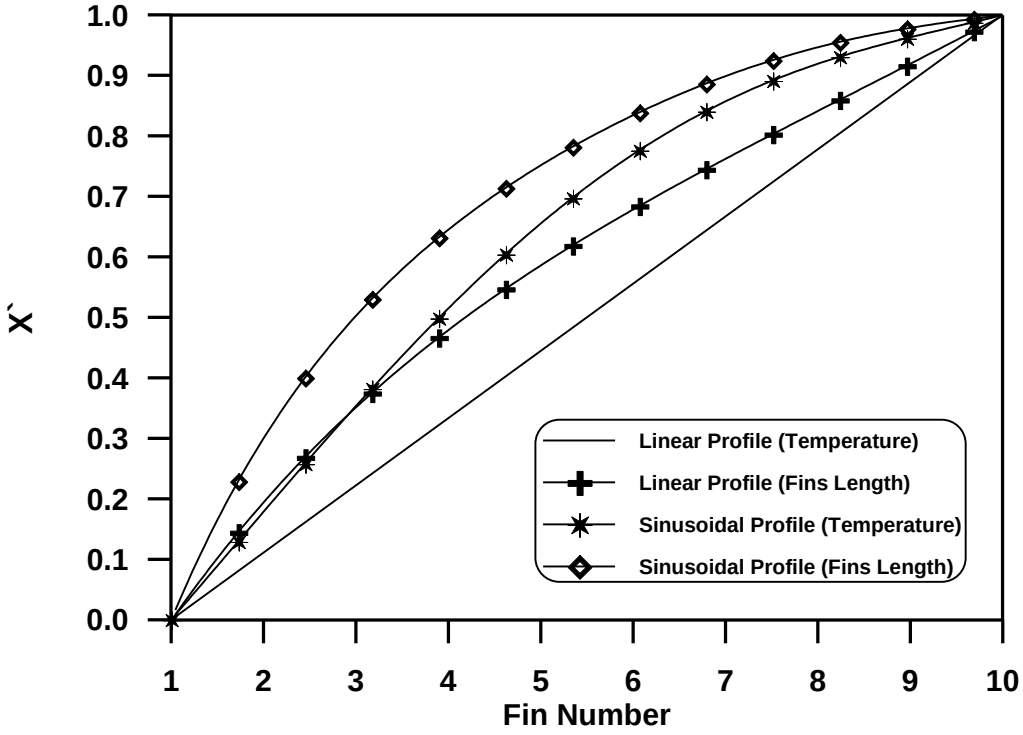

Figure (5-18) Re-scaled (X') Temperature and Fin Length Profiles for both Cases Linear and Sinusoidal Base Temperature.

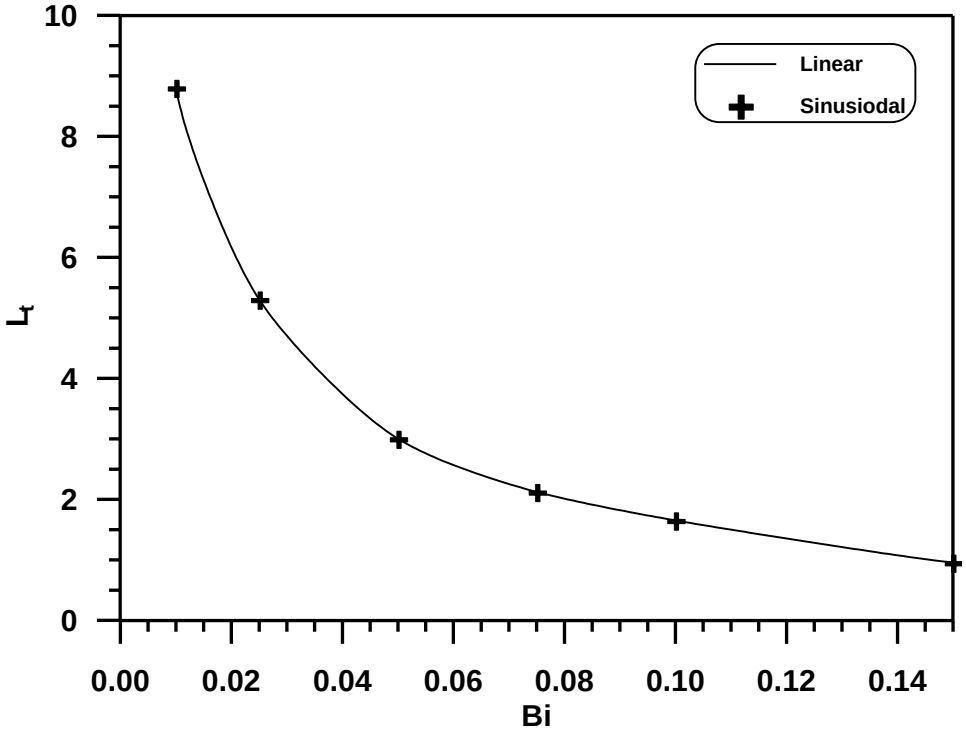

Figure (5-19) Total Fin Lengths (L_t) versus Biot Number (Bi) for Linear and Sinusoidal Base Temperature.

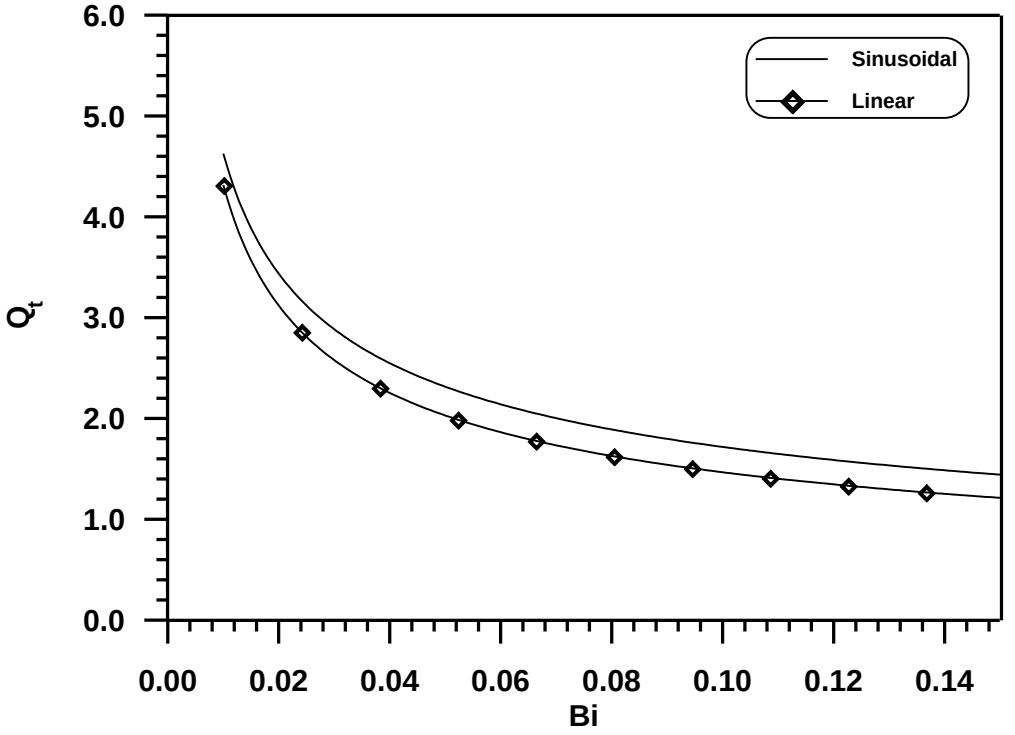

Figure (5-20) Total Heat Removed (Q_t) versus Biot Number (Bi) for Linear and Sinusoidal Base Temperature.

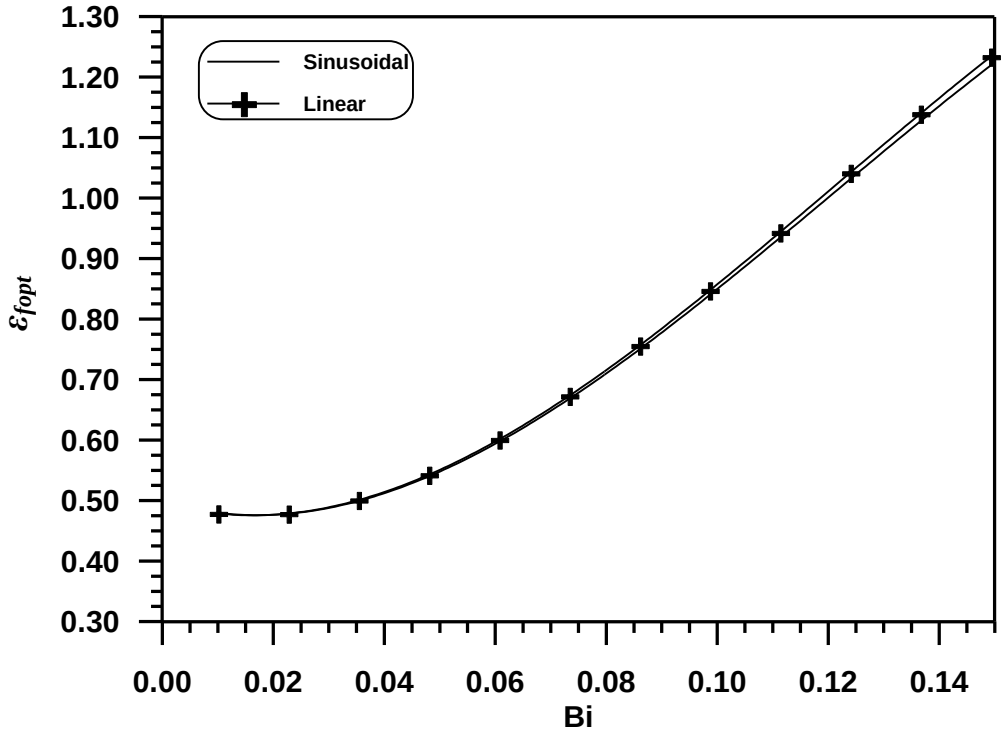

Figure (5-21) Optimum Effectiveness (ε_{fopt}) versus Biot Number (Bi) for Linear and Sinusoidal base temperature.

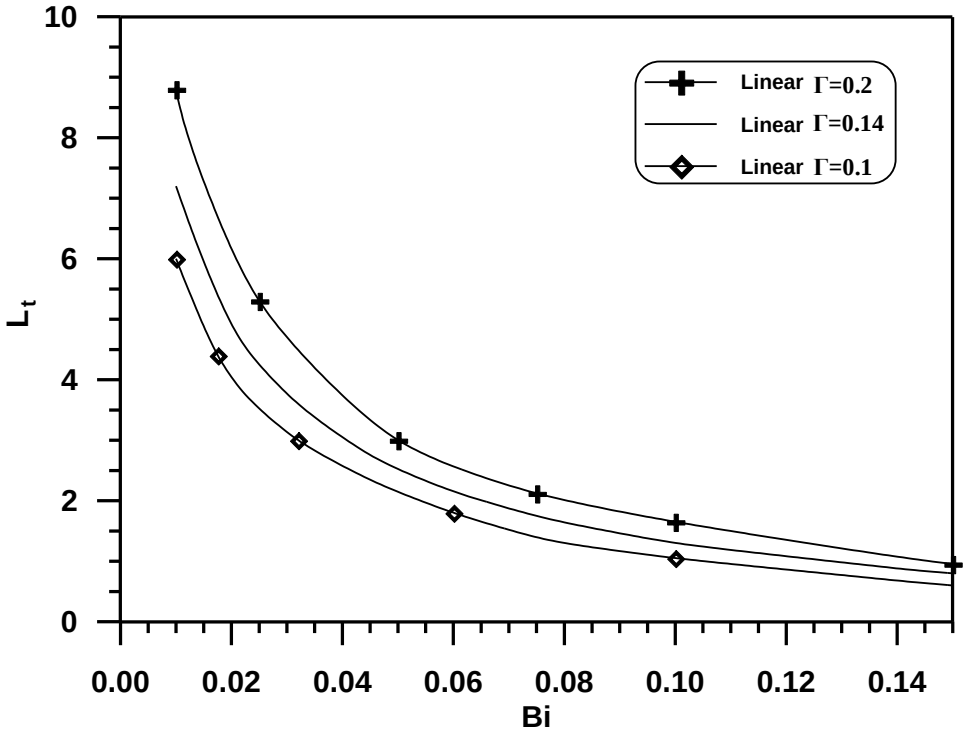

Figure (5-22) Total Fin Lengths (L_t) versus Biot Number (Bi) for Linear Base Temperature and Different Γ.

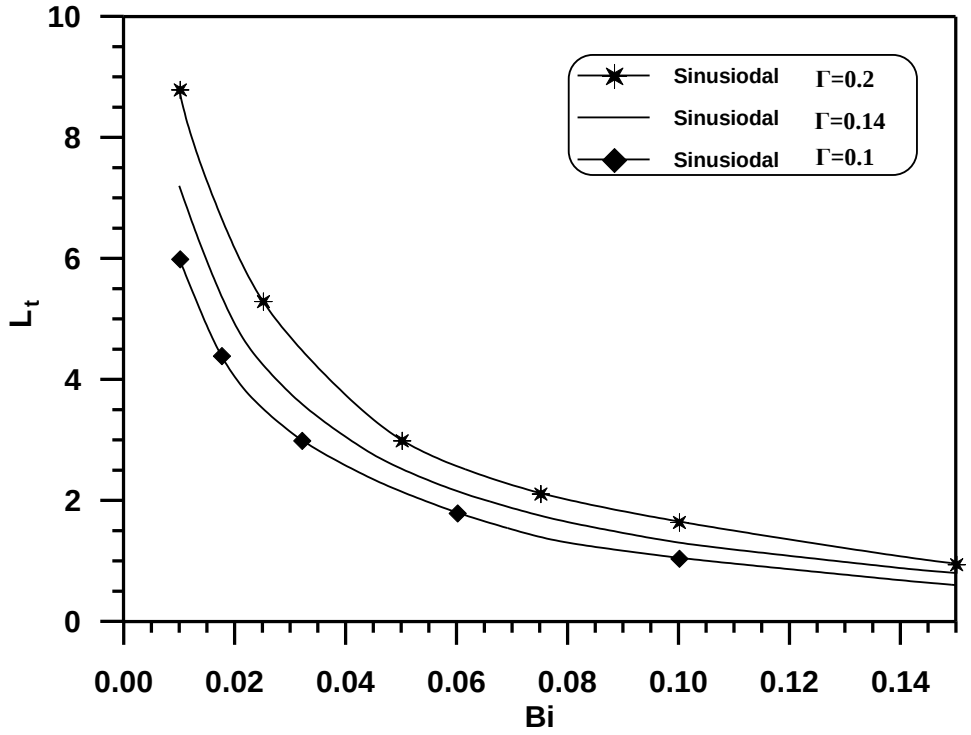

Figure (5-23) Total Fin Lengths (L_t) versus Biot Number (Bi) for Sinusoidal Base Temperature and Different Γ.

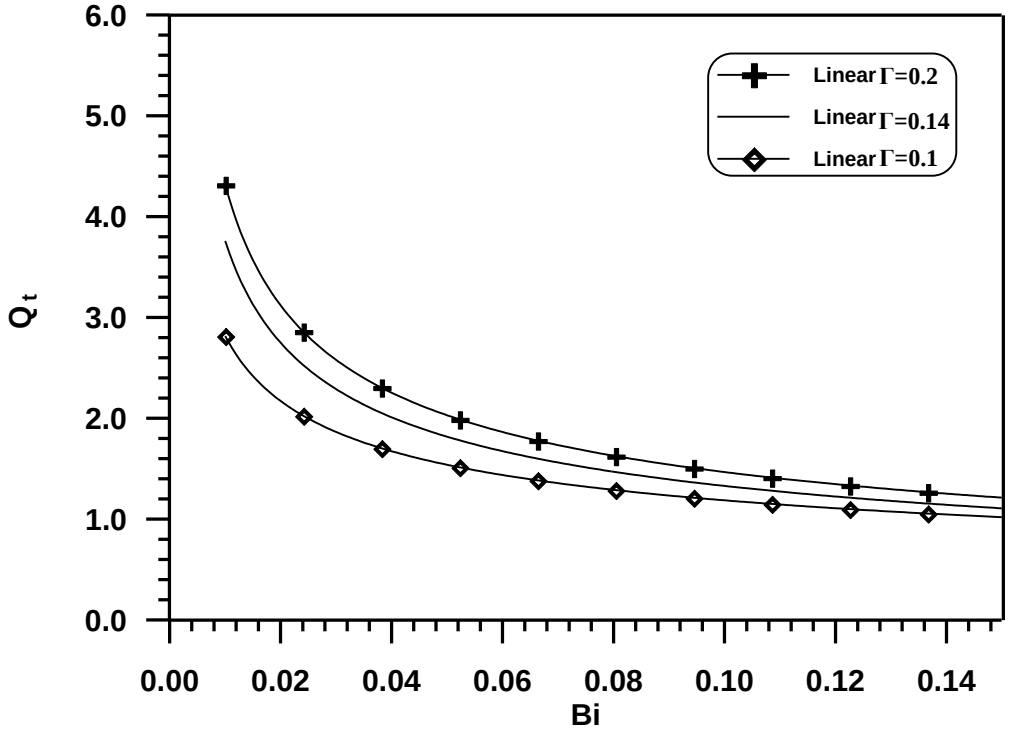

Figure (5-24) Total Heat Removed (Q_t) versus Biot Number (Bi) for Linear Base Temperature and Different Γ.

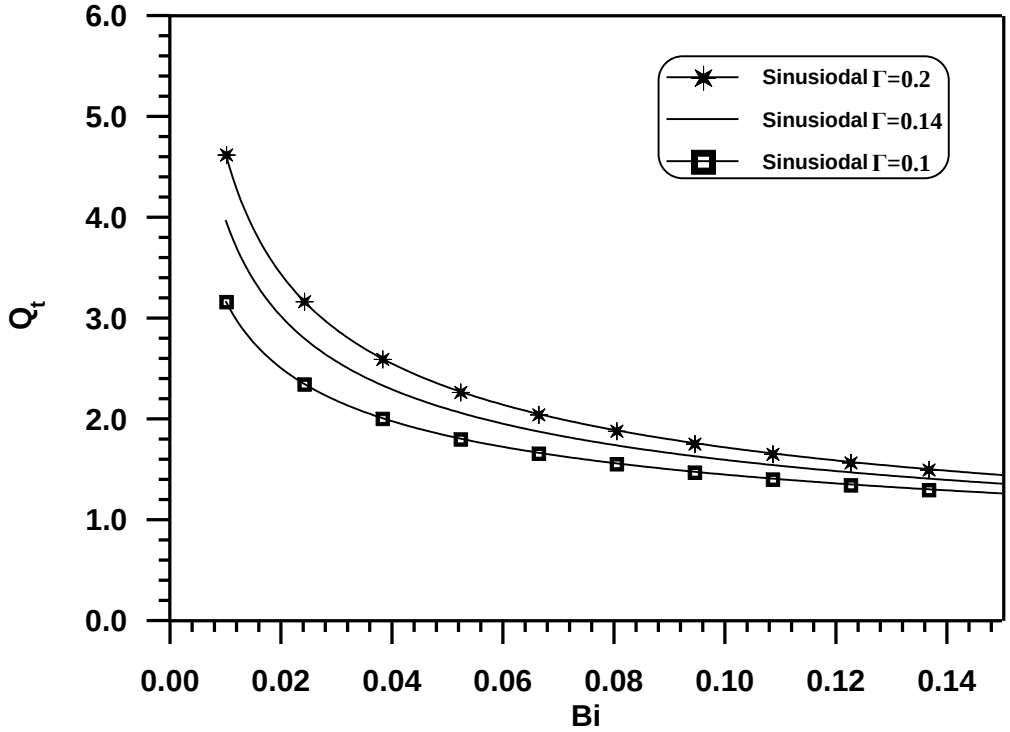

Figure (5-25) Total Heat Removed (Q_t) versus Biot Number (Bi) for Sinusoidal Base Temperature and Different Γ.

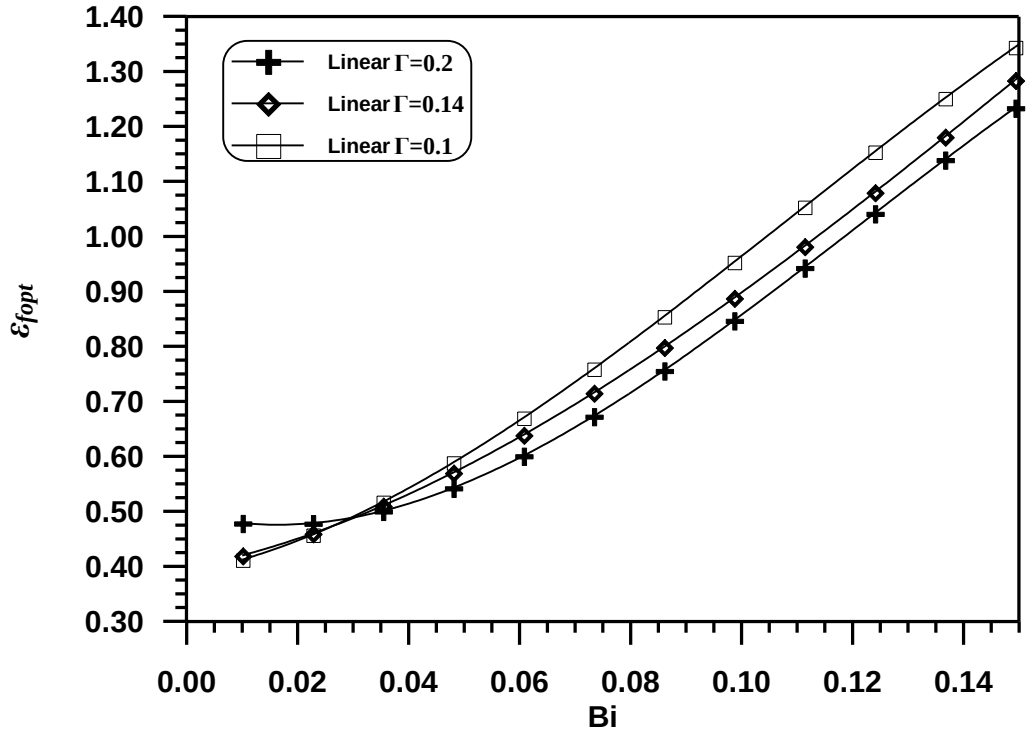

Figure (5-26) Optimum Effectiveness (ε_{fopt}) versus Biot Number (Bi) for Linear base temperature and Different Γ.

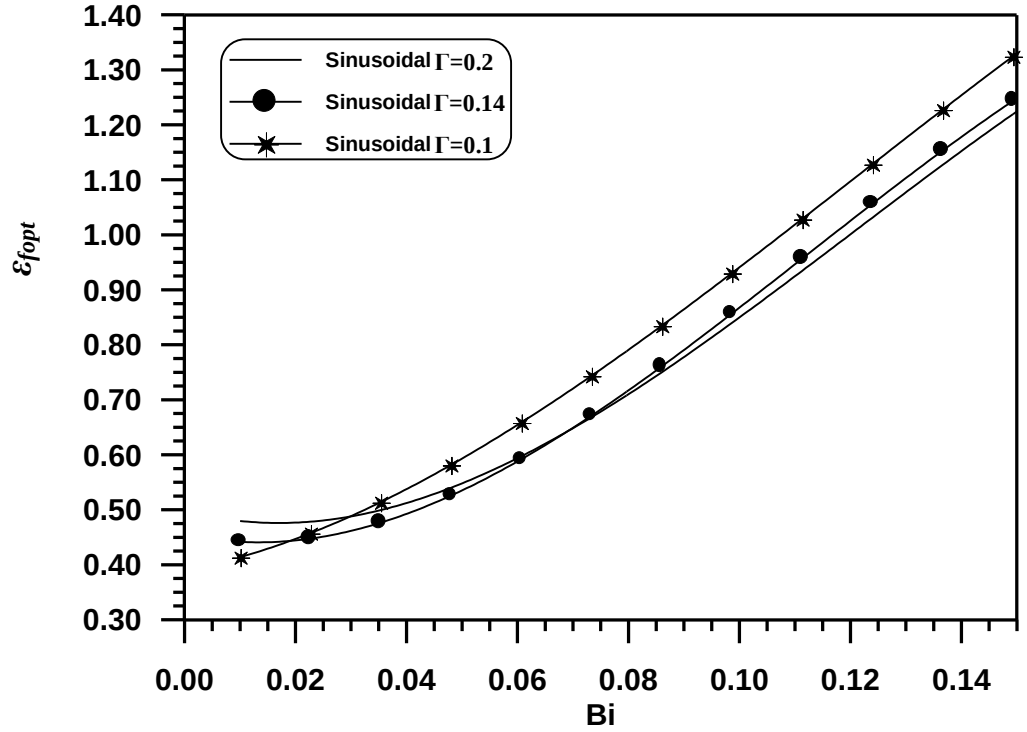

Figure (5-27) Optimum Effectiveness (ε_{fopt}) versus Biot Number (Bi) for Sinusoidal base temperature and Different Γ.

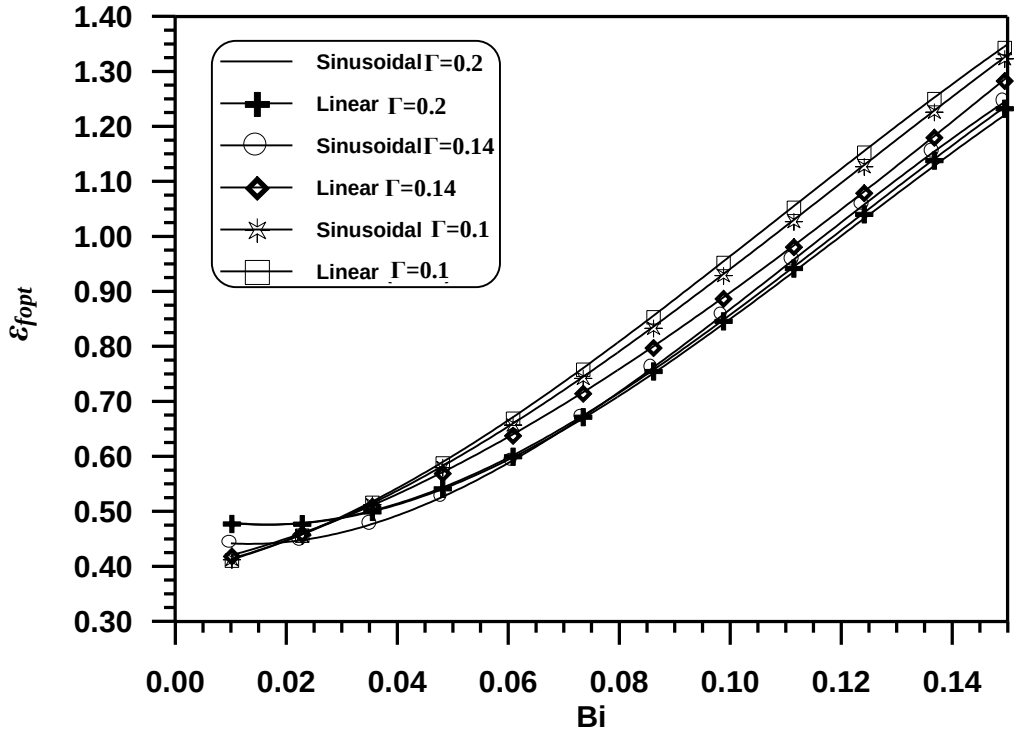

Figure (5-28) Optimum Effectiveness (ε_{fopt}) versus Biot Number (Bi) for Sinusoidal and Linear base temperature and Different Γ.

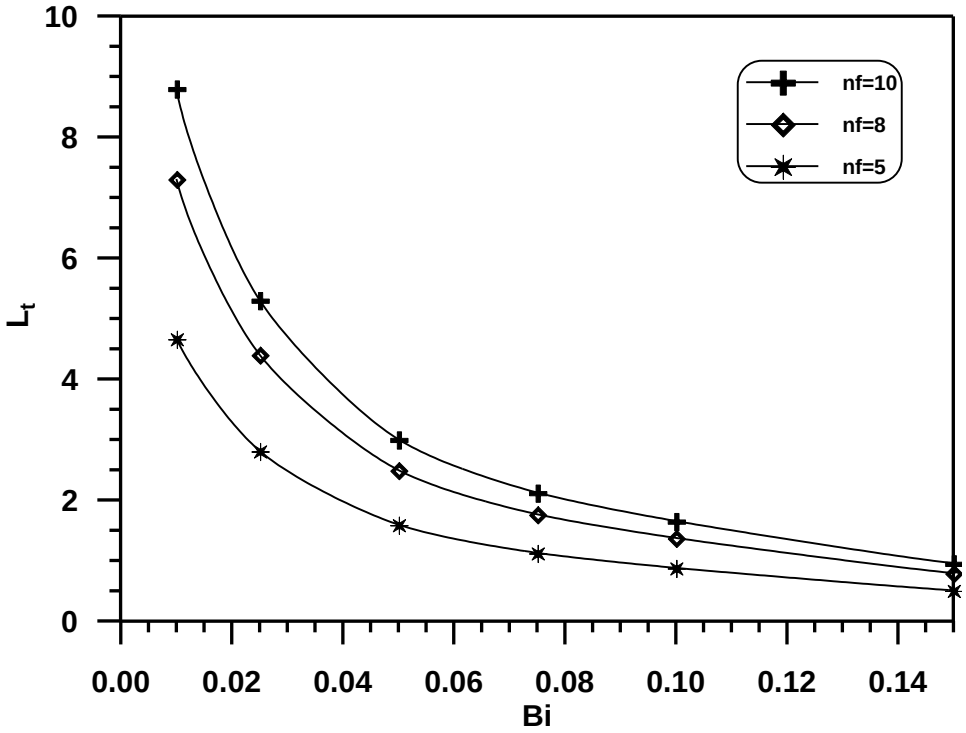

Figure (5-29) Total Fin Lengths (L_t) versus Biot Number (Bi) for Different Number of Fins.

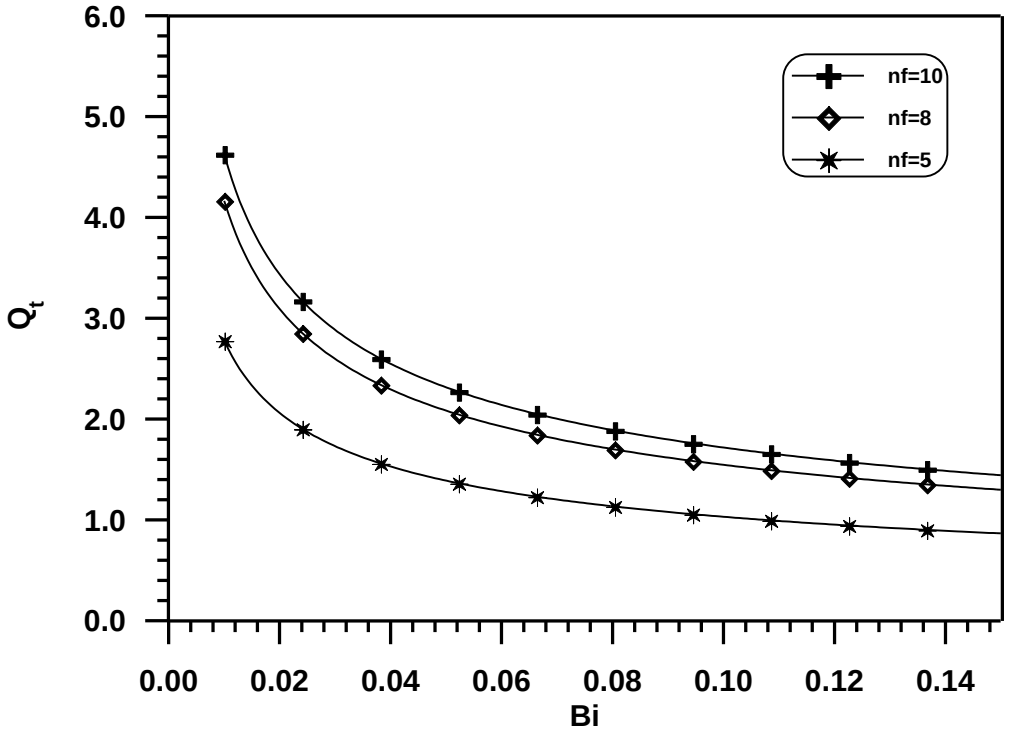

Figure (5-30) Total Heat Removed (Q_t) versus Biot Number (Bi) for Different Number of Fins.

الجمهورية العراقية
وزارة التعليم العالي و البحث العلمي
جامعة بابل/كلية الهندسة
قسم الهندسة الميكانيكية

الأبعاد المثلى للزعانف الحلقية غير المتناظرة

رسالة

مقدمة إلى كلية الهندسة في جامعة بابل

كجزء من متطلبات نيل درجة ماجستير علوم

في الهندسة الميكانيكية

أعدت من قبل

علي صفاء نوري الصائغ

بكالوريوس هندسة ميكانيكية، 2001

تشرين الأول ، 2005 شوال، 1426

الخلاصة

لقد تم اعتماد التحليل ثنائي الأبعاد في هذا البحث لدراسة الأمثلية لمصفوفة من الزعانف الحلقية ذات المقطع المستطيل بفرض إن الخواص الحرارية ثابتة. إن إجراء التصميم استند على حساب أعلى حرارة مفقودة من مصفوفة الزعانف الحلقية ذات المقطع المستطيل غير منتظمة الأطوال آخذين بنظر الاعتبار الانحدار في درجة حرارة قاعدة الزعانف.

إن معامل أداء الزعنفة هو من اكثر العوامل المميزة التي يمكن استخدامها لتمييز عملها. لإيجاد معامل أداء الزعنفة بدقة اكثر, يجب الأخذ بنظر الاعتبار تأثير وجود الزعنفة على درجة حرارة قاعدة الزعنفة مقارنةً بعدم وجود الزعنفة و الذي أهمل من قبل الكثير من الباحثين.

استخدم أسلوب العناصر المحددة (Finite Element) و المعتمدة على طريقة كليركن (Galerkin's Method) لحل المعادلات الحاكمة لمصفوفة الزعانف الحلقية ذات المقطع المستطيل حيث استخدمت عناصر ذات أشكال مثلثة.

في هذه الدراسة تم اعتماد انتقال الحرارة بالحمل القسري مع إهمال انتقالها بالإشعاع و الحمل الحر. لقد تم حساب معدل انتقال الحرارة الكلي ومعامل الأداء و الكفاءة الكلية لمصفوفة الزعانف آخذين بنظر الاعتبار انتقال الحرارة بالتوصيل خلال سطح القاعدة الذي تتصل به الزعانف و انتقال الحرارة من المسافات بين الزعانف و الحافة الخارجية لها.

تم استخدام طريقة الأمثلة العددية (Hooke and Jeeves Method) لإيجاد الطول الأمثل للزعانف بحالتين: الأولى الزعانف غير متساوية الأطوال مع تساوي المسافات الموجودة بينها (FAM) و الثانية هي الزعانف متساوية الأطوال مع تساوي المسافات الموجودة بينها (SFM). لقد وجد الطول الأمثل للزعانف في الحالتين اعتماداً على أكبر معامل أداء لوحدة الحجم لمصفوفة الزعانف. لقد تمت مقارنة النتائج التي حصلنا عليها من دراسة الامثلية المعتمدة على طريقة أطوال الزعانف المنتظمة (SFM) مع طريقة الأطوال غير المنتظمة للزعانف (FAM) و أشارت النتائج إلى أن طريقة أل(FAM) تؤدي إلى تصميم مصفوفة من الزعانف ذات معامل أداء أعلى و لحجم اقل من المواد المستخدمة لصناعة مثل هذه الزعانف.

تم اخذ نوعين من التدرج الحراري عند قاعة الزعانف لدراسة تأثير نوع التدرج الحراري عند قاعدة الزعانف على انتقال الحرارة و الصورة الجانبية للزعانف و فعالية مصفوفة الزعانف و القيم العضمى لها. التدرج الأول هو التدرج الجيبي لقاعدة الزعانف و الثاني هو التدرج الخطي. النتائج أظهرت بان الصورة الجانبية لاطوال الزعانف دائماً تختلف عن الصورة الجانبية للتدرج في درجة حرارة قاعدة الزعانف كما و أظهرت النتائج بان الكمية الكلية للحرارة المفقودة من مصفوفة الزعانف المستندة على أساس التدرج الجيبي لدرجة حرارة قاعدة الزعانف تكون دائما أعلى من تلك المستندة على أساس التدرج الخطي. كذلك فان فعالية مصفوفة الزعانف طبقاً للتدرج الخطي تكون دائماً أعلى مما هي في التدرج الجيبي كما وان كتلة مصفوفة الزعانف في حالة التدرج الخطي تكون اقل منها في حالة التدرج الجيبي.

لقد رسمت قيم كل من الكمية الكلية للحرارة المفقودة من مصفوفة الزعانف و فعالية مصفوفة الزعانف مقسومة على حجم المصفوفة ضد قيم رقم بايوت. لقد وجد من تلك الرسومات بان زيادة رقم بايوت ستؤدي إلى تقليل قيمة الحرارة الكلية المفقودة من مصفوفة الزعانف وكذلك الطوال الكلي للزعانف.

لفحص تأثير المعامل (Γ) فقد رسمت قيم الكمية الكلية للحرارة المفقودة من مصفوفة الزعانف و الطول الكلي للزعانف و فعالية الزعانف مقسومةً على حجمها ضد قيم مختلفة من رقم بايوت و قيم Γ. النتائج أظهرت بان الزيادة بقيمة المعامل Γ تؤدي إلى تقليل الفعالية لمصفوفة الزعانف.

أستخدم التحليل الرياضي الأحادي و الثنائي البعد للزعانف الحلقية المفردة و المنتظمة بصفوف للتحقق من صلاحية النتائج و قد أظهرت النتائج دقة جيدة.

REFERENCES

[1]- Arpaci, V. S., "**Conduction Heat Transfer**", Addison-Wesley, 1966.

[2]- Incropera, F. P., and DeWitt, D. P., "**Fundamentals of Heat and Mass Transfer**", John Wiley and Sons Inc., New York, 1996.

[3]- Holman, J. P., "**Heat Transfer**", McGraw Hill Inc., New York, 1989.

[4]- Abul-Rahman, G. Y., "**An Analogue System for Heat Flow Through Annular Fins of Constant Thickness**", M.Sc. Thesis, University of Mosul, Mosul, Iraq, 1978.

[5]- Schneider, P. J., "**Conduction Heat Transfer**", Addison-Wesley, 1974.

[6]- Elias, A. R., "**Comparison of Performance for the Annular Fin with Different Shapes**", M.Sc., Thesis, University of Mosul, Mosul, Iraq, 1998.

[7]- Manzoor, M., "**Heat Flow Through Extended Surface Heat Exchanger**", "**Lecture Notes in Engineering**", Springer-Verlag, Berlin Heideberg, 1984.

[8]- Kreith, F., and Bohn, M., "**Principle of Heat Transfer**", Pws Publishing Company, Boston, 1997.

[9]- Kern, D. Q., and Kraus, A. D., "**Extended Surface Heat Transfer**", McGraw-Hill, New York, 1972.

[10]- Myers, G. E., "**Analytical Methods in Conduction Heat Transfer**", McGraw-Hill, New York, 1971.

[11]- Mousa, A. H., "**Performance of Fins Subjected to Natural Convection Through Body Perforation**", Ph.D. Thesis, University of Baghdad, Baghdad, Iraq, 2000.

[12]- Suryanarayana, N. V., "**Two Dimensional Effects on Heat Transfer Rate from an Array of Straight Fins**", *ASME J. Heat Transfer*, Vol. 99, pp. 129~132, 1977.

[13]- Lienhard IV, and Lienhard V, J. H., "**A Heat Transfer Textbook**", Phlogiston Press, Cambridge, 2004. Web site, http://web.mit.edu/lienhard/www/ohtt.html

[14]- Chung, B. T. F., Abdalla, M. H., and Liu, F., "**Optimization of Convective Longitudinal Fins of Trapezoidal Profile**", *J. Chem. Eng. Comm.*, Vol. 80, pp. 211~223, 1989.

[15]- Bunday, B. D., "**Basic Optimization Methods**", Edward Arnold, USA, 1985.

[16]- Stewart, R. W., "**The Absolute Thermal Condutivities of Iron and Copper**", *Philosophical Transactions*, Royal Society of London, Eng., Vol. 184, Series A, pp. 569, 1893.Cited in Ref. [22].

[17]- Parsons, S. R., and Harper, D. R., "**Radiators of Aircraft Engines**", U.S. Bureau of Standards, Technical Paper No. 211, pp. 327~330, 1922. Cited in Ref. [22].

[18]- Harper, W.B., and Brown, D.R., "**Mathematical Equations for Heat Conduction in the Fins of Air Cooled Engine**", *NACA Report*, No. 158, 1922, Cited in Ref. [5].

[19]- Murray, W. M., "**Heat Dissipation Through an Annular Disk of Fin of Uniform Thickness**", *Trans. ASME J. Applied Mechanics*, Vol. 60, pp. A78~A80, 1938. Cited in Ref. [22].

[20]- Herman, H. E., Jr., and Arnold, E. B., "**Surface Heat-Transfer Coefficient of Finned Cylinder**", *NACA Report*, No. 676, pp. 651~665, 1939. Web site, http://naca.larc.gov/reports/

[21]- Carrier, W.H, and Anderson, S.W., "**The Resistance to Heat Flow through Finned Tubing**", Heating, Piping, and Air Conditioning, Vol. 10, pp. 304~320, 1944, Cited in Ref. [5].

[22]- Gardner, K.A., "**Efficiency of Extended Surface**", *Trans. ASME J. Heat Transfer*, Vol. 70, No. 8, pp. 621~631, 1945.

[23]- Zabronsky, H., "**Efficiency of Heat Exchanger using square Fins on Round Tubes**", USAEC, k-929. Osk Ridge Technical Information Service, 1952, Cited in Ref. [5].

[24]- Keller, H.H., and Somers, E.V., "**Heat Transfer From an Annular Fin of Constant Thickness**", *ASME J. Heat Transfer*, Vol. 81, pp. 151~156, 1959.

[25]- Yundin, V.F., and Toktorova, L.C., "**Investigation of the Correction Factor Ψ for the Theoretical Effectiveness of a Round Fin**", *Thermal Engineering*, pp. 66~68, 1973.

[26]- Lau, W., and Tan, C. W., "**Error in One-Dimensional Heat Transfer Analysis in Straight and Annular Fins**", *ASME J. Heat Transfer*, November 1973.

[27]- Heggs, P.J., Ingham, D.B., and Manzoor, M., "**The Effect of Non-uniform Heat Transfer from an Annular Fin of Triangular Profile**", *ASME J. Heat Transfer*, Vol. 103, pp. 184~185, 1981.

[28]- Ünal, H. C., "**The Effect of the Boundary Condition at a Fin Tip on the Performance of the Fin with and without Internal Heat Generation**", *Int. J. Heat Mass Transfer*, Vol. 31, No. 7, pp. 1483~1496, 1988.

[29]- Charters, W.W.S., and Theerakulpisut, S., "**Efficiency Equations For Constant Thickness Annular Fins**", *Int. Comm. Heat Mass Transfer*, Vol. 16, pp. 547~558, 1989.

[30]- Look, D.C, JR., "**Fin on a Pipe (Insulated Tip): Minimum Conditions for Fin to Be Beneficial**", *Heat Transfer Engineering*, Vol. 16, No. 3, pp. 65~75, 1995.

[31]- Look, D.C., Jr., "**Fin (on a pipe) Effectiveness: One Dimensional and Two Dimensional**", *ASME J. Heat Transfer*, Vol. 121, pp. 227~230, 1999.

[32]- Sparrow, E. M., and Hennecke, D. K., "**Temperature Depression at the Base of Fin**", *ASME J. Heat Transfer*, Vol. 92, pp. 204~206, 1970.

[33]- Levitsky, M., "**The Criterion for Validity of the Fin Approximation**", *Int. J. Heat Mass Transfer*, Vol. 15, pp. 1960~1963, 1972.

[34]- Look, D. C, Jr., "**Two-dimensional Fin with Non-constant Root Temperature**", *Int. J. Heat Mass Transfer*, Vol. 32, No. 5, pp. 977~980, 1989.

[35]- Look, D. C., and Kang, H. S., "**Effects of Variation in Root Temperature on Heat Lost from a Thermally Non-symmetrical Fin**", *Int. J. Heat Mass Transfer*, Vol. 34, pp. 1059~1065, 1991.

[36]- Kang, H. S., and Look, D. C., Jr., "**Two-Dimensional Trapezoidal Fins Analysis**", *Computational Mechanics*, Vol. 19, pp. 247~250, 1997.

[37]- Kang, H. S., and Look, D. C., Jr., "**A Comparison of Four Solution Methods for the Analysis of a Trapezoidal Fin**", *KSMA International J.*, Vol. 13, pp. 487~495, 1999.

[38]- Kraus, A. D., Snider, A. D., and Doty, L. F., "**An Efficient Algorithm for Evaluating Arrays of Extended Surface**", *ASME J. Heat Transfer*, Vol. 100, pp. 288~293, 1978.

[39]- Snider, A. D., and Kraus, A. D., "**Recent Development in the Analysis and Design of Extended Surface**", *ASME J. Heat Transfer*, Vol. 105, pp. 302~306, 1983.

[40]- Kraus, A. D., "**Analysis of Extended Surface**", *ASME J. Heat Transfer*, Vol. 110, pp. 1071~1081, 1988.

[41]- Houghton, J. M., Ingham, D. B., and Heggs, P. J., "**The One-Dimensional Analysis of Oscillatory Heat Transfer in a Fin Assembly**", *ASME J. Heat Transfer*, Vol. 114, pp. 548~552, 1992.

[42]- Schmidt, E., "**Die Warmeubertrangung Durch Rippen**", Zeit, VDI, Vol.70, pp. 885~889, 947~951, 1926, Cited in Ref. [5].

[43]- Focke, R., "Die Nadel als Kuhlelement", Forschung auf dem Gebiete des Ingenieurwesens, Vol. 13, pp. 34~42, 1942. Cited in Ref. [22].

[44]- Duffin, R. J., "**A Variational Problem Relating to Cooling Fins**", *J. Math. Mech.*, Vol. 8, pp. 46~56, 1959, Cited in Ref. [6].

[45]- Ahmadi, G., and Razani, A., "**Some Optimization Problems Related to Cooling Fin**", *Int. J. Heat Mass Transfer*, Vol.16, pp. 2369~2375, 1973.

[46]- Maday, C. J., "**The Minimum Weight One-Dimensional Straight Cooling Fin**", *J. Eng. Ind*., Vol.96, pp. 161~15, 1974.

[47]- Dahr, P. L., and Arora, C. P., "**Optimum Design of Finned Surface**", *J. of Franklin Institute*, Vol. 301, No. 4, pp. 379~392, April 1976.

[48]- Schnurr, N. M., Shapiro, A. B., and Townsend, M. A., "**Optimization of Radiating Fin Arrays with Respect to Weight**", *ASME J. Heat Transfer*, Vol. 98, pp. 643~648, 1976.

[49]- Bar-Cohen, A., "**Fin Thickness for an Optimized Natural Convection Array of Rectangular Fins**", *ASME J. Heat Transfer*, Vol. 101, pp. 564~566, 1979.

[50]- Razelos, P., and Imre, K., "**The Optimum Dimensions of Circular Fins with Variable Thermal Parameters**", *ASME J. Heat Transfer*, Vol.102, pp. 420~425, 1980.

[51]- Mikk, I., "**Convective Fin of Minimum Mass**", *Int. J. Heat Mass Transfer*, Vol. 23, pp. 707~711, 1980.

[52]- Razelos, I., and Imre, K., "**Minimum mass Convective Fins with Variable Heat Transfer Coefficients**", *J. of the Franklin Institute*, Vol. 315, No. 4, pp. 269~282, April 1983.

[53]- Khan, J., and Zubair, S. M., "**The Optimal Dimensions of convective-Radiating Circular Fins**", *Int. J. Heat Mass Transfer*, Vol. 35, No. 6, pp. 469~478, 1999. Web site, http://www.springerlink.com/

[54]- Kundu, B., and Das, P. K., "**Performance Analysis and Optimization of Annular Fin with a Step change in Thickness**", *ASME J. Heat Transfer*, Vol.123, No.3, pp. 601~604, 2001. Web site, (http://www. google.com), with key word, (heart transfer + extended surface + optimization + annular fin).

[55]- Razelos, P., and Krikkis, R. N., "**Optimum Design of Longitudinal Rectangular Fins with Base-to-Fin Radiant Interaction**", *Heat Transfer Engineering*, Vol.22, No.4, 2001. Web site, http://taylorandfrancis.metapress.com

[56]- Krikkis, R. N., and Razelos, P., "**Optimum Design of Spacecraft Radiators with Longitudinal Rectangular and Triangular Fins**", *ASME J. Heat Transfer*, Vol.124, No.5, pp. 805~811, 2002. Web site, (http://www. google.com), with key word, (heart transfer + extended surface + optimization + longitudinal fin).

[57]- Razelos, P., and Kikkis, R. N., "**The optimum Design of Radiating and Conevtive-Radiating Circular Fins**", *Heat Transfer Engineering*, Vol.24, No.3, 2003. Web site, http://www.taylorandfrancis.metapress.com/

[58]- Stewart, S. W., Shelton, S. V., and Aspelund, K. A., "**Finned Tube Heat Exchanger Optimization**", 2nd International Conference on Heat Transfer, Fluid Mechanics and Thermodynamics, Paper No. SS2, Victoria Falls, Zambia, 23~26 June 2003. Web site, (http://www.google.com), with key words (heat transfer, finned tube, extended surface, optimization).

[59]- Jacob, M., **"Heat Transfer"**, Vol.1, John Wiley and Sons, New York, 1957.

[60]- Eckert, E. R. G., and Drake, R., "**Analysis of Heat and Mass Transfer"**, McGraw-Hill, New York, 1972.

[61]- Karlekar, B. V., and Chao, B. T., "**Mass Minimization of Radiating Trapezoidal Fins with Negligible Base Cylinder Interaction**", *Int. J. Heat Mass Transfer*, Vol.6, pp. 33~48, 1963.

[62]- Brown, A., "**Optimum Dimensions of Uniform Annular Fins**", *Int. J. Heat Mass Transfer*, Vol.8, pp. 655~662, 1965.

[63]- Hrymak, A. N., McRae, G. J., and Westerbarg, A. W., "**Combined Analysis and Optimization of extended Heat Transfer**", *ASME J. Heat Transfer*, Vol.107, pp. 527~532, 1985.

[64]- Buccini, A., and Soliman, H. M., "**Optimum Dimensions of Annular Fin Assemblies**", *ASME J. Heat Transfer*, Vol.108, pp. 459~462, 1986.

[65]- Yang, X. X. "**A Study on Heat Transfer of the Optimization in Circular Fins of Parabolic profile with variable Thermal Parameters**", *Appl. Math. Mech.*, Vol. 19, pp. 267~278, 1988.

[66]- Ullmann, A., and Kalman, H., "**Efficiency and Optimized Dimensions of Annular Fins of Different Cross-Section Shapes**", *Int. J Heat Mass Transfer*, Vol.23, No.6, pp. 1105~1110, 1989.

[67]- Look, D.C., Jr., and Kang, H. S., "**Optimization of Thermally Non-symmetrical Fin: Preliminary Evaluation**", *Int. J. Heat Mass Transfer*, Vol.35, No8, pp. 2057~2060, 1992.

[68]- Al-Hattab, T. A., Abdul-Wahab, M. I., and Kasir, N. W., "**Efficiency and Optimum Dimensions of Radiated Fins**", *J. Babylon University*, *Eng. Sc.*, Vol.5, No.5, pp. 655~661, 2000.

[69]- Ali, A. M., "**Optimum Arrangement of Rectangular and Triangular Fin Arrays**", M.Sc. Thesis, University of Babylon, Babylon, Iraq, 2001.

[70]- Al-Hattab, T. A., "**Optimum Fin Length of Annular Fin Arrays**", *Iraqi J. for Mech. And Materials Eng.*, Vol.3, No.1, pp. 101~115, 2003.

[71]- Bathe, K. J., "**Finite Element Procedure in Engineering Analysis**", prentice-Hall, Englewood Cliffs, N. T., 1996.

[72]- Lewis, R. W., Morgan, K., Thomas, H. R., and Seetharamu, K. N., "**The Finite Element Method in Heat Transfer Analysis**", John Wily and Sons, 1996.

[73]- Segerlind, L. J., "**Applied Finite Element**", John Wiley and Sons, 1984.

[74]- Chaudruptla, T. R., Belegundu, A. D., "**Introduction to Finite Element in Engineering**", Second Edition, Prentice-Hall, New Delhi, 1997.

[75]- Rockey, K. C., Evans, H. S., Griffiths, D. W., and Nethercot, D. A., "**The Finite Element Method**", William Clowes and Sons, 1975.

[76]- Reddy, J. N., "**An Introduction to the Finite Element**", First Edition, McGraw-Hill, Inc., USA, 1984.

[77]- Sparrow, E. M., and Lee, L., "**Effect of Fin Base Depression in a Multi-fin Array**", ASME J. Heat Transfer, Vol. 97, pp. 63, 1975.